EAST MANCOS RIVER WATERSHED

MONTEZUMA COUNTY, COLORADO

AQUEOUS METAL SOURCES, CONCENTRATIONS, MASS LOADING, AND AQUATIC IMPACTS

MANCOS CONSERVATION DISTRICT

604 Bauer Avenue

Mancos, Colorado 81328

SEPTEMBER 25, 2020

Prepared for:

Colorado Department of Public Health and Environment
CMS Contract Routing Number 18 FEGA 104837, 01/02/2018

Prepared by:

[Sections 1, 2, and 3]

Winfield G. Wright, M.S., P.E., C.P.H.
Southwest Hydro-Logic, LLC
Durango, Colorado 81303
(970) 749-3950
win@swhydrologic.com

Prepared by:

[Section 4]

Scott Roberts, M.S.
Mountain Studies Institute
Silverton, Colorado 81433
(970) 387-5161
scott@mountainstudies.org

With funding and field support from:

Kirstin Brown
Colorado Division of Reclamation, Mining, and Safety (DRMS)
Durango, Colorado

Jeff Litteral
Colorado Division of Reclamation, Mining, and Safety (DRMS)
Ridgway, Colorado

TABLE OF CONTENTS

EAST MANCOS RIVER WATERSHED
AQUEOUS METAL SOURCES, CONCENTRATIONS, MASS LOADING, AND AQUATIC IMPACTS
Mancos Conservation District

---

1. INTRODUCTION

The Mancos River originates on the western flanks of the La Plata Mountains, a western subrange of the San Juan Mountains in southwestern Colorado. It then flows southwest through the Mancos Valley and Mancos Canyon, until it joins the San Juan River in northwestern New Mexico. The river is 116 miles in length, including major upstream tributaries, and drains an area of approximately 800 square miles. The Mancos River watershed is part of the Colorado Plateau geologic region, and is often divided into two main parts: an upper watershed of approximately 203 square miles that includes Mancos Valley and the surrounding mountains; and a lower area that begins in Mancos Canyon at the confluence of Weber Creek, and drains the mesa and desert lowland country of Mesa Verde National Park, the Ute Mountain Ute Indian Reservation, and the surrounding regions. Four main tributaries originate among the 13-thousand-foot peaks of the upper watershed—the East, Middle, and West Mancos Rivers.

With a watershed area of about 15 square miles, the East Mancos River drains a geologically mineralized region of the La Plata Mountains, southwestern Colorado **(Figure 1-1)**. Early Spanish explorers searched for gold in the East Mancos River, and since the late 1800's gold, silver, and other metals have been extracted from mines in the upper East Mancos River. With as many as 65 abandoned historical mines in the East Mancos River (and some recently active mines), acid-mine drainage and leachate from weathered waste-rock piles may contribute dissolved-metal loads to the stream. While some component of dissolved-metal loading may come from historical mines and waste-rock piles, some component of the dissolved-metal load in the East Mancos River may be caused by naturally occurring seeps and streams draining mineralized rocks of the upper basin (Neubert, 2000; CDHPE, 2005; CDPHE, 2012). Water-quality conditions are, therefore, degraded throughout the length of East Mancos River, dissolved copper and manganese have been identified as contaminants of concern, aquatic

habitat has been degraded, and fish are generally absent in the East Mancos River. The effects of impaired water-quality conditions in East Mancos River could be transported downstream, thereby impacting water quality, aquatic habitat, and agricultural irrigation in the lower Mancos River.

Historical mining in the East Mancos River began between 1897 and 1901, when the low-grade pyritic-gold deposits in Jackson Ridge were discovered at the heads of East and Middle Mancos Rivers. Placer gold deposits were discovered in the middle East Mancos River valley near the Red Arrow Mine (https://mrdata.usgs.gov/mrds/show-mrds.php?dep_id=10014163). At the turn of the century, hundreds of mine claims had been recorded, and more than 200 claims had been patented. Many of the mines had produced some ore, but the total production of the district up to 1900 was comparatively small. Some of the mines produced intermittently up to 1939, but none of the mines produced even as much as $100,000 (Eckel, 1949). Transportation costs and remote access were described as reasons for mine failures, highlighted during February 1936 when a large avalanche in Rush Basin claimed six lives, destroying the Doyle-Hesperus Mine boarding house and gold mill (A. Gulliford, "White Death of 1936," https://durangoherald.com/articles/9136, Feb. 14, 2010). Mining resumed a few years later with newly constructed buildings and milling technology such as cyanide leaching for gold extraction (Eckel, 1949). At the ore milling sites for the Doyle mines, mill tailings were dumped directly into the upper East Mancos River, and massive mill tailings deposits can be observed in the stream channel, forming ledges and ironstone dams of tailings cemented by iron and copper mineral precipitates. Locations of historical mines in the East Mancos River watershed are shown in **Figure 1-2**, and mine sites where leach testing was done on waste-rock samples also are shown on **Figure 1-2**.

1.1 Historical Water-Quality Data and Regulatory Setting

Water-quality and water-chemistry data for the East Mancos watershed are not as readily available as with other watersheds in the region (for example, Animas and Alamosa River basins), possibly due to the remote and difficult access to the upper East Mancos. Since about 1998, intermittent water-quality samples have been collected by the CDPHE, River Watch of Colorado, the Mancos Watershed Group, and the Colorado Division of Reclamation, Mining, and Safety (DRMS). Some of the data are available in the USEPA WQX data base (https://www.epa.gov/waterdata/water-quality-data-wqx). Water-quality samples collected at the

mouth of the watershed, combined from CDPHE and River Watch during 1998-2007, show fluctuations in dissolved copper, manganese, zinc, and hardness over time **(Figure 1-3)**. Streamflow discharge measurements were not always performed by these entities; therefore, dissolved-metal mass loading estimates were not available. Dissolved copper, manganese, and zinc concentrations appear to increase from 1998 to 2009; however, this might be caused by more frequent sample collection during 2006-09. Throughout the period, dissolved-copper concentrations exceeded the chronic and acute water-quality standards, dissolved manganese exceeded the standard, but dissolved zinc did not exceed the standards **(Figure 1-3)**. Hardness concentrations also fluctuated over time, occasionally decreasing to a low of about 50 mg/L.

As part of a state-wide effort to describe naturally occurring degraded waters, the Colorado Geological Survey collected water-chemistry samples from upper East Mancos River near Rush Basin (Neubert, 2000). From collection of samples on September 18, 1999 (late-summer low flow conditions), the report describes extensive bog-iron deposits and acidic stream waters with high concentrations of dissolved metals, concluding (p. 63):

> Past mining activities between this test site and the upper sample sites may affect water quality, but the effects are apparently dwarfed by the degraded runoff from the large exposures of altered bedrock and talus further upstream.

In 2005, the Colorado Department of Public Health and Environment Hazardous Materials and Waste Management Division (CDPHE, 2005) conducted a reconnaissance study of the East Mancos watershed to examine impacts of historical mining on human health and the environment. The report describes elevated concentrations of cadmium, copper, iron, manganese, nickel, and zinc in stream water and bed sediments, concluding (p. 22):

> Based on the available data, it is apparent that impacts to water quality in the drainage originate from naturally occurring source areas in Rush Basin and attenuate prior to the confluence with the main Fork of the Mancos River. While mining activity has occurred in the drainage, ongoing impairments to surface water quality do not appear to be attributable to historic mineral extraction activities.

In 2012, under USEPA regulations to establish Total Maximum Daily Loading (TMDL) criteria for every watershed in the US (Code of Federal Regulations, 40 CFR, Vol. 23, Sec. 130.7), the CDPHE revisited historical data in the East Mancos watershed to address the reported elevated concentrations of copper and manganese (CDPHE, 2012). The East Mancos River (Segment COSJLP04a) was identified for impairment with regards to dissolved copper and manganese, and was subsequently listed on the 303(d) list of impaired waters, concluding:

> (p. 1): The sources of pollutants in this watershed are mixed. There are apparent unpermitted point source discharges of pollutants to the East Mancos River from historic mine activity in the area, in addition to natural non-point sources.
>
> (p. 2): The sources of pollutants in this watershed were thought to be predominately related to historic mining, either inactive or abandoned.
>
> (p. 3): The entire segment is water quality impaired. The source of dissolved copper is predominately from historic gold mining features in the drainage.
>
> (p. 16): The average copper load reduction for the East Mancos River (COSJLP04a) would be approximately 50%. The highest load reductions occur in the higher flow months of April through June, with reductions ranging between 72% and 70%.
>
> (p. 21): Non-point sources and background were given approximately 15% of the allowable load.

The East Mancos TMDL report established water-quality standards for dissolved copper (hardness-based equations for acute and chronic toxicity) and manganese (maximum concentration of 50 ug/L), and described the mass loading reductions necessary to attain the standards. While technical descriptions of methods used to calculate load reductions are brief and ambiguous (for example, arbitrarily assigning non-point sources 15% of the load), the TMDL report nonetheless presents tables with specific mass loading reductions for dissolved copper and manganese. The water quality target and goal for the TMDL was attainment of the dissolved copper and dissolved manganese water-quality standards established for the entire San Juan River Basin (latest update CDPHE, 2017), thereby improving water quality to "ensure that it is safe and protective of all its assigned uses," including Coldwater 1 aquatic life, recreation, agriculture, and water supply. With USEPA approval of the 2012 TMDL report, the Upper East Mancos River was shown as removed from the 2018 Colorado 303(d) impaired waters list. However, as of 2020 the lower East Mancos River from the U.S. Forest Service boundary to confluence with the Middle Mancos River remains on the 303(d) list for dissolved lead, macroinvertebrates, and dissolved oxygen. In addition, the mainstem Mancos River remains on the 2020 Colorado 303(d) list for dissolved arsenic, dissolved copper, dissolved iron, dissolved lead, sulfate, macroinvertebrates, and dissolved oxygen.

The East Mancos River has been classified by USEPA as abandoned mine lands, and site assessments have been performed by USEPA to characterize the abandoned mine lands in the East Mancos River drainage according to Comprehensive Environmental Response, Compensation, and Liability Action (https://cumulis.epa.gov/supercpad/cursites/csitinfo.cfm?id=0801922, CERCLA ID CO0012947186).

1.2 Physical, Hydrologic, and Geologic Setting

The East Mancos River begins its course surrounded by 13,000 ft peaks in the La Plata Mountains, and flows 10 ½ miles down steep canyons and waterfalls to the semi-desert mouth of the watershed at 7,475 ft near Mancos, Colorado. The elevation profile of the stream course highlights the steep terrain, with an average stream channel slope of 7 percent per mile, and maximum slope of 32 percent per mile **(Figure 1-4)**. The East Mancos can be classified as an alpine stream, where the sources of streamflow come from snowmelt, high-altitude lakes, and cirque basins. However, the East Mancos does not fit other characteristics of alpine streams, such as low dissolved-constituent concentrations and diverse aquatic-life communities.

Annual surface-water runoff of the East Mancos River is variable from year to year depending on the amount of snowpack. A streamflow gaging station at the mouth of the watershed was operated by the U.S. Geological Survey during 1937-51 (https://waterdata.usgs.gov/, Site 09369000). Streamflow discharges during the period ranged from a minimum of 0.2 ft^3/sec to a maximum of 260 ft^3/sec (cubic feet per second) on May 12, 1941 **(Figure 1-5A)**. Mean daily discharges ranged from 1.3 ft^3/sec to 64 ft^3/sec **(Figure 1-5B)**. The snowmelt runoff period generally occurs from mid-March to early-July of each year **(Figure 1-5B)**. Average annual watershed yield of the East Mancos for the period was about 3.8 million acre-ft per year.

In the East Mancos watershed, the combination of mineralized igneous intrusives and altered and metamorphosed sedimentary rocks makes for a unique and complex geological, geochemical, and mineralogical setting **(Figure 1-6)**. In general, the La Plata Mountains are a laccolithic uplift of Mesozoic sedimentary rocks, intruded by numerous stocks, dikes, and sills (Eckel, 1949; Mutschler and others, 1998). Injection of great quantities of porphyry magma was largely responsible for the forming of the La Plata structural dome. Extensive faulting due to the 24-km wide domal structure resulted in mineralized ore veins, replacement deposits, and breccia zones (Summerlin, 2014) **(Figure 1-6)**. The igneous intrusive rocks of the La Plata Mountains are of late Cretaceous or Tertiary age, and vary widely in composition and in form, but all of them can be grouped in two general types: porphyritic and nonporphyritic (Eckel, 1949). Porphyry deposits are high temperature (>700°C), deep-seated (10-20 km) stockwork intrusives within associated sub-volcanic porphyritic intrusive bodies and surrounding country rock. In contrast, epithermal deposits are shallow (<1 km deep) disseminated, stockwork, or vein deposits that

were hydrothermally formed. The porphyritic rocks are intermediate between diorite and monzonite in composition, but some bodies are syenitic or mafic. The nonporphyritic rocks, which are in general younger than the porphyries, consist of syenite, monzonite, and diorite and occur as irregular stocks accompanied by dikes. The porphyritic bodies were intruded forcibly between the layers of sedimentary rock and were thus a major factor in the uplifting of the La Plata dome, whereas the nonporphyritic rocks cut across the sedimentary formations and the sills, few of them having disturbed the preexisting attitude of the beds.

Diorite-monzonite porphyry in the East Mancos watershed is intermediate in composition between the typical diorite porphyry and typical monzonite porphyry, and contains phenocrysts of white feldspar and of dark-green to black hornblende, set in a gray to brown dense groundmass (Summerlin, 2014). There is clear evidence that the porphyry bodies of the upper East Mancos (Rush Basin) are surrounded by an aureole of rather intensely altered sedimentary rocks (Eckel, 1949, Summerlin, 2014) **(Figure 1-6)**. The porphyry bodies intruded forcibly between the layers of sedimentary rock which created deposits of metallic mineral ores. The Allard stock, located beneath and between the East Mancos watershed and Bedrock Creek **(Figure 1-6)**, is a multi-phase syenite stock hosting sub-economic copper deposits that are partly exposed at the surface (Werle and others, 1984). Alteration and pyritization are widespread and extend into sedimentary rocks beyond the stock. Pyrite and chalcopyrite are abundant and are the dominant metallic minerals. Gold, silver, platinum, and palladium also occur in the Allard Stock, primarily as telluride minerals.

The sedimentary rocks exposed in the La Plata Mountains **(Figure 1-6)** range from the Hermosa formation of Pennsylvania age to the Mancos shale of Upper Cretaceous age. Sedimentary rocks underlying the East Mancos include the upper Jurassic Morrison, Junction Creek, Wanakah, Entrada Sandstone, and upper Triassic Dolores and Junction Creek Formations. The upper Permian Cutler Formation occurs in the central part of the watershed **(Figure 1-6)**. The Wanakah Formation is comprised of shale, sandstone, and the Pony Express Limestone member. These sedimentary rocks have all been hydrothermally altered in the upper basin due to porphyry intrusives, and many of the limestone beds have been completely silicified (Eckel, 1949).

Three important and distinct classes of metallic ores occur in the East Mancos (Eckel, 1949): (1) Porphyry deposits containing metals such as copper, molybdenum, gold, tungsten, and tin; (2)

hydrothermal veins containing copper, lead, zinc, silver, and gold; and (3) hydrothermal or metamorphic alteration and replacement of sedimentary rocks. The porphyry deposits also are known to contain platinum-group elements (PGE), including platinum, palladium, rhodium, ruthenium, iridium, and osmium (Summerlin, 2014). Massive veins of pyrite occur as the "Doyle blanket" which are replacement deposits in the Pony Express limestone. While the massively bedded limestone has been completely silicified and replaced by fine grained quartz, several locations within the exposed Pony Express exhibit thick veins of fine to coarsely granular pyrite (Doyle blanket), which also may contain gold and some chalcopyrite. The underground workings of the North Star-Sundown Mine of the Doyle Group, for example, consist of a maze of interconnected rooms which distinctively resembles a map of a typical limestone cave. The Doyle blanket deposits might represent paleokarst voids (ancient cave systems filled with secondary deposits) in the Pony Express that were replaced by pyrite, hence the occurrence of pockets or “rooms” of the Doyle blanket.

The most pronounced structural geology feature of the La Plata Mountains is the domal uplift of the sedimentary rocks. The uplift is quite considerable such that, for example, the base of the Dolores formation has been elevated in the center of the dome nearly 6,000 feet above its normal position (Eckel, 1949). The East Mancos is located along a structural hinge zone where the beds generally dip outward at angles of 25° to 60°. In places the rocks are sheared and brecciated along the hinge fold, and many of the ore-bearing vein fractures are concentrated within or near the hinge fold, which is exposed on the ridge between Spiller and Burwell Peaks in upper East Mancos (Eckel, 1949).

Glaciers played a role in the formation of the East Mancos River valley. Glacial ice filled the valley of the East Mancos River at least as far downstream as Gold Run (Atwood and Mather, 1932; Eckel, 1949). Valley floors are likely filled with combinations of glacial till, alluvium, and colluvium; however, little information is available regarding alluvium thicknesses in the East Mancos.

1.3 Objectives and Scope

The overall goal is to restore and protect water quality and aquatic habitat in the East Mancos River watershed. Dissolved copper and manganese have been identified as primary metals of

concern. Previous publications are contradictory with regard to the sources of aqueous metal concentrations, with some reports concluding that natural sources provide the dominant contributions, and regulatory references concluding that historical mines are the primary cause of high dissolved-metal concentrations in the East Mancos River.

This report represents a reconnaissance-level investigation, with an anticipation that further detailed studies will be pursued to decipher the complex hydrogeochemical setting in the East Mancos River. This report consists of four objectives:

(1) Characterize sources of metals in water (total and dissolved) from selected springs, streams, and draining mines.
(2) Characterize leachate from waste-rock piles in the East Mancos River.
(3) Compare water-quality results with toxicity thresholds for aquatic life.
(4) Mine site characterization and preliminary remedial alternatives (Colorado DRMS).

1.4 Methods of Investigation

As part of the East Mancos study, water-quality samples were collected from springs, streams, and mines and analyzed for major ions, total and dissolved metals, and dissolved organic carbon **(Table 1-1)**. Waste-rock soil samples were collected and analyzed for leachate potential using leachate extractions analyzed for dissolved metals. Water-quality and leachate samples for the East Mancos River Source study were analyzed by the laboratory at CDPHE-LSD in Denver, Colorado. CDPHE-LSD will provide sample bottles and coolers. Water-quality samples for dissolved organic carbon (DOC) and other parameters (silica, chloride, and fluoride) were analyzed by Green Analytical Laboratories (GAL) in Durango, Colorado, and GAL will provide sample bottles, transport coolers, and chain of custody forms for those samples.

Field data collection include measurement of the field water-quality parameters temperature, pH, specific conductance, and dissolved oxygen. Data collection include discharge measurements at each water-quality site, performed by flow anemometer (pygmy or AA), velocity sensor (e.g. Hach 950), portable flume, or volumetric method. Field laboratory data include analytical determinations for alkalinity, cupric copper (Cu^{2+}), and ferrous iron (Fe^{2+}).

Geographic coordinates of water-quality sampling sites were determined using the Global Positioning System (GPS) referenced to latitude and longitude (in decimal degrees) within the World Geodetic System of 1984 (WGS 84). Altitudes of sampling sites, in feet above mean sea level, were determined through a combination of topographic maps and GPS. Tools used to collect site coordinate data included the navigation software Gaia GPS™ operating on smart-phone platform, where multi-layered maps display the topography and aerial photography, and where site photographs can be acquired and stored.

1.4.1 Collection and Processing of Water-Quality Samples

Laboratory analytical determinations included major ions and trace metals. Concentrations of major ions and trace constituents were determined through a combination of inductively-coupled plasma optical emission spectroscopy (ICP-OES), flame atomic absorption spectrometry (Flame AA), ion chromatography (IC), and cold vapor atomic absorption spectrometry (cold vapor AA). Field analytical methods include analyses of ferrous iron by spectrophotometry, alkalinity (bicarbonate) by incremental titration, and cupric copper by ion-selective electrode **(Table 1-1)**.

Methods and reporting limits for water-quality field parameters are shown in **Table 1-2**. Field meters were calibrated in the morning on the day of water-quality sample collection. If the meters drifted because of ambient temperature or pressure changes, the meters were recalibrated. Measurement of pH values in water was done using double-junction electrodes to prevent dissolved-silver interferences in the silver/silver chloride electrode. If the waters were in the pH 4 to 7 range, the pH meters were calibrated to a pH 4 and 7 standards. If the waters were below pH 4, the pH meters were calibrated to pH 2 and 4 standards, and the pH probes were conditioned in pH 2 standard for at least 2 hours prior to measurement. If the waters were below pH 2, the pH meters were calibrated to pH 1.68 and 2 standards. Specific conductance (SC) meters were calibrated to two standards that bracket the range of SC expected in the field. SC probes were rinsed with deionized water between sites. Dissolved-oxygen (DO) meters were calibrated to the saturated DO of water according to tables presenting the DO at the ambient temperature and pressure of the site. DO meters also were checked against a zero-DO standard (sodium sulfite added to deionized water to saturation with sodium sulfate). If the waters were near zero DO (typical for deep ground-water-flow springs and collapsed mines), DO meters were checked using a zero DO standard. Water temperature were measured with a digital

thermometer and checked with other sensors (thermistors in the pH probe, SC probe, and DO probe). Quality control for field meters includes maintenance of field meter logbooks where calibration data were recorded. Probe conditions can be tracked by recording slope calculations after each calibration. Ferrous iron determinations by spectrophotometry were calibrated to stock Fe^{2+} standards. Cupric copper determinations by ion-selective electrode were calibrated against stock Cu^{2+} standards, and calibration regression equations were developed for determination of dissolved-copper concentration using the readout from a portable millivolt meter. Alkalinity (bicarbonate concentration) were determined by incremental titration of the sample to pH 4.0 using a 0.16N sulfuric-acid titrant, where the slope breakpoint is used for final determination of alkalinity.

To determine toxicity of dissolved copper in low-hardness waters, the Biotic Ligand Model (USEPA, 2007) utilizes dissolved organic carbon (DOC), dissolved major ions, copper concentration, pH, and alkalinity as input for calculation of toxicity thresholds. DOC samples were collected at sites along the mainstem East Mancos River where favorable fish habitat were indicated, and DOC were collected from selected springs and mines to determine sources of DOC.

Water-quality samples were processed using a peristaltic pump, positive-displacement sample pump, and(or) a 60-milliter syringe. From the width-integrated sample container, or directly from spring or mine, site water were passed through a 0.45 μm (micrometer) filter into sample bottles within a portable glove box, and samples were acidified and preserved within the glove box. Unfiltered samples were placed directly into the sample bottles. Ferrous iron were determined for selected groundwater sites, and samples were analyzed in the field or within 24 hours of collection using a Hach spectrophotometer (DR-2000 or DR-820). Field measurements and instrument calibrations were recorded on Water-Quality Field Forms **(Appendix 3)**. Streamflow discharge measurements were performed by wading the stream according to methods developed by the U.S. Geological Survey (Rantz, 1982). Selected discharge measurement field forms are shown in **Appendix 3**. Field meter calibrations, measurements, sample filtration, and sample preservation were done according to water-quality field methods developed by the USGS (Horowitz, 1994; Wilde, 2014).

Water-quality samples were collected along the lower reach of the East Mancos River to characterize toxicity thresholds for survival of aquatic life. Water from selected sites was analyzed for major ions, trace constituents, and DOC. Toxicity thresholds for survival of rainbow trout were described for dissolved aluminum, cadmium, cobalt, copper, nickel, lead, silver, and zinc using the Biotic Ligand Model (BLM) (USEPA, 2007). Toxicity thresholds for dissolved manganese and other metals were described using hardness-based water-quality standards (CDPHE, 2017).

Portable glove boxes were used to collect all field water-quality samples. Prior to going in the field, empty water-sample bottles for each site were pre-bagged in clear plastic bags that will include a disposable cartridge filter, powderless surgical gloves, absorbent chem wipes, and lengths of sample tubing. A portable PVC frame were used to support the plastic bag, which forms the glove box. Sample filtration and preservation will occur inside of the glove box, and the plastic bag were sealed after sample collection. Water-sample bottles were chilled to 4^{o}C following sample collection. Labels on each sample bottle will identify the site name, sample date, sample time, and sample type. Water samples were shipped to the laboratory in coolers that contain ice to maintain water sample temperatures at 4 to 6^{o}C. The coolers were shipped to the laboratory via express shipping, and chain-of-custody tags will indicate sample security. Equipment that were re-used at sites (for example, sieves, stream sampling equipment) were cleaned with a sequential cleaning procedure of liquinox, then a rinse with tap water, then a wash with 2 percent hydrochloric acid mixed in analyte-free water, then two final rinses with analyte-free water. Water sample bottles to be used for collection of dissolved metals in the field were washed with a 2 percent nitric acid solution in analyte-free water, then rinsed with analyte-free water. In some cases, pre-cleaned sample bottles can be purchased from supply vendors. Upon collection of the water sample in the field, the sample bottles were rinsed two times with the site water. Every sample had a unique barcode identification number, with a barcode printed on weatherproof address labels, and affixed to the exterior of each bottle set prior to a given sample trip. Barcodes associated with each sample were affixed to the chain of custody forms for shipping and delivery to the laboratory.

Quality-assurance samples were collected equaling approximately 10 percent of all samples collected during this investigation. This includes equipment blanks and replicate samples. The

equipment blank consists of running inorganic-blank, analyte-free water through the pump, disposable tubing, and filter unit. The blanks were acidified using nitric acid. Equipment blanks also were performed for DOC using organic-blank, analyte-free water.

1.4.2 Collection and Processing of Mine Waste Rock Leachate Samples

Historical waste-rock piles were sampled for potential to leach metals into the East Mancos River. Due to the mineralized terrain in upper East Mancos River, waste-rock analyses were compared with background soil analyses. Sites for testing of leachate potential are shown in **Figure 1-2**. Waste rock and soil samples were collected from a minimum of ten to thirty locations at each site. Acid-washed 100-mL plastic beakers or plastic spoons were used to collect the top two inches of material. Sub-samples were composited in a 1-gallon re-sealable plastic bag, thoroughly mixed by inverting the plastic bag several times. Waste rock and soil samples were screened through a 2 millimeter stainless steel sieve. For leachable metals, 150 mL of sample were placed in a 1-liter plastic beaker along with 150 mL of deionized water. Sample were mixed for 15 seconds using a magnetic stirrer and stir bar. Plastic wrap was placed over the beaker, and allowed to settle for 90 minutes. Aliquots of the raw and filtered samples were used for measuring pH, specific conductance, acidity, and cupric copper concentration. Samples were filtered using a 0.45 μm high-capacity filter into a 250 mL sample bottle and acidified to pH < 2 using concentrated nitric acid for analysis of dissolved metals **(Table 1-3)**. Acidity titrations were performed on aliquots immediately following leachate tests, and cupric copper determinations were made using an ion-selective electrode. From the acidity titrations, the acid-neutralizing requirement was calculated (in kilograms of calcium carbonate per 1000 liters of leachate) in order to treat or remediate the waste rock leachate. Waste-rock leachate field sample collection forms are shown in **Appendix 4**.

Dissolved metal mass loadings were estimated for snowmelt runoff from waste rock piles. Laboratory analyses of dissolved metal concentrations were multiplied by the annual precipitation snow-water equivalent (multiplied by 0.8 to account for snow sublimation and evaporation) and the waste rock pile surface area, over a 90-day snowmelt duration. Waste-rock leachate percolates through the ground to reach the stream during low flow; therefore, the waste-rock mass loadings were added to low-flow mass loadings in the stream.

Descriptions of selected mine sites in the East Mancos River watershed are presented in a separate report by the Colorado Division of Reclamation, Mining, and Safety (DRMS). In the report, mines are characterized and prioritized for dissolved copper in waste rock leachate and mine drainage. Maps and photographs are provided, and suggestions are presented for reclamation at each site.

1.4.3 Geochemical Modeling Methods

Results from geochemical models provide an understanding of the dissolved metal species present in water samples. While water-quality standards address concentration of a dissolved element (for example, copper, symbol Cu), there are many forms of dissolved copper such as copper carbonate ($CuCO_3$), copper hydroxide ($CuOH^+$), copper phosphate ($CuPO_4^-$), copper sulfate ($CuSO_4$), copper silicate ($CuSiO_2$), copper chloride (CuCl), and cupric or "free" copper (Cu^{+2}) (Stumm and Morgan, 1981). Copper readily complexes with organic carbon (Nordstrom and Munoz, 1994), and these metal-organic complexes affect aquatic toxicity (USEPA, 2007). Supersaturation of dissolved metal species occurs with just the right combination of dissolved metal cations and complexing anions to form solid precipitates on the stream bottom (for example, cupriferrite, symbol $CuFeO_3$). In order to describe the distribution of dissolved-metal species and solid phases, the Wateq4f and Phreeqc geochemical models were implemented, which are computer programs written by the U.S. Geological Survey describing multicomponent, multiphase equilibrium and geochemical processes (Parkhurst and Appelo, 1999; Ball and Nordstrom, 1991; Nordstrom and Munoz, 1994).

1.4.4 Source Characterization and Natural Background

Water-chemistry studies have been published by the U.S. Geological Survey regarding natural background dissolved constituents and historical mining in the Upper Animas Watershed, Colorado (Wright, 1995; Wright, 1997; Wright and Nordstrom, 1999; Yager and others, 2000; Church and others, 2007; Mast and others, 2007). These studies have shown a direct connection between aqueous metal concentrations in water from springs, streams, and mines, and the degree of geologic alteration. For example, water from springs and streams in weakly altered rocks can have water chemistry with neutral pH and low dissolved-metal concentrations, whereas water from springs and streams in highly altered rocks can have poor water chemistry with acidic pH

and high dissolved-metal concentrations (Mast and others, 2007). Water from some draining mines can have extremely high concentrations of dissolved metals, while water from other mines may have neutral pH and relatively low dissolved-metal concentrations.

Water-quality samples were collected at selected stream and spring sites throughout the East Mancos watershed during summer low flow in 2018 and high flow 2019. Sites and samples were assigned categories of natural background and mining impact as published by the U.S. Geological Survey in Mast and others (2007). Because historical mining disturbance is so extensive throughout the study area, determining whether a spring or stream has or has not been affected by mining is a challenge. Many of the water-quality sampling sites are obviously affected by historical mining activity, yet at other sites the extent to which mining activity has affected water quality is less certain. To address this issue, the USGS ranking system was utilized to evaluate the potential for the effects of mining on water quality **(Table 1-4)**. The ranking system consists of four categories (I–IV), ranging from category I, having no evidence of mining activity, to category IV, having direct discharges from inactive mine sites. If a site appeared unaffected, but not unequivocally, the site was ranked category II. Conversely, sites that were not directly affected but had upgradient mining activity that likely affected the water quality were ranked as category III. Numbers of sites and samples are relatively small for this East Mancos study; therefore, sites were grouped together as Category I-II representing natural background samples, and Category III-IV representing mining-impacted samples.

2. METAL CONCENTRATIONS, MASS LOADING, AND AQUEOUS GEOCHEMISTRY

2.1 East Mancos River Water-Quality Results, 2018-19

The East Mancos River watershed has a wide variety of physical, geologic, and hydrothermal alteration settings. The upper East Mancos, originating in Rush Basin surrounded by 13,000 ft peaks, is mostly comprised of high-altitude settings above tree line, with geologic mineralization related to combinations of hydrothermal veins and porphyry intrusive bodies. Rush Basin has a particularly unique geologic setting because of the effects of the copper-molybdenum porphyry

(Allard Stock) that was intruded into sedimentary rocks. The porphyry intrusive had unique effects on sedimentary rocks due to the "alteration halo" radiating outward from the intrusive body.

In the nearby upper Animas River, for example, the host rocks are volcanic lavas and welded tuffs, where the rock matrix may be comprised of silicate and titanium, and most of the mineralization occurs as vein-related sulfides. In the upper Animas, dissolved aluminum, copper, iron, and zinc in streams are the primary constituents of concern, and recent efforts have focused on toxicity of zinc and aluminum to aquatic life. In water from springs and streams in the upper Animas River basin, many of the chemical elements and metals tested in water samples are below the detection limits of the laboratory analysis.

In contrast, porphyry intrusive alteration in sedimentary environments of the upper East Mancos has provided a unique variety of dissolved minerals in water. In the upper East Mancos, high dissolved-metal concentrations and acidic pH are prevalent in water from streams, springs, and mines. Water-quality results indicate that almost every element and metal tested in water from the upper basin during this study showed positive results. Whereas the upper Animas needs to be concerned with toxicity of dissolved zinc and aluminum, the East Mancos needs to consider the combined effects of numerous metal constituents in water, including antimony, arsenic, cadmium, copper, iron, manganese, thallium, uranium, vanadium, and zinc.

The lower East Mancos drains a few high peaks (for example, Madden Peak at 11,972 ft), yet the lower slopes consist of dense forest, and geologic mineralization in the lower basin is limited to hydrothermal veins, with an absence of porphyry intrusives as compared with the upper basin. In the lower basin (while not studied in detail in this report), water from streams, springs, and mines has relatively low dissolved-metal concentrations and circumneutral pH values. Water-quality conditions of the upper basin are the focus of this report, with an emphasis on natural background conditions of the upper basin.

Many of the historical mines are located in highly mineralized and altered areas of the upper basin. Because of the combined effects of hydrothermal alteration and historical mines, to attribute low pH values and high trace-metal concentrations to either source is difficult. However, several historical mines clearly have high dissolved-metal concentrations in water

from draining adits. To a great extent, mineralized springs and diffuse groundwater inflows contribute the most to low pH and high trace-metal concentrations in upper East Mancos River Creek watershed.

As part of low-flow sampling during September 2018, which was a near-record drought year, water-quality samples were collected from 21 sites in the East Mancos River watershed. Springs and streams in the upper basin were documented and sampled, but very few of the mines showed any water drainage. As the sampling progressed downstream, it was apparent that the stream was a losing reach, where stream flows measured upstream were greater than stream flows measured in downstream reaches. Hence, surface water discharges were lost to infiltration into the groundwater system. The lost discharge may or may not return to the stream channel, depending on glacial valley fill, regional groundwater flow, faults, and fissure controls on groundwater movement. The 2018 drought provided a unique opportunity to witness the losing stream reach; otherwise, higher flows would mask the effects of lost discharge and would be more difficult to quantify.

During high-flow sampling of June-July 2019, water-quality samples were collected from 31 sites in the East Mancos River watershed. Many of the historical mines in the upper basin had water drainage, which provided the opportunity to collect water samples from draining mines that was missed during the drought of 2018. This indicates that groundwater flow through the high-altitude mines may have relatively short-lived travel paths from the top of Jackson Ridge to the adit; therefore, the upper mines probably dry up seasonally every year, especially during drought periods. If mine drainage is not manifested at the adit or portal, the effects of underground mines on deep groundwater metal concentrations and inflows to streams is difficult to document, and was not addressed as part of this report.

Water-quality results are presented in **Appendix 1**. Site descriptions, locations, dates of sample collection, field measurements, and laboratory results are shown in the Appendix. Mass loading calculations for each site also are shown in the Appendix. The discussion below emphasizes the low-flow water-quality data collected during September 2018.

2.1.1 Major Ions in Water

Water-quality data from the springs and streams sampled during low-flow of September 2018 are plotted on a trilinear diagram **(Figure 2-1)**. This diagram, referred to as a Piper diagram, shows the relations among concentrations of major cations (positively charged ions) and anions (negatively charged ions). The values are expressed as percentages of the total milliequivalents per liter of cations (lower left triangle) or of anions (lower right triangle) and are not shown as actual concentrations. The central quadrilinear graph shows the combined cationic and anionic chemical quality of the water by a third point, which is at the intersection of the rays projected from the points on the cation and anion plots. Major ions are present in water at milligrams per liter (parts per million) levels, whereas dissolved metals are usually present in water at micrograms per liter (parts per billion) levels. In the case with the upper East Mancos, dissolved metal concentrations are extremely high (in the milligrams per liter range), hence the Piper diagram does not reflect dissolved metals at major-ion levels in water from these sites.

During low-flow conditions of September 2018, water from source lake EM-WQ-01 and Middle Mancos River site EM-WQ-26 are described as a calcium-magnesium-bicarbonate type waters because these are the dominant major ions. Headwater sites in Rush Basin (02, 03, and 12) are described as calcium-magnesium-potassium-sodium-sulfate type waters; however, aluminum, copper, and iron (not reflected in the Piper diagram) are present in high concentrations in water from these sites. Headwater sites 02 and 03 have low calcium-magnesium concentrations, elevated dissolved zinc concentrations, and relatively high sodium and potassium (Na+K) due to acid dissolution of feldspars, also reflected by high silicate (SiO_2) concentrations. Signature of water from site 12 is dominated by the signature of water from sites 02 and 03. Water from Doyle Group (site 07), lies on the diagram as a calcium-magnesium-sulfate type water; however, with aluminum and copper concentrations, water from the Doyle Group during low-flow could be described as aluminum-calcium-copper-sulfate type water. Porphyry Spring site 09 and Burwell Tributary site 11 lie on the piper as a calcium-sulfate type water, but really represents a calcium-magnesium-aluminum-copper-manganese-sulfate type water, with elevated dissolved zinc. Site EM-WQ-19 located below the Thunder Mine, has characteristics similar to stream site EM-WQ-24, likely not reflecting drainage from the Thunder Mine area. From site 16 to 18 to 24, the stream water remains consistent as a calcium-sulfate type water, until site 25 where the

water acquires some bicarbonate to represent a calcium-magnesium-sulfate-bicarbonate type water.

2.1.2 Trace Metals in Water - Principal Components Analysis

Synoptic sampling results in a large number of water-chemistry samples. Classification of these samples into groups of similar chemical characteristics helps highlight their similarities and differences. Because water-rock reactions with altered and unaltered mineral assemblages may lead to particular chemical signatures among inflows to the stream, the classification can help to distinguish different sources and also to recognize geochemical processes. Patterns in the chemistry and pH of stream and inflow samples were evaluated by using Principal Components Analysis (PCA), a multivariate analysis technique (Daultrey, 1976; Grundy and Miesch, 1987). Principal components represent a set of new, transformed reference axes that are linear combinations of the original variables; it is a transformation of data, not a statistical treatment. A principal components transformation orients the data points so that the first of the new axes, principal component 1 (PC1), is oriented along the direction of the greatest variance in the data. The second principal component (PC2) is orthogonal to PC1 and is oriented to show the next greatest amount of variance in the data. This can be pictured in two dimensions if one imagines drawing a line that would go through the two most distant points in a bivariate plot of data; that would be the direction of PC1. It would be at some angle to the original x and y axes, but any point along the line could be described by a linear equation. PC2 would be drawn perpendicular to PC1 and would have its own linear equation. In multidimensional space, each subsequent principal component is orthogonal to the first two and represents a decreasing amount of the total variance. Typically, the first two or three principal components show enough of the variance in the data set to enable the recognition of groups among samples; this is the advantage of using the method for multivariate data. Water samples are plotted by their PCA scores, which are the coordinates of the original data points on the new principal component axes. Principal component loadings are interpreted as the coefficients of the linear combination of the initial variables from which the principal components are constructed. Adding loading vectors representing the correlations of original variables with the new principal component axes to the plot of scores creates what is called a biplot. The vectors help identify variations in chemistry among the groups of samples.

For East Mancos samples collected during low-flow conditions of September 2018, using logarithmic transformations of dissolved chemical concentrations, the PCA identified two distinct groupings related to mineralization **(Figure 2-2)**. The vectors showing iron (Fe), arsenic (As), and lead (Pb) likely relates to arsenopyrite mineralization. The vectors surrounding copper (Cu), cadmium (Cd), manganese (Mn), nickel (Ni), and selenium (Se) relate to porphyry mineralization **(Figure 2-2A)**. Therefore, values in the upper right of the biplot show sites with high concentrations of Cu, Cd, Mn, Ni, and Se, while in the lower right of the biplot show sites with high concentrations of Fe, As, and Pb. For example, in the lower right corner of the biplot, drainage from the Thunder Mine plots the furthest along the Fe axis, while the opposite end of the Fe axis shows site 24, which has low Fe concentration **(Figure 2-2B)**. Sites in the Burwell Trib (09, 10, and 11) plot in the area with high Cu, Cd, Mn, Ni, and Se **(Figure 2-2B)**. Sites 05, 22, and 25 plot in the area with low Cu, Cd, Mn, and Ni **(Figure 2-2B)**. Sites 02, 03, and 12 are a mix of high concentration Fe, but also containing high concentrations of Cu and Cd. Mixing of waters from upstream sources results in the East Mancos at Silver Falls (site 16) having a mixed signature of upstream sites **(Figure 2-2B)**. East Mancos River near mouth (site 25) has the lowest principal component loadings of all the dissolved metals **(Figure 2-2B).**

2.1.3 Distribution of Dissolved and Total Metals

Dissolved copper and manganese have been identified as constituents of concern for the East Mancos River. For brevity, many of the following maps and discussions will focus on these constituents. In the following text and graphics some site numbers might be abbreviated; for example, site EM-WQ-25 might also be referred to as EM-25, or site 25. The complete set of water-quality data, including low-flow and high-flow concentrations and loads, are shown in **Appendix 1** of this report. Water quality field notes for each site and water-quality sample are shown in **Appendix 3**.

2.1.3.1 Concentrations

During low-flow conditions of September 2018, dissolved copper concentrations in water from sites in the East Mancos ranged from < 2.2 to 22,100 µg/L (micrograms per liter), with a median value of 3,110 µg/L. Many of the high dissolved copper concentrations originate from sites in the Burwell Trib **(Figure 2-3)**. Dissolved manganese concentrations in water from sites in the

East Mancos ranged from 3.3 to 7,210 µg/L, with a median value of 1,560 µg/L. High dissolved manganese concentrations appeared to be present during low flow in water from many sites in the upper and middle East Mancos **(Figure 2-4)**.

During high-flow conditions of June-July 2019, dissolved copper concentrations in water from sites in the East Mancos ranged from < 5.5 to 20,400 µg/L, with a median value of 154 µg/L. Many of the high dissolved copper concentrations originate from sites in the upper East Mancos (Rush Basin and Burwell Trib), including drainage from mine sites that were dry during September 2018 **(Figure 2-5)**. Drainage from mine sites in the middle basin also had elevated dissolved copper concentrations. Dissolved manganese concentrations in water from sites in the East Mancos ranged from < 1 to 2,480 µg/L, with a median value of 95.4 µg/L. The highest dissolved manganese concentrations appear to have originated from the Burwell Trib **(Figure 2-6)**; however, elevated dissolved manganese concentrations also were present in drainage from mine sites in the middle basin **(Figure 2-6)**.

2.1.3.2 Loads

During low-flow conditions of September 2018, dissolved copper loads in water from sites in the East Mancos ranged from 0.01 to 8.42 pounds per day (lb/d), with a median value of 1.2 lb/d. Many of the high dissolved copper loads originate from sites in the Burwell Trib **(Figure 2-7)**. Dissolved manganese loads during low flow in water from sites in the East Mancos ranged from 0.01 to 4.3 lb/d, with a median value of 0.2 lb/d. Most of the elevated dissolved manganese loads appeared to have originated in the upper basin **(Figure 2-8)**.

During high-flow conditions of June-July 2019, dissolved copper loads in water from sites in the East Mancos ranged from 0.0 to 110.8 lb/d, with a median value of 3.4 lb/d. Sources of elevated dissolved copper loads were unclear, but appeared to have originated mainly from the Burwell Trib **(Figure 2-9)**. Dissolved copper loads appeared to increase between mainstem sites 12 and 16, and between mainstem sites 16 and 18, yet the causes or sources are uncertain. Dissolved manganese loads during high flow in water from sites in the East Mancos ranged from 0.01 to 36.8 lb/d, with a median value of 1.63 lb/d. The highest dissolved manganese concentrations appear to have originated from the Burwell Trib **(Figure 2-10)**. As with dissolved copper loads,

dissolved manganese loads appeared to increase between mainstem sites 12 and 16, and between sites 16 and 18, yet the causes or sources are uncertain.

2.1.4 Stream Profiles of Concentrations and Loads

Longitudinal profile of streamflow discharge during low-flow conditions (drought) of September 2018 shows decreases in streamflow, illustrating the "losing stream reach" as discussed above. Longitudinal concentration profiles along the length of mainstem East Mancos show increasing and decreasing concentrations of dissolved and total metals **(Figures 2-11A, B, C)**. Longitudinal profiles of dissolved and total metals shows that most of the high concentrations during low flow originate from the upper basin (Rush Basin and Burwell Trib). Buffering constituents such as calcium and magnesium increase in a downstream direction as the stream leaves the areas altered by the Allard Stock **(Figures 2-11A, B, and C)**, along with increasing barium and strontium concentrations consistent with weathering of sedimentary rocks. Dissolved and total lead are variable along the mainstem, increasing in the middle part of the basin possibly due to vein mineralization in the middle basin **(Figure 2-11B)**. Decreasing metal concentrations in a downstream direction are likely caused not only by dilution, but also due to mineral complexation, supersaturation, and precipitation. Due to geologic alteration, rocks in the upper basin are acidic and devoid of buffering minerals such a calcium and magnesium. As the stream exits geologically altered areas and flows through unaltered sedimentary rocks, the pH of water increases and metals are removed from the dissolved phase through chemical reactions.

Focusing on copper and manganese **(Figure 2-12)**, longitudinal stream profiles of dissolved and total mass loadings during low- and high-flow conditions show increasing and decreasing loads through the East Mancos River mainstem. During low-flow conditions of September 2018, dissolved and total copper and manganese loads increased through the upper basin **(Figures 2-12A and 2-12B)** as the stream has incised canyons through geologically altered rocks, and mining-impacted waters possibly enter the stream diffusely from the Jackson Ridge area (although there were no draining mines documented along Jackson Ridge during low flow 2018). During low flow, dissolved and total copper and manganese decrease through the middle East Mancos due to chemical reactions and metal attenuation **(Figures 2-12A and 2-12B)**; loads increase slightly towards the end of the middle reach; and metal loads are almost removed by the end of the lower reaches (mouth of the watershed) **(Figures 2-12A and 2-12B)**. During high-

flow conditions of June-July 2019, there were significant increases in discharge and mass loadings between sites EM-12 and EM-16 **(Figures 2-12C and 2-12D)**. [This is the stream reach past Gibbs Peak, where there is known geologic alteration and mineralization due to porphyry intrusions **(Figure 1-6)**. More information are needed for this reach of the East Mancos during low- and high-flow conditions.] During high flow, dissolved copper loads were significantly attenuated in the lower reaches; however, total copper loads were less affected by attenuation **(Figures 2-12C and 2-12D)**. Dissolved and total manganese were not significantly attenuated in the lower reaches **(Figures 2-12C and 2-12D)**.

2.1.5 Effects of Snowmelt Runoff on Water Quality

During March-July 2019, at the East Mancos River near mouth (site EM-WQ-25), plans were to sample and measure discharge on a weekly basis (late March through June) in order to capture the spring snowmelt runoff hydrograph. After an early start to weekly sampling on March 20, 2019, the weather shifted to cooler temperatures and increased precipitation during May, and weekly sampling was curtailed. Runoff sampling resumed during June and July, resulting in 10 samples collected at EM-WQ-25 to represent the snowmelt runoff hydrograph.

For the Mancos River near Mancos, Colorado (site MANMANCO, collected by the Colorado Division of Water Resources), the snowmelt runoff hydrograph for the Mancos River basin shows the rising limb during March-June (increasing discharges due to snowmelt), and the falling limb (decreasing discharges after snowmelt) **(Figure 2-13A)**. At site EM-WQ-25, streamflow discharges were measured concurrently with collection of water-quality samples during the snowmelt runoff period. Streamflow discharges for the Mancos River were correlated with discharges for the East Mancos River **(Figure 2-13B)**. Using the regression correlation equation, discharges for the East Mancos River were modeled (estimated), showing the approximate snowmelt runoff hydrograph for the East Mancos, with the hydrograph peak occurring on June 14, 2019 **(Figure 2-13C)**. This provides an idea of snowmelt discharges to be expected in the East Mancos watershed; however, there are only seven data points in the correlation, and likely some error in the modeled East Mancos discharges. Dots on the hydrograph indicate when samples were collected at site EM-WQ-25.

From water-quality samples and discharge measurements collected at EM-WQ-25 during March-July 2019, increasing discharges were shown during March-May, with sampling of the discharge peak occurring on June 12 (**Figure 2-14**, top three graphs). Time series showing metal mass loadings indicates that the loads for many constituents peaked before the streamflow peak **(Figure 2-14)**. Other constituent loads such as dissolved copper and dissolved zinc peaked with the discharge peak, and continued to increase after the peak **(Figure 2-14)**. During fall and winter low flow periods, metal solids accumulated on the streambed throughout the upper and middle reaches due to mineral supersaturation. Then during runoff, these metal solids were flushed from the streambed **(Figure 2-15)**, causing increased total metal loads at the mouth of the watershed. Given that water-quality synoptic sampling of many alpine watersheds in Colorado usually occurs after snowmelt (June-July), and therefore the high country can be accessed, these data from the East Mancos show that maximum dissolved and total metal concentrations and loads occurred before the streamflow peak. Therefore, the typical high-flow synoptic events by agencies and stakeholders have been conducted too late to capture the worst water-quality conditions from these geologically altered terrains. Seasonally variable processes of metal weathering, deposition, mobilization, and transport in the East Mancos River watershed are not fully understood, partly due to access problems, including poor roads, inclement weather, downed trees, rock slides, and avalanches.

2.1.6 Aqueous Geochemistry and Mineral Species Distribution

Aqueous mineral species, which are represented in the water-quality sample, can describe the source rocks and minerals that result from chemical weathering. Aqueous mineral speciation represents compounds that are dissolved in the water samples under certain water-chemistry conditions, and yet under different water-chemistry conditions, clay particles or colloids can precipitate from stream water onto the streambed, and colloids can be transported downstream for many miles. The colors of precipitates reflect the chemical composition of the water: Red and orange indicate presence of iron in the water; black and dark brown indicates manganese; blue-green, aqua-blue, and rust-brown indicates copper; yellow precipitates indicate sulfur and sulfates; and white precipitates represent aluminum (likely as aluminum sulfate). Plotting East Mancos data points on the stability field diagram for copper and iron compounds shows that the cupric ferrite in water from some sites was present in the dissolved phase **(Figure 2-16)**. As the

stream flows from altered geologic settings into sedimentary rocks, pH of water increases due to neutral inflows, and the cupric ferrite transitions from dissolved to solid phase minerals, which are then precipitated on the streambed. This is confirmed by the voluminous amounts of red-brown-orange precipitates that were present during low flow of 2018 in the upper and middle parts of the watershed **(Figure 2-17A and 2-17B)**. These precipitates are known to occur in geologically mineralized watersheds (for example, Cement Creek in the upper Animas River basin); however, with high concentrations of copper in waters of the East Mancos, these precipitates can have a copper-rust color, and dried copper precipitates on bank rocks can display a multi-colored rainbow-like patina.

Water-chemistry data from low-flow samples (Sept. 2018) in the East Mancos were input to the geochemical model Phreeqc (Parkhurst and Appelo, 1999). The activity (or concentration) of dominant mineral species were identified, and the saturation index (SI) of the mineral species indicated whether the mineral was dissolving or precipitating (negative SI--dissolving; positive SI--precipitating). The predominant mineral species with high activity identified in streams of the East Mancos included the minerals cupric ferrite ($CuFe_2O_4$) and manganese oxide (Mn_3O_4). Longitudinal profiles of Phreeqc results show elevated cupric ferrite activity from the headwaters to the mouth of East Mancos **(Figure 2-18A)**. Longitudinal stream profiles of saturation index shows that cupric ferrite was supersaturated from the headwaters to the mouth of the stream **(Figure 2-18B)**. Other copper mineral species identified in the geochemical model with high activity values included cuprite (Cu_2O), cuprous ferrite ($CuFeO_2$), chrysocolla ($CuSiH_4O_5$), and copper chromate ($CuCr_2O_4$).

Longitudinal stream profile of Phreeqc results show high activities for manganese oxide (MnO_3) from the headwaters to the mouth of the East Mancos **(Figure 2-18C)**. Other manganese species were identified such as manganese hydroxide ($MnOH_2$), manganese dioxide (MnO_2), rhodonite ($MnSiO_3$), and rhodocrosite ($MnCO_3$). In contrast to the above copper example, longitudinal profile of manganese oxide shows undersaturation of the mineral **(Figure 2-18D)**; therefore, manganese would more easily remain in the dissolved phase.

2.1.7 Non-Conservative Constituent Behavior

In theory, mineral precipitation should decrease dissolved metal concentrations with removal of the metal ions from water. In stream systems, this frequently happens with mixing of different pH waters, and is called non-conservative constituent behavior. For example, non-conservative metals (such as copper and iron) should not be used as tracers to track the transport of metal molecules in a downstream fashion because copper and iron readily precipitate from water. Other examples of non-conservative dissolved constituents include aluminum, arsenic, selenium, and sulfur. In contrast, conservative constituents include dissolved major ions and trace metals that persistently remain dissolved in water, being so soluble that these conservative elements are minimally subject to chemical or biological activity in water (Stumm and Morgan, 1981). Examples of dissolved conservative constituents include sodium and chloride (NaCl, or table salt). In addition to supersaturation of mineral species, dissolved metals can adsorb to and co-precipitate with other metals such as iron and manganese. Formation of colloids in water is known to be a microbial process, and the resulting flocculants can have high surface areas where trace metals are readily adsorbed. Algae and biological films accumulative on the streambed also can uptake and sequester dissolved-constituent concentrations.

Phreeqc modeling results show supersaturation and precipitation of several iron clay mineral species, including potassium nontronite ($KFeAlSiO_2$) and jarosite ($KFeSO_4$). Using the Phreeqc model, mineral mass precipitation was calculated between stream sites (from upstream to downstream), and the resulting precipitated mass was multiplied by streamflow discharge to obtain the weight of mineral precipitated between stream sites. Results indicate that during low-flow conditions of September 2018, cupric ferrite, nontronite, and jarosite precipitation occurred throughout the length of the East Mancos River. Up to 18 tons per day (tons/d) of cupric ferrite, 6.5 tons/d of nontronite, and 58 tons/d of jarosite were precipitated between stream sites **(Figure 2-19)**. Deposition of the minerals during low flow was confirmed by field observations **(Figure 2-17)**, and during snowmelt runoff these mineral solids were scoured from the streambed and transported out of the watershed **(Figure 2-15)**.

2.1.8 Natural Background Characterization

Water-quality samples were collected at selected stream and spring sites throughout the watershed during summer low flow September 2018 and high flow June-July 2019. Because historical mining disturbance is so extensive throughout the study area, determining whether a spring or stream has or has not been affected by mining is a challenge. Many of the water-quality sampling sites are obviously affected by historical mining activity, yet at other sites the extent to which mining activity has affected water quality is unclear. To address this issue, the USGS ranking system was utilized (Mast and others, 2007) to evaluate the potential for the effects of mining on water quality **(Table 2-1)**. The ranking system consists of four categories (I–IV), ranging from category I, having no evidence of mining activity, to category IV, having direct discharges from inactive mine sites.

Statistical summaries of selected dissolved constituent concentrations for background streams and springs (Category I and II sites) are compared with mining affected sites (Category III-IV) in **Table 2-2**. During low flow September 2018, the Category I-II sites had a wide variation in chemical composition; pH ranged from 3.43 to 8.51, and specific conductance ranged from 62 to 1,528 µs/cm (microsiemens per centimeter). Sulfate concentrations ranged from 7.3 to 1,640 mg/L, dissolved copper concentrations ranged from 1.0 to 12,200 µg/L, and dissolved manganese concentrations ranged from 4.5 to 5,580 µg/L. Sites with high pH values (pH>5.4) typically had measurable concentrations of alkalinity and lower aluminum, copper, and iron concentrations, whereas sites with low pH values (pH<5.4) had little measurable alkalinity and elevated concentrations of aluminum, copper, and iron. Category III-IV sites during low flow showed a wide variation in chemistry, with pH ranging from 2.74 to 6.55, and specific conductance ranging from 98.4 to 1,605 µs/cm. Sulfate ranged from 11.9 to 690 mg/L, and dissolved copper concentrations ranged from 6.6 to 23,600 µg/L. This highest dissolved copper concentration was in water from the Burwell Trib, which was likely affected by elevated natural-background and mining-affected copper concentrations; for example, water from a Category I spring in the Burwell Trib (EM-WQ-09) had a dissolved copper concentration of 11,700 µg/L.

During high flow of June-July 2019, the Category I-II sites had a wide range of chemical compositions, where pH values of background sites ranged from 4.11 to 8.71, and specific

conductance values ranged from 7 to 229 µs/cm. Sulfate ranged from 1.2 to 134 mg/L, dissolved copper concentrations ranged from 69.1 to 9,690 µg/L, and dissolved manganese concentrations ranged from 1.0 to 2,180 µg/L. Category III-IV sites during high flow also had a wide variation of water chemistry, where pH values ranged from 2.63 to 7.04, and specific conductance values ranged from 21.7 to 1,832 µs/cm. Sulfate concentrations ranged from 3.56 to 473 mg/L, dissolved copper concentrations ranged from 9.2 to 20,400 µg/L, and dissolved manganese concentrations ranged from 1.4 to 2,480 µg/L.

Statistical summaries of selected dissolved constituents in **Table 2-2** show similar chemical characteristics when comparing background sites (Category I-II) and mining-affected sites (Category III-IV). Boxplots of selected constituents similarly show little differences between Category I-II and Category III-IV concentrations of selected dissolved and total metals **(Figure 2-20)**. From these data, it would be challenging to conclude which category of site contributes the highest concentrations of dissolved constituents to the East Mancos watershed.

2.2 Mine Waste Rock Leachate Results

As part of this report, more than 65 historical mine sites were documented in the East Mancos River watershed **(Figure 1-2)**. Given the short project time frame, many of the mine sites were not visited or sampled, and some were located using topographic maps or visual observance in the field. From 32 of these mine sites (most of them in the upper basin), in addition to three background sites, soil/waste-rock samples were collected from waste rock and mill tailing sites, and laboratory leachate potential tests were performed on sieved samples **(Table 2-3)**. Results indicate that pH values of leachate ranged from 2.10 to 7.03, with a median value of 4.22. Specific conductance values ranged from 14 to 5,230 µs/cm, with a median of 84.0 µs/cm. From titrations, acidity values ranged from 10.0 to 6,080 mg/L as $CaCO_3$, with a median of 20.0 mg/L as $CaCO_3$. Acid neutralizing requirements for leachate stabilization ranged from 0.01 to 12.4 kg $CaCO_3$/1000 L, with a median value of 0.13 kg $CaCO_3$/1000 L. Cupric copper concentrations in leachate water ranged from 79.5 µg/L to 1,032,720 µg/L. The lowest pH values, highest specific conductance values, and highest acidity values occurred in leachate water from waste rock piles at the Doyle Group (2, 3, 6, 8) and the Thunder Mine. Results from mine sites in the lower basin (Gold Dollar, Kentucky, Red Arrow) were different than most sites in the upper basin, with pH

values ranging from 4.91 to 6.81, and a median value of 5.73; specific conductance values ranged from 37.0 to 541 μs/cm, with a median of 87.5 μs/cm; acidity titrations were less than the detection limit of 1.0 mg/L as $CaCO_3$; and one site had cupric copper concentration of 79.5 μg/L. The differences between high waste rock leachate potential in the upper basin as compared to low waste rock leachate potential in the lower basin reflects the differences in geology, mineralization, and porphyry alteration in the upper reaches of the East Mancos watershed. Laboratory analytical results for waste rock leachate samples are shown in **Appendix 2**. Waste rock field data collection sheets showing site sketches and locations are shown in **Appendix 4**. Waste rock leachate laboratory testing sheets are shown in **Appendix 5**.

2.2.1 Leachate Concentrations

Waste-rock leachate samples were filtered and sent to the laboratory for dissolved metal analyses. Concentrations of dissolved metals in water from leachate samples were extremely high in some samples.

- Dissolved aluminum ranged from 27.3 to 65,500 μg/L, with a median value of 144.0 μg/L.
- Antimony ranged from 7.60 to 3,380 μg/L, with a median of 224.0 μg/L.
- Arsenic ranged from 0.03 to 9,290 μg/L, with a median of 0.3 μg/L.
- Cadmium ranged from 0.01 to 382 μg/L, with a median of 0.2 μg/L.
- Copper ranged from 2.6 to 3,870 μg/L, with a median of 48.7 μg/L.
- Iron ranged from 2.6 to 3,870 μg/L, with a median of 49.5 μg/L.
- Lead ranged from 0.04 to 133.0 μg/L, with a median of 0.9 μg/L.
- Manganese ranged from 2.0 to 23,600 μg/L, with a median of 133.0 μg/L.
- Silver ranged from 0.04 to 0.79 μg/L, with a median of 0.08 μg/L.
- Zinc ranged from 5.8 to 1,060 μg/L, with a median of 33.60 μg/L.

The highest concentrations of dissolved copper occurred in water from leachate testing of waste rock from the Thunder Mine and site WR-1 in the headwaters of the Burwell Trib. Waste rock leachate samples from the Doyle Group also had high dissolved copper concentrations. The highest concentrations of dissolved manganese occurred in water from leachate testing of waste rock from the Red Arrow Gold Run Mine and Red Arrow Tailings.

2.2.2 Estimated Waste-Rock Loads

Dissolved metal mass loadings were estimated for snowmelt runoff from waste rock piles. Laboratory analyses of dissolved metal concentrations were multiplied by the waste rock pile surface area and the annual precipitation snow-water equivalent over a 90-day snowmelt duration (multiplied by 0.8 to account for snow sublimation and evaporation). Snowmelt waste rock runoff discharge ranged from 0.0004 to 0.0336 ft^3/sec, with a median value of 0.0027 ft^3/sec, and total summed discharge of 0.136 ft^3/sec. Given that copper and manganese are the primary constituents of concern, dissolved mass loading estimates are described below.

- Dissolved copper mass loading ranged from 0.0001 to 0.067 lb/d, with a median value of 0.0009 lb/d, with total summed load of 0.246 lb/d.
- Dissolved manganese mass loading ranged from 0.00001 to 0.259 lb/d, with a median of 0.0019 lb/d, and total summed load of 0.736 lb/d.

Waste-rock leachate likely percolates through the ground to reach the stream during low flow. Considering dissolved manganese to be more conservative than copper, during low flow of 2018, dissolved manganese waste-rock loads comprised 17 percent of the manganese load at site EM-WQ-16, and about 3 percent during high flow. These mass loading estimates do not include the dissolution and mobilization of metals during overland flow of summer rainfall runoff. In addition, the underground workings of mines can serve as conduits for capture and deep percolation of contaminated groundwater. Exposure of fresh mineral surfaces in mines to water and oxygen dramatically increases dissolved metal concentrations in water. Estimates of the effects of underground mines on metals concentrations in groundwater were beyond the scope of this report.

3. TMDL REQUIREMENTS AND MASS LOADING SUMMARY

Regulations for water-quality planning and management (40 CFR Part 130) establishes the program and policies that implement the Clean Water Act section 303(d) requirements (USEPA, 1991). Within the regulations, Section 130.7 describes the Total Maximum Daily Load (TMDL) process and the State's responsibility for identifying waters requiring TMDL's, setting priorities and developing TMDL's, submitting the waters identified with priority rankings and the TMDL's to USEPA for approval, and the incorporation of the TMDL's into the State's Water Quality Management Plan.

To implement the program, the regulation establishes the following definitions for loading capacity, load allocation, waste load allocation, total maximum daily load, water quality-limited segments and water quality limited segments still requiring TMDL's (USEPA, 1991).

[*Italics* added, this report]

Loading capacity (LC) - The greatest amount of loading that a water can receive without violating water quality standards. (40 CFR 1302(f))

Load allocation (LA) - The portion of a receiving water's loading capacity that is attributed either to one of its existing or future nonpoint sources of pollution or to *natural background sources*. Load allocations are best estimates of the loading, which may range from reasonably accurate estimates to gross allotments, depending on the availability of data and appropriate techniques for predicting the loading. Wherever possible, *natural and nonpoint source loads should be distinguished*. (40 CFR 130.2(g))

Waste load allocation (WLA) - The portion of a receiving water's loading capacity that is allocated to one of its existing or future point sources of pollution. WLAs constitute a type of water quality-based effluent limitation. (40 CFR 1302(h))

Total maximum daily load (TMDL) - The sum of the individual WLAs for point sources and LAs for *nonpoint sources and natural background*. If a receiving water has only one point source discharge, the TMDL is the sum of that point source WLA plus the LA for any nonpoint sources of pollution and natural background sources, tributaries, or adjacent segments. (40 CFR 1302(i))

Margin of Safety (MOS) - A required component of the TMDL that accounts for the uncertainty about the relationship between the pollutant loads and the quality of the receiving waterbody (CWA section 303(d)(l)(C)). The MOS is normally incorporated into the conservative assumptions used to develop TMDL's (generally within the calculations or models). If the MOS needs to be larger than that which is allowed through the conservative assumptions, additional MOS can be added as a separate component of the TMDL

A TMDL is comprised of the Load Allocation (LA), which is that portion of the pollutant load attributed to *natural background or the nonpoint sources*, the Waste Load Allocation (WLA), which is that portion of the pollutant load associated with point source discharges, and a Margin of Safety (MOS) (Eqn. 1).

$$TMDL = LC = WLA + LA + MOS \quad \text{Eqn. (1)}$$

In the East Mancos River watershed during September 2018, near-record drought conditions persisted during the low-flow sampling events. Few of the historical mines exhibited any mine drainage or water features (water from only five mine sites was measured and sampled). While there were probably mining-related metal concentrations entering the stream through diffuse groundwater flow paths, these inflows were not easily distinguishable from natural background sources. Loss of concentrations and dissolved metal loads (non-conservative behavior) were documented; in addition, streamflow losses were documented. Therefore, identification and calculation of WLA was particularly challenging.

Identification of natural background mass loadings (LA in Eqn. 1) also turned out to be challenging. As part of this report, many stream reaches were hiked, climbed, and waded to conduct a reconnaissance of springs, mines, and tributaries in the East Mancos River. Many of the stream reaches were impossible to negotiate, not only due to steep canyons and waterfalls, but frequently due to trees (logjams) blocking the channel, where logjams were sometimes caused by avalanche debris, and sometimes caused by erosion and runoff from logging, placer mining, roads, and grazing, which result in severe stream channel blockage and bed sediment aggradation. Hence, only a small fraction of the springs and inflows to the East Mancos River were documented. The quantification of natural background sources through Load Allocation (LA) would, therefore, require further detailed investigation.

Given the challenges quantifying the different WLA and LA sources, instream mass loadings of dissolved metals were compared to the measurable mining-affected (Category III-IV sites) mass loadings for low-flow and high-flow conditions **(Table 3-1)**. Results indicate that during low flow, dissolved and total metal loadings in the East Mancos River were much greater than the measurable mass loadings from Category III-IV sites **(Table 3-1)**. Considering dissolved manganese to be more conservative than dissolved copper, during low flow of September 2018,

summation of Category III-IV loads and waste-rock leachate loads comprised about 17 percent of the dissolved manganese loads at site EM-WQ-16, and about 40 percent of the dissolved manganese load at site EM-WQ-24. During high flow of June-July 2019, summation of Category III-IV loads and waste-rock leachate loads comprised about 3 percent of the dissolved manganese loads at site EM-WQ-16, and about 4 percent of the dissolved manganese load at site EM-WQ-24. These estimates do not account for Category III-IV inflows from diffuse groundwater flow paths and weathering of instream mill tailing deposits. Quantification of diffuse inflows and distinction of dissolved metal sources could be accomplished using stream tracer-injection tests (Kimball and others, 2007) or isotopic fingerprinting of sulfate sources (Nordstrom and others, 2007).

The Total Maximum Daily Load (TMDL) approach assumes that constituents of concern behave conservatively in water, that the sources of dissolved constituents of concern can be identified, and source loads in a watershed can be summed in a balance sheet. In the East Mancos River, however, non-conservative behavior of dissolved constituents has been identified through sampling, observations, and geochemical modeling. In addition, the East Mancos River is a losing stream reach (further documentation is needed); therefore, dissolved constituent concentrations and loads are being removed from the stream system due to the lost streamflow discharge and associated loads. In the East Mancos River watershed, therefore, the TMDL theory of conservative constituent behavior has been violated by numerous conditions, and really should not be applied here, especially for dissolved copper. If remedial measures were to be implemented, then measurement and quantification of water-quality improvements would be difficult to document due to non-conservative constituent behavior. In contrast, the use of more conservative constituents in water—such as dissolved barium, cadmium, sulfate, uranium, or vanadium—might yield better results to distinguish mass loadings from different sources.

4. EAST MANCOS FISHERY, WATER-QUALITY STANDARDS, AND AQUATIC TOXICITY

4.1 Status of the East Mancos River Fishery

Over the past several decades, surveys by various agencies have documented fishery conditions in the East Mancos River. In 1960 and ’66, Colorado Department of Wildlife (CDOW) stocked

native cutthroat trout fingerlings in the East Mancos River. The U.S. Forest Service (USFS) documented a small trout population in 1969 near White Rocks (Horn, 2010; B.U.G.S. Consulting, 2009). Subsequent CDOW fish stocking of rainbow and brook trout fry occurred in the East, West, and Middle Mancos reaches in 1971, '72, '75, '77, '78, '83, and '87. Records from surveys conducted in 1977 indicate that the fishery in the lower East Mancos River, below the confluence with the Middle Mancos, comprised of rainbow trout, mottled sculpin, and speckled dace, with rainbow trout making up the majority of biomass (Horn, 2010). In stark contrast to these observations of a fishery in the lower East Mancos River that receives higher water quality from the Middle Mancos, CDOW reported that further upstream in the East Mancos, there were no fish in 1975 and '77. In 1986, a breach of the then obstructed Gold Dollar Mine discharged metal-laden water into the East Mancos River and there were anecdotal reports of substantial fish kills (Horn, 2010; B.U.G.S. Consulting, 2009). Two years after the Gold Dollar Mine event, the USFS documented that habitat conditions near White Rocks (downstream of the Gold Dollar Mine) were unsuitable for fish survival. In 1990, CDOW reported an absence of fish in the East Mancos River (B.U.G.S. Consulting, 2009). More recent fish sampling and stocking efforts in 2003 and 2009 occurred downstream on the mainstem Mancos River, with no fish sampling records on the East Mancos River since 1990 (Horn, 2010).

4.2 Aquatic Toxicity of the East Mancos River, This Study 2018-19

The suitability of water quality conditions for aquatic life were evaluated in the East Mancos River, Middle Mancos River, and East Mancos tributaries by assessing observed metal concentrations in context of estimated toxicity thresholds. To assess potential toxicity of copper, the Biotic Ligand Model (BLM) was used (USEPA, 2007), which incorporates dissolved organic carbon (DOC) and major ion concentrations, pH and alkalinity of water to derive acute and chronic toxicity estimates for dissolved copper. Similarly, to assess potential toxicity of aluminum, the EPA water quality criteria for aluminum (for samples with parameters within model assumptions), which incorporates DOC, hardness, and pH to derive acute and chronic toxicity estimates for aluminum (USEPA, 2018). For other metals, water-quality concentrations were compared with toxicity-based water quality standards developed by Colorado Department of Public Health and Environment (CDPHE) for the protection of aquatic life from acute (brief, short-term) and chronic (persistent, long-term) exposure to metals in surface water. Several

CDPHE water-quality standards incorporate water hardness. Due to the impairment status of the East Mancos for copper and manganese, for this report toxicity assessment focused on those analytes. In **Table 4.1**, observed metal concentrations are compared with water-quality standards and estimates of toxicity for each site, expressed as a hazard quotient (HQ). HQ's were calculated as the ratio of measured exposure (i.e., observed metal concentration) to water-quality standards or toxicity estimates. HQ values equal to or greater than one indicate a potential for ecological risk and HQ values below one indicate a low probability of ecological risk. For the purpose of broadly comparing potential toxicity of multiple metals among sites, an aggregate measure of HQs is presented as a Cumulative Criteria Unit (CCU), defined as the sum of HQs for each site (Clements, 2000) **(see Figures 4-9 to 4-12 and Table 4-1)**.

Results from toxicity assessment indicate that water quality conditions in much of the East Mancos are not suitable for aquatic life, and have a high toxicity risk during high-flow and low-flow periods **(see Figures 4-1 through 4-12)**. Multiple metals had concentrations above toxicity thresholds including aluminum, cadmium, copper, iron, manganese, mercury, nickel, selenium, silver, and zinc. HQ's indicated substantial toxicity in the upper watershed with the highest HQs occurring in the Burwell Tributary where the concentration of copper during high flow was more than 400,000 times greater than the BLM chronic toxicity threshold. Hazard Quotients and the number of metals occurring at potential toxic levels were far lower in the downstream reaches of the East Mancos. In the lowermost reaches (sites 24, 25, and 27), the only metals that occurred at potential toxic levels were aluminum, cadmium, and copper. During high-flow conditions, potential acute toxicity of copper and chronic toxicity of aluminum and copper extended throughout the East Mancos all the way downstream to the mouth of the East Mancos at site 27. During low-flow conditions, potential acute toxicity of copper and chronic toxicity of aluminum, copper, and cadmium extended downstream to site 24. At site 25 during low flow, there was potential for chronic copper toxicity, but no metals surpassed acute toxicity thresholds. In addition to samples collected in low-flow and high-flow conditions, multiple samples were collected at site 25 from March-July of 2019. These samples allow for a higher temporal understanding of seasonal toxicity at this location. The highest potential for aluminum toxicity occurred on 6/3/19 while the highest potential for copper toxicity occurred on 7/3/19 **(Table 4-1)**. Downstream site 27 (East Mancos at CR44) was dry during low flow 2018; therefore we were unable to assess metal toxicity. The lack of persistent flow through the furthest

downstream reach of the East Mancos during low flow periods clearly eliminates opportunities for aquatic life occurrence.

Elevated copper concentrations occurred throughout the entire East Mancos at levels indicative of aquatic life toxicity. However, the toxicity of manganese, which in addition to copper is listed as an impairment for the East Mancos, was not as high as copper throughout the East Mancos. During high-flow conditions, concentrations of manganese were below acute and chronic toxicity thresholds at all sampling locations. During low-flow conditions, concentrations of manganese surpassed acute and chronic toxicity thresholds in headwater reaches, with HQ's greater than one only occurring upstream of the Thunder Mine and site EM-WQ-18.

Metal concentrations during high flow and low flow in the Middle Mancos River were not high enough to surpass toxicity thresholds.

Potential toxicity in the East Mancos River decreased from site EM-WQ-23 (below Red Arrow Mine) to site 24 (USFS boundary) and to site 25 (above Middle Mancos), especially during low-flow conditions **(Figure 4-13)**. For example, potential acute toxicity of copper during high flow was more 49,000 times greater than the toxicity threshold at site 23, but only 185 times greater than the toxicity threshold at site 24. Further downstream at site 25, the concentration of copper during high flow was below the acute toxicity threshold. A greater spatial frequency of sampling locations between site 23 and 25 is needed to further understand the extent of suitable water-quality conditions for aquatic life in the lower reaches of the East Mancos River.

Given the high hazard quotients for multiple metals in the upper East Mancos, substantial metal reductions would need to occur to improve water quality to a condition suitable for aquatic life. In the downstream reaches of the East Mancos, we observed lower hazard quotients (aluminum, cadmium, and copper) **(Figure 4-13)**, suggesting that it is possible that moderate metal reductions could improve water-quality conditions for aquatic life. However, natural sources in the upper East Mancos would likely continue to contribute aluminum and copper loads even if anthropogenic sources could be minimized.

4.3 Status of East Mancos Benthic Macroinvertebrate Communities

Comparison of observed water quality in the East Mancos River to water quality standards and toxicity thresholds clearly suggest that conditions are not suitable for aquatic life. The most recent information we have on the status of aquatic life in the East Mancos River is from a benthic macroinvertebrate survey conducted by Mancos Conservation District (MCD) in the fall of 2019. MCD used the Colorado River Watch sampling methodology to collect benthics from three locations: East Mancos above Middle Mancos, Middle Mancos above East Mancos, and Mancos at Viets Diversion. There are substantial differences in the diversity and abundance of benthic macroinvertebrates in the East Mancos compared to the Middle Mancos and downstream Mancos River location. The East Mancos River had extremely low benthic abundance, only nine individuals per square meter. In contrast, the Middle Mancos and Mancos River at Viets had more than 1,000 individuals per square meter **(Figure 4-14)**. Diversity was reduced in the East Mancos as well, with fewer total taxa and lower diversity of Ephemeroptera (mayflies), Plecoptera (stoneflies), and Trichoptera (caddisflies) taxa, which are groups of macroinvertebrates known to be sensitive to, or intolerant of, poor water quality **(Figures 4-15 and 4-16)**. These observations of lower abundance and diversity of benthic macroinvertebrates in the East Mancos as compared to the Middle Mancos are consistent with previous observations from 2009 (B.U.G.S., 2010). Mayflies are generally known to be particularly sensitive to elevated metal concentrations (Kiffney and Clements, 1993; Besser and Leib, 2007; Clark and Clements, 2006). In the East Mancos, only one mayfly taxa was present (and only two individual mayflies were found), while the Middle Mancos had nine mayfly taxa and the Mancos River at Viets Diversion had six. The mayfly families Ephemerellidae and Heptageniidae are known from the nearby Animas River watershed to be intolerant of elevated metals (Courtney and Clements, 2002; Roberts, 2017). Ephemerellidae and Heptageniidae were present in the Middle Mancos, but none were present in the East Mancos. Somewhat surprisingly, the large differences in abundance and density among sites were only minimally reflected in the Colorado Multi-metric Index (MMI) scores, which indicated that all three sites are in attainment for aquatic life use **(Figure 4-17)**.

Water quality varies greatly throughout the East Mancos River. Additional benthic sampling at locations further upstream from the Middle Mancos confluence would be informative, especially

in the reach near White Rocks where fish were documented historically. Benthic communities are dynamic and can vary from year to year (Scarsbrook et al. 2000). It can be problematic to assess the condition of aquatic life communities based solely on one sampling event unless the natural inter-annual variability of benthic populations have been established (Mazor et al. 2009; Resh et al. 2013). Additional years of benthic observations will provide a more conclusive understanding of the status of aquatic life in the East Mancos River.

5. SUMMARY AND CONCLUSIONS

Water-quality degradation throughout the length of East Mancos River is directly related to geologic mineralization and porphyry alteration. With the prevalence of natural background and mining-induced aqueous metals, aquatic habitat has been degraded, and fish are generally absent from the East Mancos River. Geology of the upper East Mancos is extremely complex, with sedimentary rocks that have been hydrothermally altered by intrusive igneous rocks (copper-molybdenum porphyry stock). With the mineralization, mining and mineral exploration has been historically active in the watershed, but many of the underground mines in the upper basin were of limited extent due to low-grade ore, room-like nature and termination of ore bodies, high sulfur (pyrite) content, and remote access. Structural geology features show considerable uplift of sedimentary beds such that, for example, the base of the Dolores formation has been elevated in the center of the dome nearly 6,000 feet above its normal position. The East Mancos is located along a structural hinge zone where the beds generally dip outward at angles of 25° to 60° and rocks are sheared and brecciated along the hinge fold, where many of the ore-bearing vein fractures are concentrated within or near the hinge fold. Uplift and glacial weathering contribute to the steep gradients of the East Mancos River, averaging 7 percent per mile, with several steep sections of waterfalls and stream gradient greater than 30 percent.

Over the past few decades, only limited water-quality studies have been performed in the East Mancos River watershed. There are differences in conclusions within the various technical reports regarding the causes of water-quality degradation in the East Mancos, with some reports citing natural background sources as the cause of water-quality degradation, and other reports citing historical mining as the cause of water-quality degradation. Data presented in this report provide more information to address these concerns. However, the water quality and aqueous geochemistry of the East Mancos are extremely complex compared with other mineralized

watersheds in Colorado. Therefore, the summary and conclusions of this report reflect a small data set collected during a short time period (2018-19), which represents a reconnaissance-level investigation.

As part of this report, water-quality samples were collected and analyzed for an expanded water-quality parameter list (more than 30 metals). Every metal constituent tested in water from the upper basin during this study showed positive results, which is not common compared to other watersheds, and is likely related to the weathering of mineralized and hydrothermally altered sedimentary rocks and near-surface exposure of the copper-molybdenum porphyry complex. High dissolved-metal concentrations and acidic pH are present in water from streams, springs, and mines. While dissolved copper and manganese have been identified as main constituents of concern in the East Mancos watershed, there are likely to be combined effects of numerous metal constituents in water, including antimony, arsenic, cadmium, copper, iron, manganese, thallium, uranium, vanadium, and zinc.

As part of low-flow sampling during September 2018, which was a near-record drought year, water-quality samples were collected from 21 sites in the East Mancos River watershed. Springs and streams in the upper basin were documented and sampled, but very few of the mines showed any water drainage. As the sampling progressed downstream, it was apparent that the stream was a losing reach, where stream flows measured upstream were greater than stream flows measured in downstream reaches. Hence, surface water discharges were lost to infiltration into the groundwater system. The lost discharge may or may not return to the stream channel, depending on glacial valley fill, regional groundwater flow, faults, and fissure controls on groundwater movement. The 2018 drought provided a unique opportunity to witness the losing stream reach; otherwise, higher flows would mask the effects of lost discharge and would be more difficult to quantify.

During high-flow sampling of June-July 2019, water-quality samples were collected from 31 sites in the East Mancos River watershed. Many of the historical mines in the upper basin had water drainage, which provided the opportunity to collect water samples from draining mines that was missed during the drought of 2018. This indicates that groundwater flow through the high-altitude mines may have relatively short-lived travel paths from the top of Jackson Ridge to the adit; therefore, the upper mines probably dry up seasonally every year, especially during

drought periods. If mine drainage is not manifested at the adit or portal, the effects of underground mines on deep groundwater metal concentrations and inflows to streams is difficult to document, and was not addressed as part of this report.

During low-flow conditions of September 2018, dissolved copper concentrations in water from sites in the East Mancos ranged from < 2.2 to 22,100 µg/L, with a median value of 3,110 µg/L. Many of the high dissolved copper concentrations originate from sites in the Burwell Trib. Dissolved manganese concentrations in water from sites in the East Mancos ranged from 3.3 to 7,210 µg/L, with a median value of 1,560 µg/L. High dissolved manganese concentrations appeared to be present during low flow in water from many sites in the upper and middle East Mancos.

During high-flow conditions of June-July 2019, dissolved copper concentrations in water from sites in the East Mancos ranged from < 5.5 to 20,400 µg/L, with a median value of 154 µg/L. Many of the high dissolved copper concentrations originate from sites in the upper East Mancos (Rush Basin and Burwell Trib), including drainage from mine sites that were dry during September 2018. Drainage from mine sites in the middle basin also had elevated dissolved copper concentrations. Dissolved manganese concentrations in water from sites in the East Mancos ranged from < 1 to 2,480 µg/L, with a median value of 95.4 µg/L. The highest dissolved manganese concentrations appear to have originated from the Burwell Trib; however, elevated dissolved manganese concentrations also were present in drainage from mine sites in the middle basin.

During low-flow conditions of September 2018, dissolved copper mass loading in water from sites in the East Mancos ranged from 0.01 to 8.42 lb/d, with a median value of 1.2 lb/d. Many of the high dissolved copper loads originate from sites in the Burwell Trib. Dissolved manganese mass loading during low flow in water from sites in the East Mancos ranged from 0.01 to 4.3 lb/d, with a median value of 0.2 lb/d. Most of the elevated dissolved manganese loads appeared to have originated in the upper basin.

During high-flow conditions of June-July 2019, dissolved copper mass loading in water from sites in the East Mancos ranged from 0.0 to 110.8 lb/d, with a median value of 3.4 lb/d. Sources of elevated dissolved copper loads were unclear, but appeared to have originated mainly from the

Burwell Trib. Dissolved copper loads appeared to increase between mainstem sites EM-WQ-12 and EM-WQ-16, and between mainstem sites EM-WQ-16 and EM-WQ-18, yet the causes or sources are uncertain. Dissolved manganese mass loading during high flow in water from sites in the East Mancos ranged from 0.01 to 36.8 lb/d, with a median value of 1.63 lb/d. As with dissolved copper loads, dissolved manganese loads appeared to increase between mainstem sites 12 and 16, and between sites 16 and 18, yet the causes or sources are uncertain.

Longitudinal profiles of dissolved and total metals shows that most of the high concentrations during low flow originate from the upper basin (Rush Basin and Burwell Trib). Buffering constituents such as calcium and magnesium increase in a downstream direction as the stream leaves the areas altered by the porphyry intrusive, along with increasing barium and strontium concentrations consistent with weathering of sedimentary rocks. Dissolved and total lead are variable along the mainstem, increasing in the middle part of the basin possibly due to vein mineralization in the middle basin. Decreasing metal concentrations in a downstream direction are likely caused not only by dilution, but also due to mineral complexation, supersaturation, and precipitation.

Much of the aqueous metal mobilization and transport in the East Mancos occurs during high flow conditions. Many of the historical mines did not exhibit water drainage at the adits during low flow, but drainage was noted and sampled during high flow. During low and high flow conditions, metal loads increase between EM-WQ-03 and EM-WQ-12, which flows past the upper Doyle Group and mill, and loads increase between EM-WQ-12 and EM-WQ-16, which flows past the lower Doyle Group, plus the Georgia Girl Mines and unidentified site WR-7, but this reach also flows past Gibbs Peak and the porphyry intrusive. More information are needed for this reach of the East Mancos during low-flow and high-flow conditions. Loads for other metals (arsenic, antimony) also increased through the reach EM-WQ-03 to EM-WQ-12 and EM-WQ-12 to EM-WQ-16, but the sources of these metals (natural background or mining-related) requires further investigation. Dissolved and total lead (Pb) loading increases from EM-WQ-21 to EM-WQ-23, which flows past the Red Arrow Mine. This reach also shows indications of historical placer mining and streambed disturbance.

During low flow of September 2018, there were voluminous amounts of red, brown, orange, and white precipitates present on the streambed in the upper and middle parts of the watershed.

These precipitates are known to occur in geologically mineralized watersheds (for example, Cement Creek in the upper Animas River basin); however, precipitates in waters of the upper East Mancos have a copper-rust color due to extremely high concentrations of copper. The precipitates were identified as the mineral cupric ferrite by the geochemical model; however, further verification of this is needed. White precipitates occur on the streambed during low flow downstream from the confluence of the acidic East Mancos mainstem and neutral pH tributaries such as Fall Creek. Photo documentation during 2018-19 shows that these precipitates deposited during low flow were scoured and flushed downstream during high flow snowmelt runoff.

Statistical summaries of selected dissolved constituent concentrations for background streams and springs (Category I and II sites) were compared with mining-affected sites (Category III-IV). During low flow September 2018, the Category I-II sites had a wide variation in chemical composition; pH ranged from 3.43 to 8.51, and specific conductance ranged from 62 to 1,528 µs/cm. Sulfate concentrations ranged from 7.3 to 1,640 mg/L, dissolved copper concentrations ranged from 1.0 to 12,200 µg/L, and dissolved manganese concentrations ranged from 4.5 to 5,580 µg/L. Sites with high pH values (pH>5.4) typically had measurable concentrations of alkalinity and lower aluminum, copper, and iron concentrations, whereas sites with low pH values (pH<5.4) had little measurable alkalinity and elevated concentrations of aluminum, copper, and iron. Category III-IV sites during low flow showed a wide variation in chemistry, with pH ranging from 2.74 to 6.55, and specific conductance ranging from 98.4 to 1,605 µs/cm. Sulfate ranged from 11.9 to 690 mg/L, and dissolved copper concentrations ranged from 6.6 to 23,600 µg/L. This highest dissolved copper concentration was in water from the Burwell Trib, which was likely affected by elevated natural-background and mining-affected copper concentrations; for example, water from a Category I spring in the Burwell Trib (EM-WQ-09) had a dissolved copper concentration of 11,700 µg/L. During high flow of June-July 2019, the Category I-II sites had a wide range of chemical compositions, where pH values of background sites ranged from 4.11 to 8.71, and specific conductance values ranged from 7 to 229 µs/cm. Sulfate ranged from 1.2 to 134 mg/L, dissolved copper concentrations ranged from 69.1 to 9,690 µg/L, and dissolved manganese concentrations ranged from 1.0 to 2,180 µg/L. Category III-IV sites during high flow also had a wide variation of water chemistry, where pH values ranged from 2.63 to 7.04, and specific conductance values ranged from 21.7 to 1,832 µs/cm. Sulfate

concentrations ranged from 3.56 to 473 mg/L, dissolved copper concentrations ranged from 9.2 to 20,400 µg/L, and dissolved manganese concentrations ranged from 1.4 to 2,480 µg/L. Statistical summaries of selected dissolved constituents in show similar chemical characteristics when comparing background sites (Category I-II) and mining-affected sites (Category III-IV). Boxplots of selected constituents similarly show little differences between Cat. I-II and Cat. III-IV concentrations of selected dissolved and total metals. From these data, it would be challenging to conclude which category of site contributes the highest concentrations of dissolved constituents to the East Mancos watershed.

As part of this report, more than 65 historical mine sites were documented in the East Mancos River watershed. Waste rock samples were collected from 32 of these mine sites (most of them in the upper basin), including three background sites. Laboratory leachate potential tests were performed on sieved waste-rock samples. Results indicate that pH values of waste-rock leachate ranged from 2.10 to 7.03, with a median value of 4.22. Specific conductance values ranged from 14 to 5,230 µs/cm, with a median of 84.0 µs/cm. From titrations, acidity values ranged from 10.0 to 6,080 mg/L as $CaCO_3$, with a median of 20.0 mg/L as $CaCO_3$. Acid neutralizing requirements for leachate stabilization ranged from 0.01 to 12.4 kg $CaCO_3$/1000 L, with a median value of 0.13 kg $CaCO_3$/1000 L. Cupric copper concentrations in leachate water ranged from 79.5 µg/L to 1,032,720 µg/L. Concentrations of dissolved metals in water from leachate samples were extremely high in many samples. The highest concentrations of dissolved copper occurred in water from leachate testing of waste rock from the Thunder Mine and site WR-1 in the headwaters of the Burwell Trib. Waste rock samples from the Doyle Group also had high dissolved copper concentrations. The highest concentrations of dissolved manganese occurred in water from leachate testing of waste rock from the Red Arrow Gold Run Mine and Red Arrow Tailings. Dissolved metal mass loadings were estimated for snowmelt runoff from waste rock piles. While non-conservative constituent behavior makes it difficult to draw conclusions, the summation of waste-rock runoff mass loadings for copper ranged from 5 to 11 percent of the low-flow mass loading at site EM-WQ-24, and waste-rock mass loadings for manganese ranged from 15 to 40 percent of the mass loading at site EM-WQ-24. Concentrations of other dissolved metals were extremely high; therefore, mass loading of other dissolved metals from waste rock leachate would likely contribute to mass loadings of the at the mouth of the watershed.

A Total Maximum Daily Load (TMDL) is comprised of the Load Allocation (LA), which is that portion of the pollutant load attributed to natural background or the nonpoint sources, the Waste Load Allocation (WLA), which is that portion of the pollutant load associated with point source discharges, and a Margin of Safety (MOS). Identification of natural background mass loadings (LA) turned out to be particularly challenging in the East Mancos. Non-conservative constituent behavior and seasonal streamflow variation makes it difficult to choose a single monitoring point in time or space. Therefore, instream mass loadings of dissolved metals were compared to the measurable mining-affected mass loadings for low-flow and high-flow conditions. Considering dissolved manganese to be more conservative than dissolved copper, during low flow of September 2018, summation of measurable Category III-IV loads and waste-rock leachate loads comprised about 17 percent of the dissolved manganese load at site EM-WQ-16, and about 40 percent of the dissolved manganese load at site EM-WQ-24. During high flow of June-July 2019, summation of measurable Category III-IV loads and waste-rock leachate loads comprised about 3 percent of the dissolved manganese load at site EM-WQ-16, and about 4 percent of the dissolved manganese load at site EM-WQ-24.

The TMDL approach assumes that constituents of concern behave conservatively in water. In the East Mancos River, however, non-conservative behavior of dissolved constituents has been identified through sampling, observations, and geochemical modeling. In addition, the East Mancos River is a losing stream reach (further documentation is needed); therefore, dissolved constituent concentrations and loads are being removed from the stream due to the lost streamflow discharge and associated loads. In the East Mancos River watershed, therefore, the TMDL theory of conservative constituent behavior has been violated by numerous conditions. Attempted balancing of aqueous metal loading sources shows that the mining-related metal loads (Category III-IV sites) are much smaller than metal loads in the East Mancos stream; however, this balance does not account for undocumented diffuse sources due to the impacts of historical mining and milling.

Results from toxicity assessment indicate that water quality conditions in much of the East Mancos are not suitable for aquatic life, and have a high toxicity risk during high-flow and low-flow periods. Multiple metals had concentrations above toxicity thresholds including aluminum, cadmium, copper, iron, manganese, mercury, nickel, selenium, silver, and zinc. HQ's indicated

substantial toxicity in the upper watershed with the highest HQs occurring in the Burwell Tributary where the concentration of copper during high flow was more than 400,000 times greater than the BLM chronic toxicity threshold. Hazard Quotients and the number of metals occurring at potential toxic levels were far lower in the downstream reaches of the East Mancos. In the lowermost reaches (sites 24, 25, and 27), the only metals that occurred at potential toxic levels were aluminum, cadmium, and copper. During high-flow conditions, potential acute toxicity of copper and chronic toxicity of aluminum and copper extended throughout the East Mancos all the way downstream to the mouth of the East Mancos at site 27. During low-flow conditions, potential acute toxicity of copper and chronic toxicity of aluminum, copper, and cadmium extended downstream to site 24. At site 25 during low flow, there was potential for chronic copper toxicity, but no metals surpassed acute toxicity thresholds. In addition to samples collected in low-flow and high-flow conditions, multiple samples were collected at site 25 from March-July of 2019. These samples allow for a higher temporal understanding of seasonal toxicity at this location. The highest potential for aluminum toxicity occurred on 6/3/19 while the highest potential for copper toxicity occurred on 7/3/19. Elevated copper concentrations occurred throughout the entire East Mancos at levels indicative of aquatic life toxicity. However, the toxicity of manganese, which in addition to copper is listed as an impairment for the East Mancos, was not as high as copper throughout the East Mancos. During high-flow conditions, concentrations of manganese were below acute and chronic toxicity thresholds at all sampling locations. During low-flow conditions, concentrations of manganese surpassed acute and chronic toxicity thresholds in headwater reaches. Potential toxicity in the East Mancos River decreased from site EM-WQ-23 (below Red Arrow Mine) to site 24 (USFS boundary) and to site 25 (above Middle Mancos), especially during high-flow conditions.

Benthic macroinvertebrate samples were collected from three locations: East Mancos above Middle Mancos, Middle Mancos above East Mancos, and Mancos at Viets Diversion. There are substantial differences in the diversity and abundance of benthic macroinvertebrates in the East Mancos compared to the Middle Mancos and downstream Mancos River location. The East Mancos River had extremely low benthic abundance, only nine individuals per square meter. In contrast, the Middle Mancos and Mancos River at Viets had more than 1,000 individuals per square meter. Diversity was reduced in the East Mancos as well, with fewer total taxa and lower diversity of Ephemeroptera (mayflies), Plecoptera (stoneflies), and Trichoptera (caddisflies) taxa,

which are groups of macroinvertebrates known to be sensitive to, or intolerant of, poor water quality. These observations of lower abundance and diversity of benthic macroinvertebrates in the East Mancos as compared to the Middle Mancos are consistent with previous observations from 2009. Mayflies are generally known to be particularly sensitive to elevated metal concentrations. In the East Mancos, only one mayfly taxa was present (and only two individual mayflies were found), while the Middle Mancos had nine mayfly taxa and the Mancos River at Viets Diversion had six. The mayfly families Ephemerellidae and Heptageniidae are known from the nearby Animas River watershed to be intolerant of elevated metals. Ephemerellidae and Heptageniidae were present in the Middle Mancos, but none were present in the East Mancos. Somewhat surprisingly, the large differences in abundance and density among sites were only minimally reflected in the Colorado Multi-metric Index (MMI) scores, which indicated that all three sites are in attainment for aquatic life use.

In the high-altitude setting of Rush Basin, mill tailings were dumped directly into the upper East Mancos River, and massive mill tailings deposits can be observed in the stream channel, forming ledges and rimstone dams of tailings cemented by iron and copper mineral precipitates. In several locations, the historical mines are near the stream, and mine waste rock was placed directly into the stream. Tailings and waste rock have likely been transported downstream as streambed sediments, and could act as sources for dissolved metal concentrations in the East Mancos River. Concentrations and sources of metals in streambed sediments were not addressed as part of this report.

The foremost conclusion of this report is that natural background *and* mining-related aqueous metal sources occur in the East Mancos River. While natural background metals are prevalent and contribute to water-quality degradation, historical mines also are impacting the stream. Given the high hazard quotients for multiple metals in the upper East Mancos, substantial metal reductions would need to occur to improve water quality to a condition suitable for aquatic life in the upper basin. In the downstream reaches of the East Mancos, however, lower hazard quotients were observed for aluminum cadmium, and copper, suggesting that dissolved metal reductions in the upper East Mancos would improve water-quality conditions for aquatic life in the lower reaches. However, natural sources in the upper East Mancos would likely continue to contribute aluminum and copper loads even if anthropogenic sources could be minimized.

Additional studies are needed to focus on the reaches where loading increases were identified by this report. The effects of deep groundwater contamination from underground mine workings needs to be investigated. Sources and concentrations of metals in streambed sediments need to be identified. Using innovative ideas and state-of-the-art remediation technologies, water-quality conditions in the East Mancos River can be improved. To determine feasible water-quality standards and remediation goals, there is a need for a Use Attainability Analysis (UAA) for the East Mancos River Watershed.

6. REFERENCES CITED

Besser, J. and K. Leib, 2007, Toxicity of metals in water and sediment to aquatic biota. In S. Church, P. von Guerard, and S. Finger (Eds.), Integrated investigations of environmental effects of historical mining in the Animas River watershed, San Juan County, Colorado. USGS Professional Paper 1651.

B.U.G.S. Consulting. 2009. East Mancos River. Presentation for Mancos Conservation District.

B.U.G.S. Consulting. 2010. Benthic Macroinvertebrates on the East Mancos River. Report prepared for Mancos Conservation District.

CDPHE, 2005, Combined Assessment – Site Inspection, Draft Analytical Results Report, East Fork of Mancos River, Montezuma County, Colorado, July 22, 2005, Colorado Department of Public Health and Environment Hazardous Materials and Waste Management Division, 46 p.

CDPHE, 2012, Total Maximum Daily Load Assessment, East Mancos River, San Juan and Dolores River Basin, Segment COSJLP04a, Montezuma County, Colorado: Colorado Department of Public Health and Environment, Water Quality Control Division, 29 p.

CDPHE, 2017, Regulation No. 34 – Classifications and Numerical Standards for the San Juan River and Dolores Basins, Colorado Water Quality Control Commission, 5 CCR 1002-34, August 7, 2017.

Clark, J., and W. Clements. 2006. The use of in situ and stream microcosm experiments to assess population- and community-level responses to metals. Environmental Toxicology and Chemistry, 25(9):2306-2312.

Courtney, L. and W. Clements. 2002. Assessing the influence of water and substratum quality on benthic macroinvertebrate communities in a metal-polluted stream: an experimental approach. Freshwater Biology, 47: 1766-1778.

Clements, W., D. Carlisle, J. Lazorchak, and P. Johnson, 2000. Heavy metals structure benthic communities in Colorado mountain streams. Ecological Applications, 10:626-638.

Colorado Parks and Wildlife, 2010, Macroinvertebrate Collection and Habitat Assessment Instructions, Version 6.10, 31 p.

Eckel, E.B., 1949, Geology and ore deposits of the La Plata District, Colorado: U.S. Geological Survey Professional Paper 219, 179 p.

Hermansson, H.P., 2004, The Stability of Magnetite and its Significance as a Passivating Film in the Repository Environment: Swedish Nuclear Power Inspectorate, SKI Report 2004:07, January 2004, 47 p.

Horn, B. 2010. Mancos River Fishery Summary. Colorado Division of Parks and Wildlife.

Horowitz, A.J., Demas, C.R., Fitzgerald, K.K., Miller, T.L., and Rickert, D.A., 1994, U.S. Geological Survey protocol for the collecting and processing of surface-water samples for subsequent determination of inorganic constituents in filtered water: U.S. Geological Survey Open-File Report 94-539, 57 p.

Kiffney, P., and W. Clements. 1993. Bioaccumulation of heavy metals by benthic invertebrates at the Arkansas River, Colorado. Environmental Toxicology and Chemistry, 12(8): 1507-1517.

Lonsdale, J.T., 1921, The Geology and ore deposits of Bedrock Gulch, La Plata County, Colorado: M.S. Thesis, Graduate College, University of Iowa, Iowa City, 1921, 60 p.

Mancos River Watershed Plan, 2011, Mancos Valley Watershed Group, 58 p.

Mancos Source Water Protection Plan, 2009, Mancos Valley Watershed Group, 75 p.

Mathsoft, Inc., 1998, S-Plus Guide to Statistics: Mathsoft, Inc., Seattle Washington, 902 p.

Meyer, W.A., 1993, Natural geochemical processes of acid rock drainage, East Mancos River, La Plata Mountains, Colorado: M.S. Thesis, Dept. of Geology, Northern Arizona University, December 1993, 105 p.

Mutschler, F.E., Larson, E.E., and Ross, M.L., 1998, Potential for Alkaline Igneous Rock-Related Gold Deposits in the Colorado Plateau Laccolithic Centers, in Friedman, J.D., and Huffman, A.C., Jr., Eds., Laccolith complexes

of Southeastern Utah: Timing of emplacement and tectonic setting – workshop proceedings: U.S. Geological Survey Bulletin 2158, p. 233-252.

Neubert, J.T., 2000, Naturally Degraded Surface Waters Associated with Hydrothermally Altered Terrane in Colorado: Colorado Geological Survey, Open-File Report 00-16, 158 p.

Rantz, S.E., and others 1982, Measurement and computation of streamflow: Volume 1, Measurement of state and discharge: U.S. Geological Survey Water-Supply Paper 2175.

Roberts, S. 2017. Bonita Peak Mining District, 2016 benthic macroinvertebrate assessment. Mountain Studies Institute.

Schiowitz, D., 2008, Gold potential mapping using fuzzy logic, La Plata Mountains, Colorado: B.S. Thesis, Department of Geology, Fort Lewis College, Durango, Colorado, 25 p., 1 plate.

Summerlin, E.S., 2014, PGE mineralization at the Allard stock: Implications for the porphyry to epithermal transition, La Plata Mountains, Colorado: M.S. Thesis, Dept. of Geology and Geography, Auburn University, May 2014, 141 p.

Taylor, J.K., 1987, Quality assurance of chemical measurements: Chelsea, Michigan, Lewis Publishers, Inc., 328 p.

USEPA, 2000, Data Quality Objectives Process for Hazardous waste Site Investigations: United States Environmental Protection Agency (EPA QA/G-4HW).

USEPA, 2007, Aquatic Life Ambient Freshwater Quality Criteria Using the Biotic Ligand Model: U.S. Environmental Protection Agency, CAS 7440-50-8, February 2007.

USEPA, 2018. Final aquatic life ambient water quality criteria for aluminum. United States Environmental Protection Agency (EPA-822-R-18-001).

Werle, J.L., Ikramuddin, M., and Mutschler, F.E., 1984, Allard stock, La Plata Mountains, Colorado—an alkaline rock-hosted porphyry copper – precious metal deposit: Canadian Journal of Earth Sciences, v. 21, n. 6, p. 630-641.

Wilde, F., and others, 2014, National field manual for the collection of water-quality data: U.S. Geological Survey Techniques of Water-Resources Investigations, Book 9, Chaps. A1-A10, available online at http://pubs.water.usgs.gov/twri9A.

ATTACHED AS SEPARATE FILES

FIGURES FOR SECTIONS 1 AND 2

TABLES FOR SECTIONS 1, 2, AND 3

FIGURES AND TABLES FOR SECTION 4

APPENDIX 1. WATER -QUALITY DATA BASE.

APPENDIX 2. WASTE -ROCK LEACHATE DATA

APPENDIX 3. WATER QUALITY FIELD NOTES, EAST MANCOS RIVER, 2018-19

APPENDIX 4. WASTE-R OCK FIELD DATA SHEETS

APPENDIX 5. WASTE-ROCK LEACHATE LABORATORY SHEETS

Figures for *East Mancos River Watershed – Aqueous Metals Sources, Concentrations, Mass Loading, and Aquatic Impacts*

Section 1. INTRODUCTION

Section 2. METAL CONCENTRATIONS, MASS LOADING, AND AQUEOUS GEOCHEMISTRY

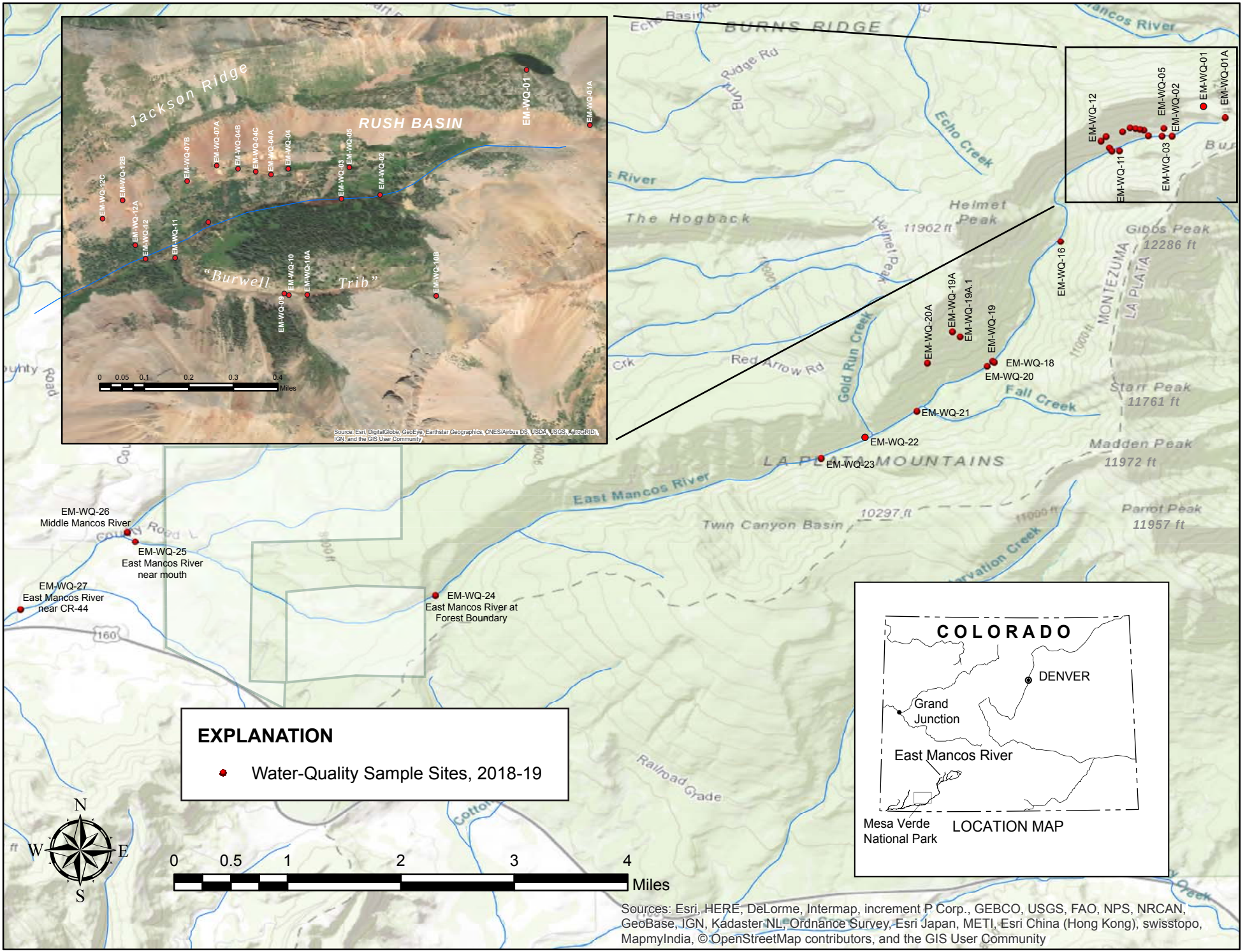

Figure 1-1. Location of water-quality sampling sites in the East Mancos River watershed, 2018-2019.

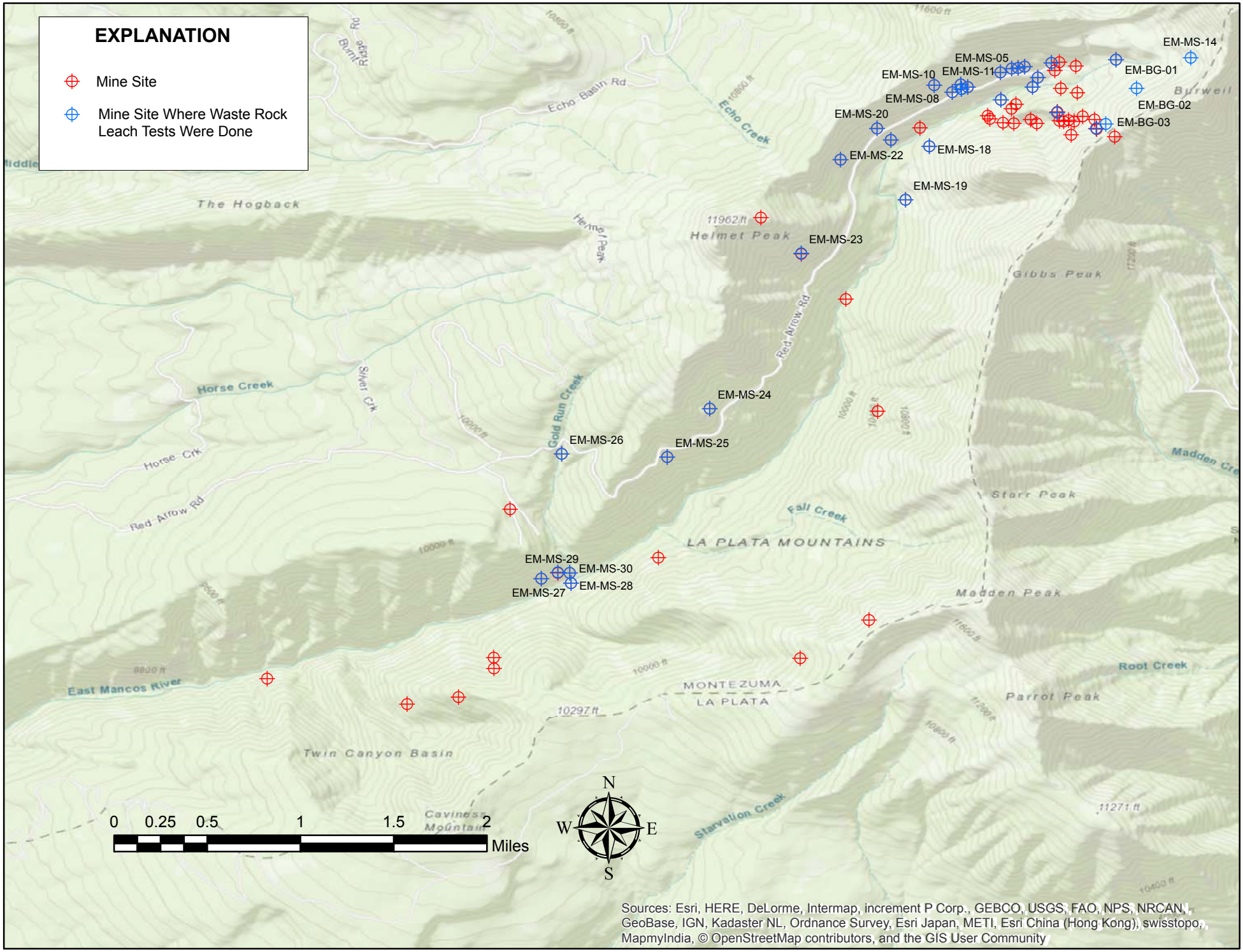

Figure 1-2. Location of historical mines sites in the East Mancos River watershed, and mine sites where waste-rock leachate tests were done.

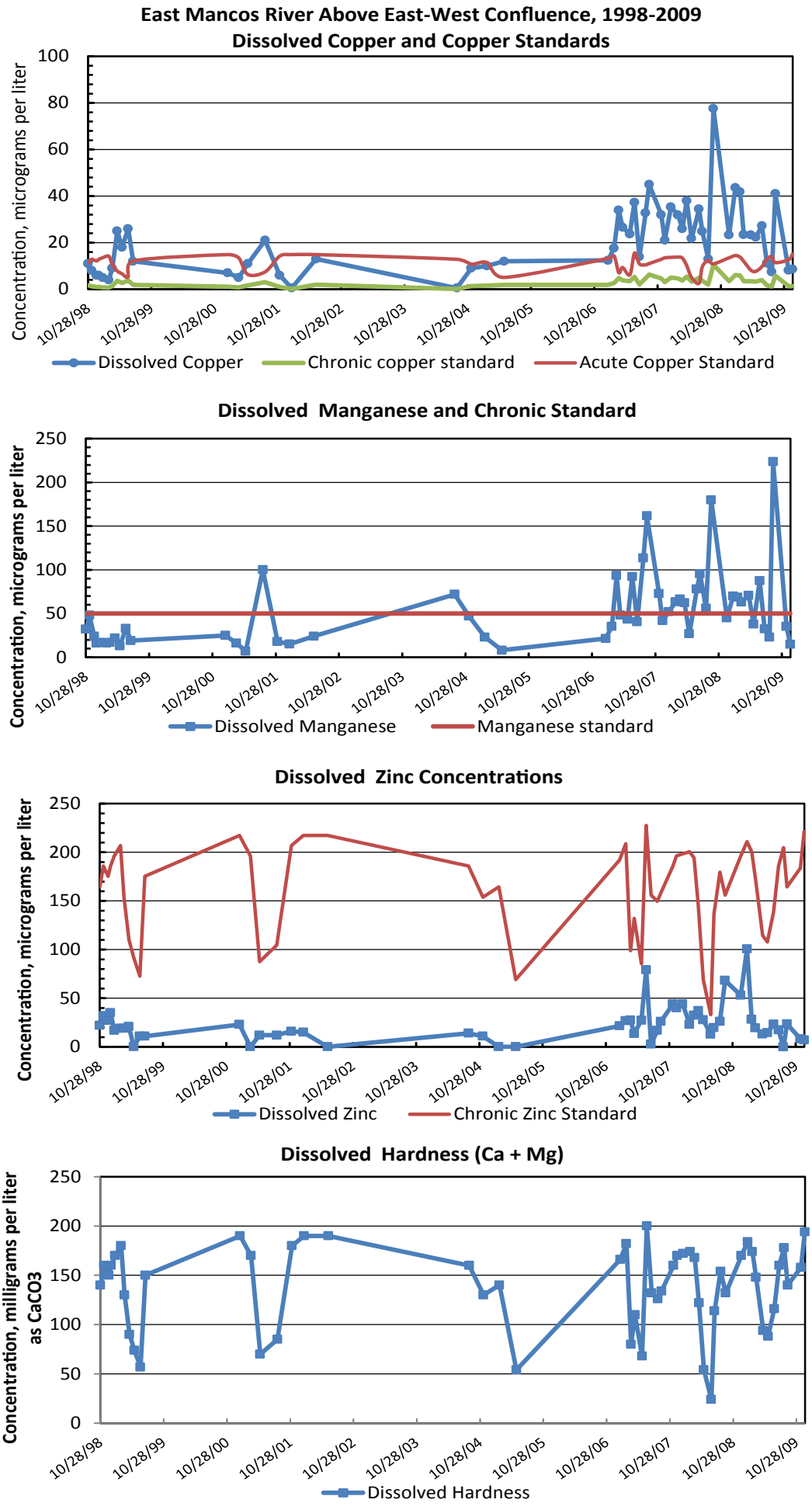

Figure 1-3. Historical water-quality data for the East Mancos River (combined CDPHE and River Watch data).

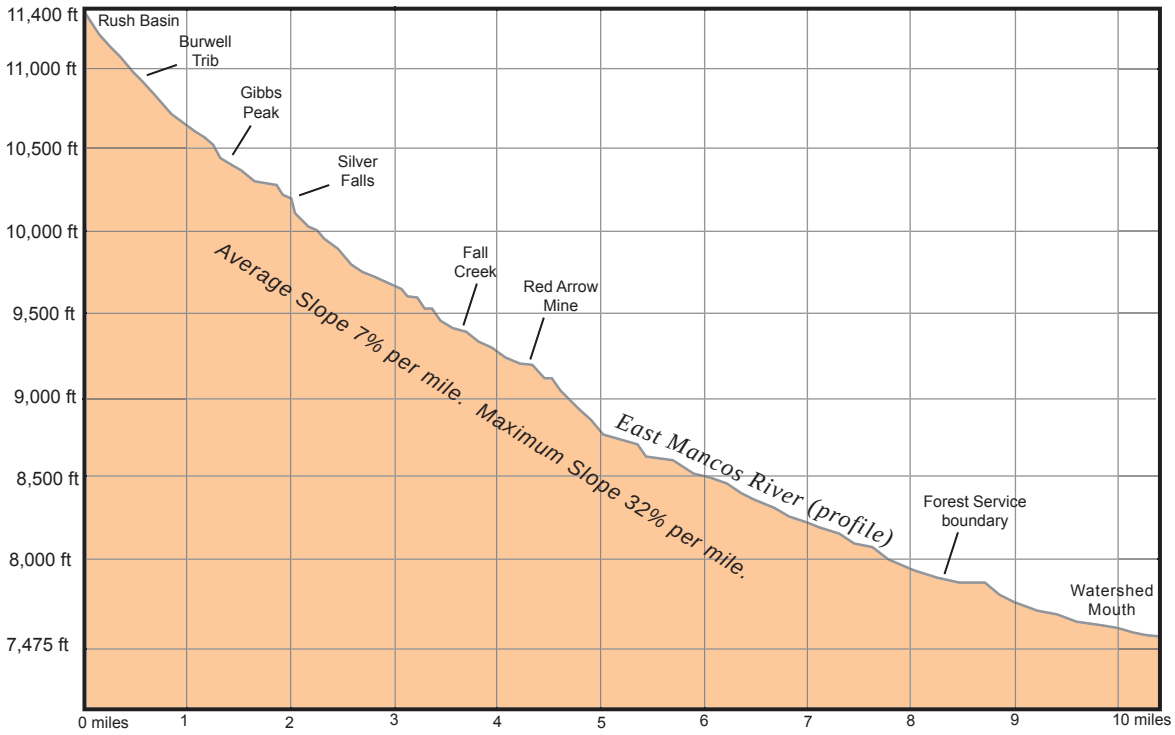

Figure 1-4. Elevation profile (looking southeast) for the East Mancos River.

Southwest Hydro-Logic, Durango, Colo.

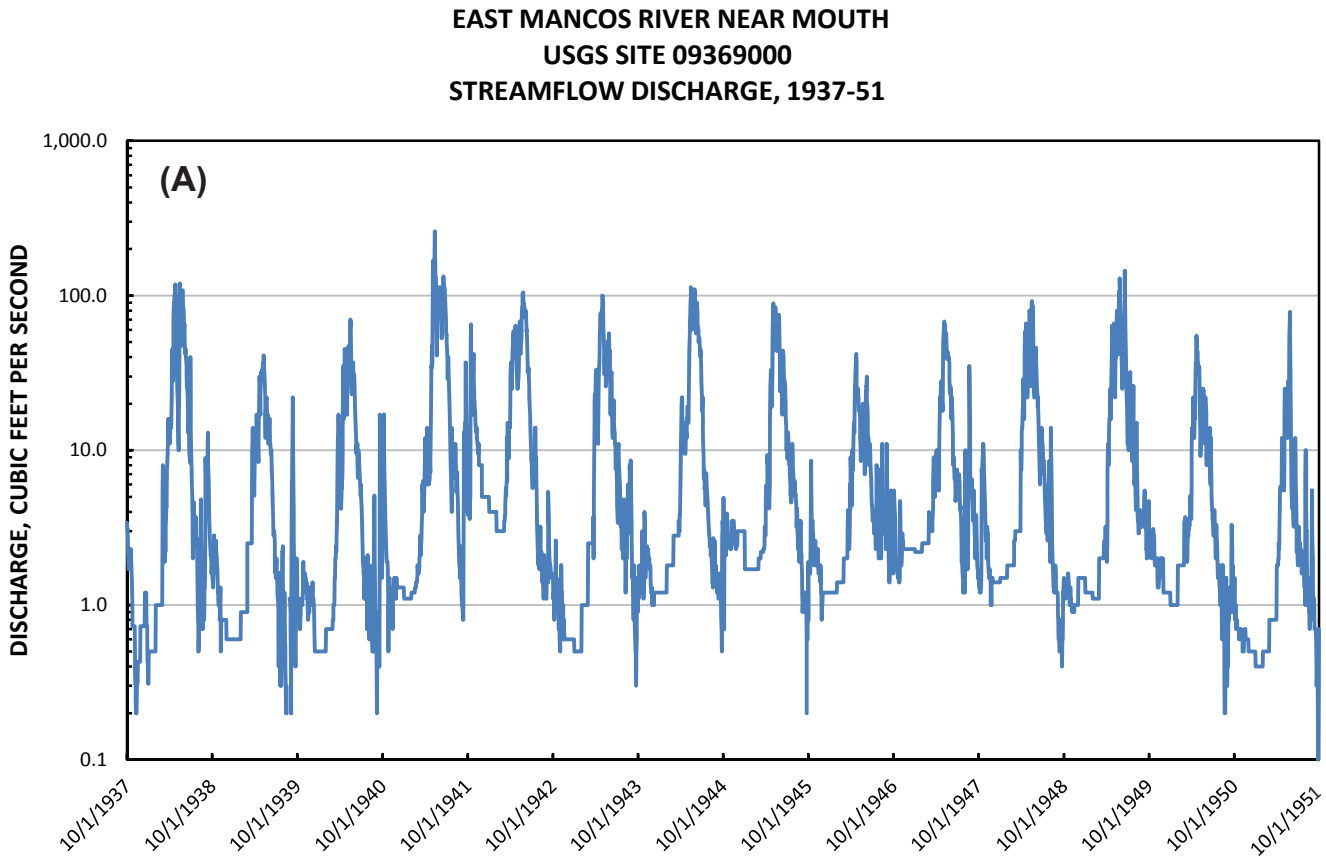

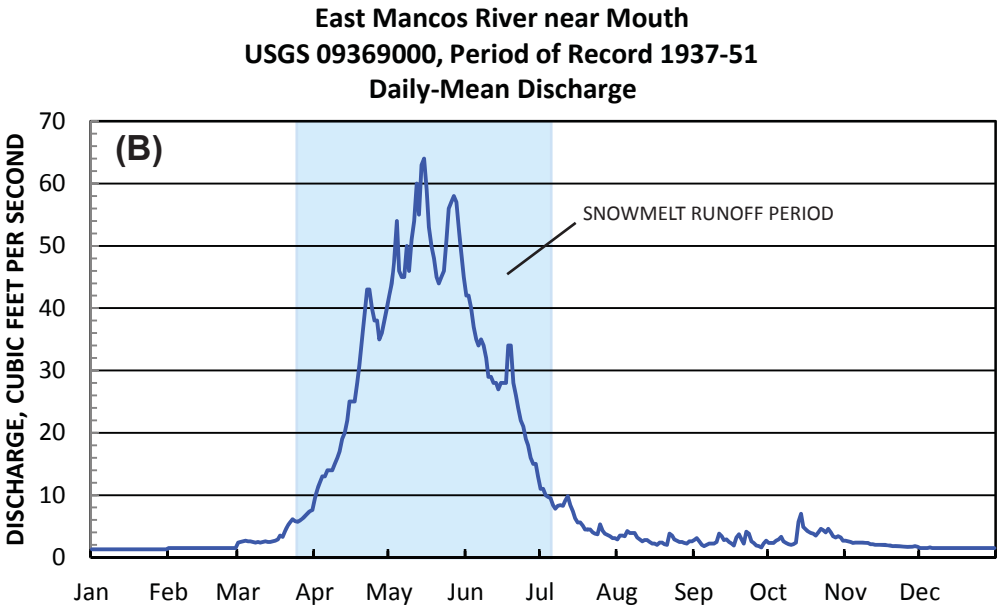

Figure 1-5. (A) Streamflow hydrograph for East Mancos River near mouth for the period of record 1937-51. (B) Daily-mean discharge hydrograph for East Mancos River showing snowmelt runoff period.

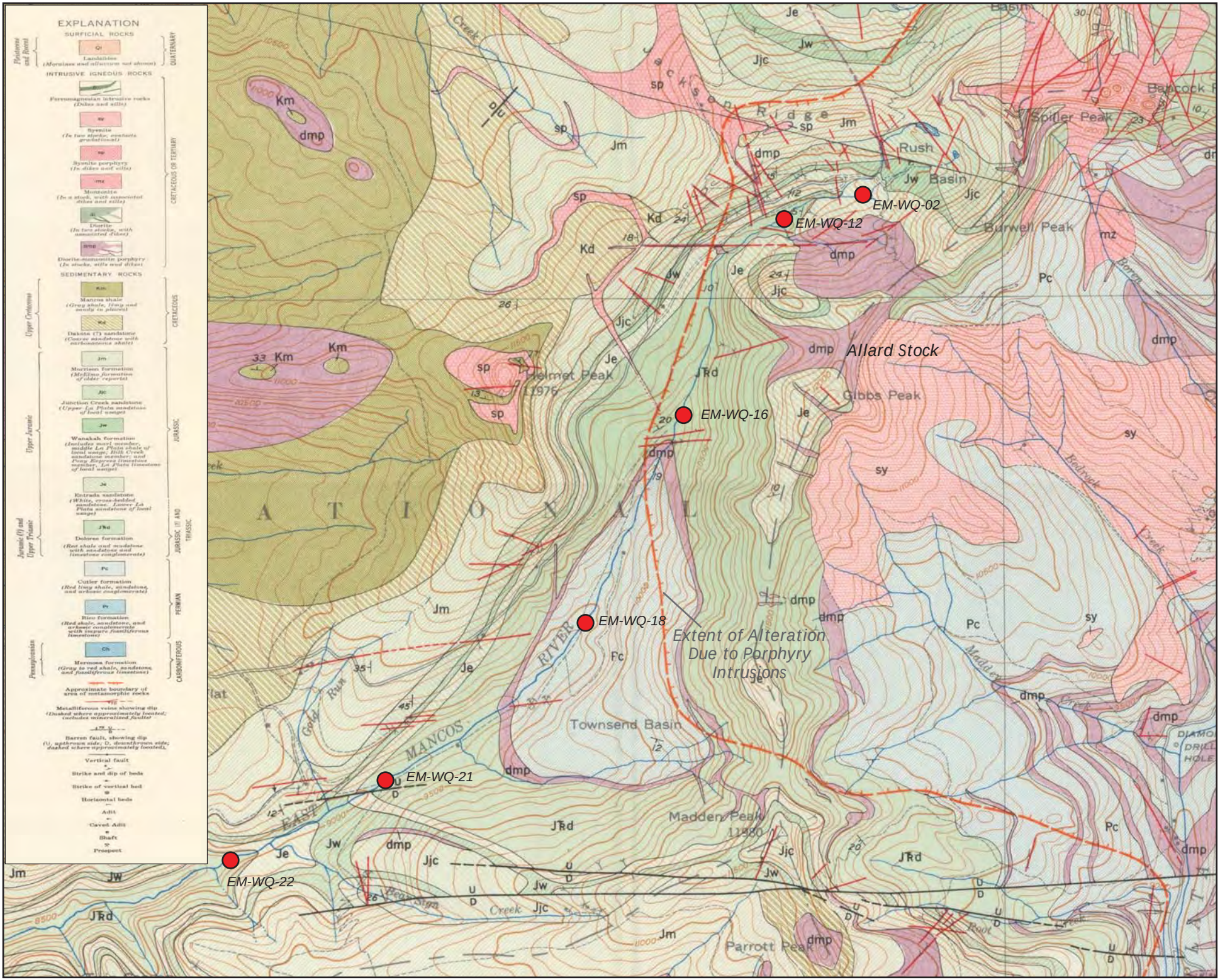

Figure 1-6. Geologic map of the upper East Mancos River watershed (Eckel, 1949).

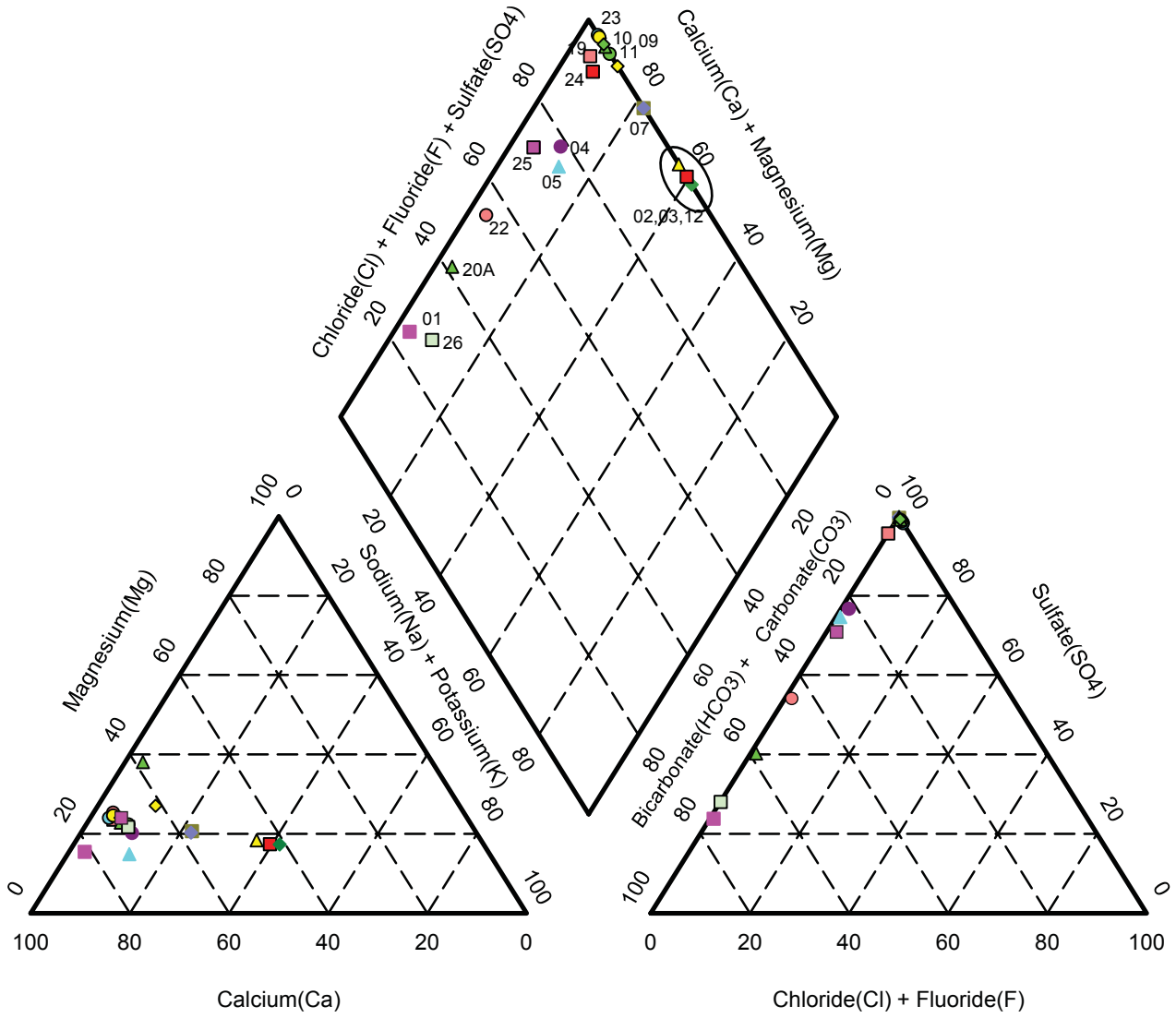

Figure 2-1. Tri-linear diagram (Piper Diagram) showing major-ion distribution for water-quality sites in the East Mancos River watershed.

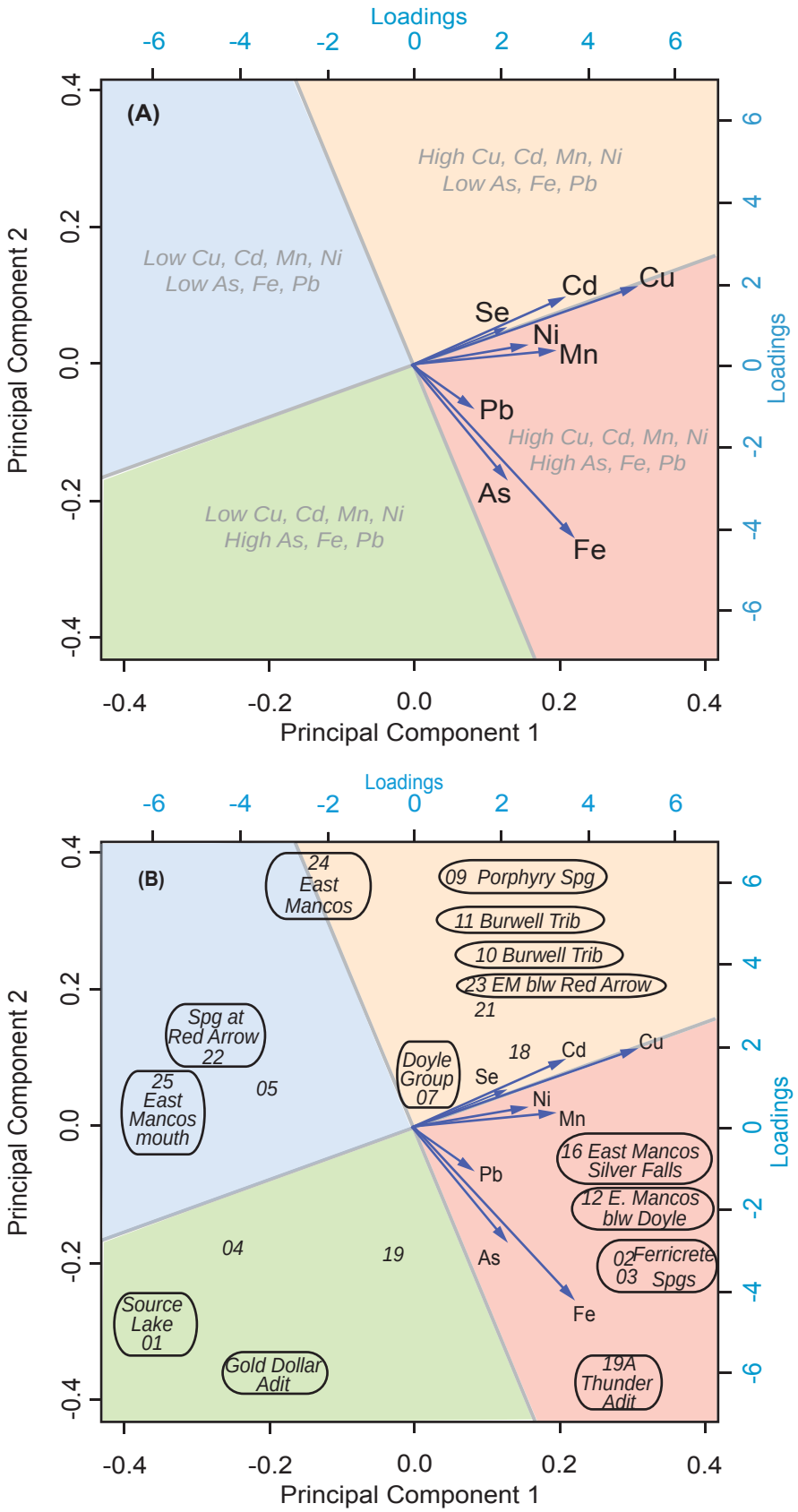

Figure 2-2. Principal components analysis biplot (A) showing rotated axes oriented according to groupings of dissolved metals, and (B) PCA biplot with site locations shown.

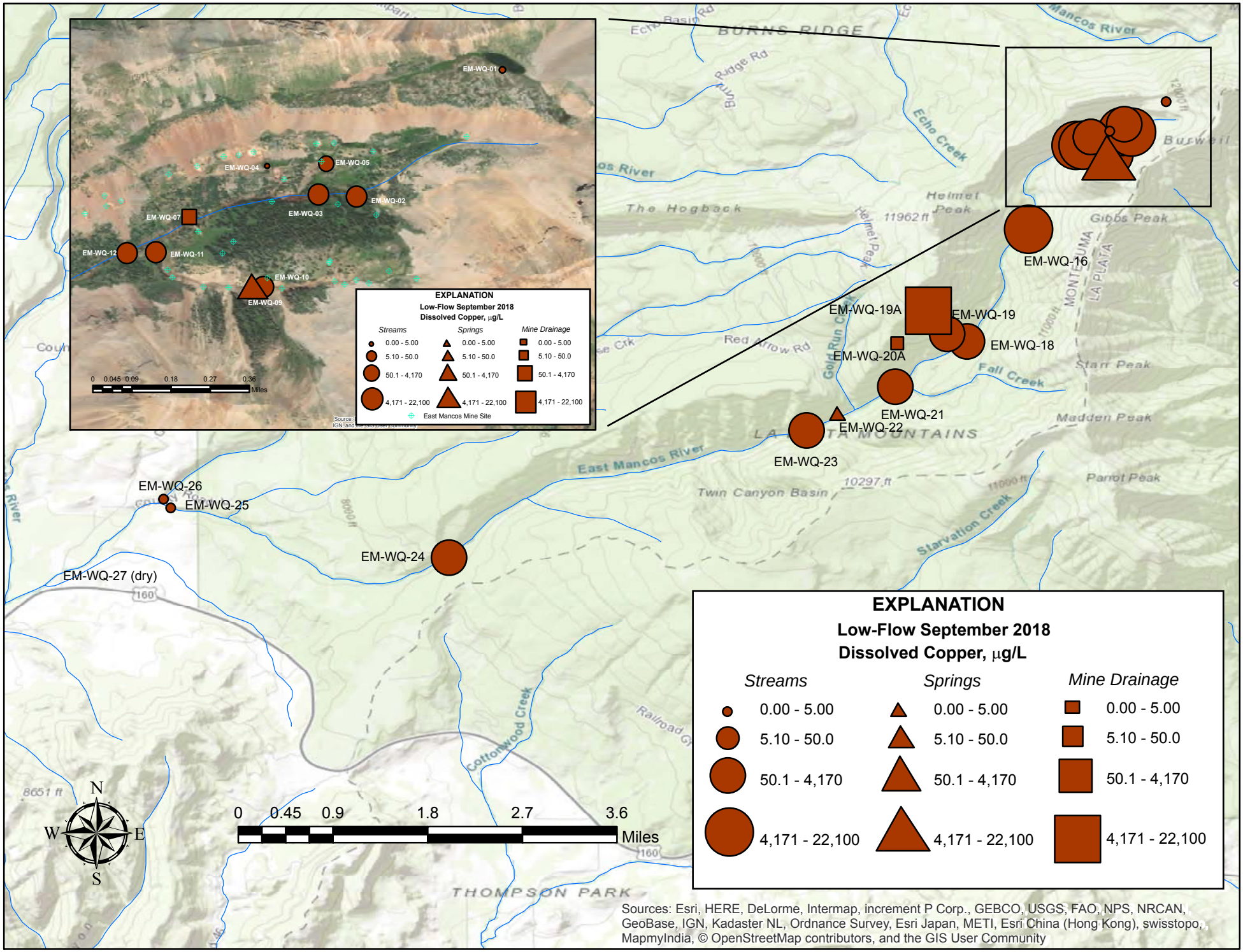

Figure 2-3. Distribution of dissolved copper concentrations during low flow in water from springs, streams, and mines in the East Mancos Watershed.

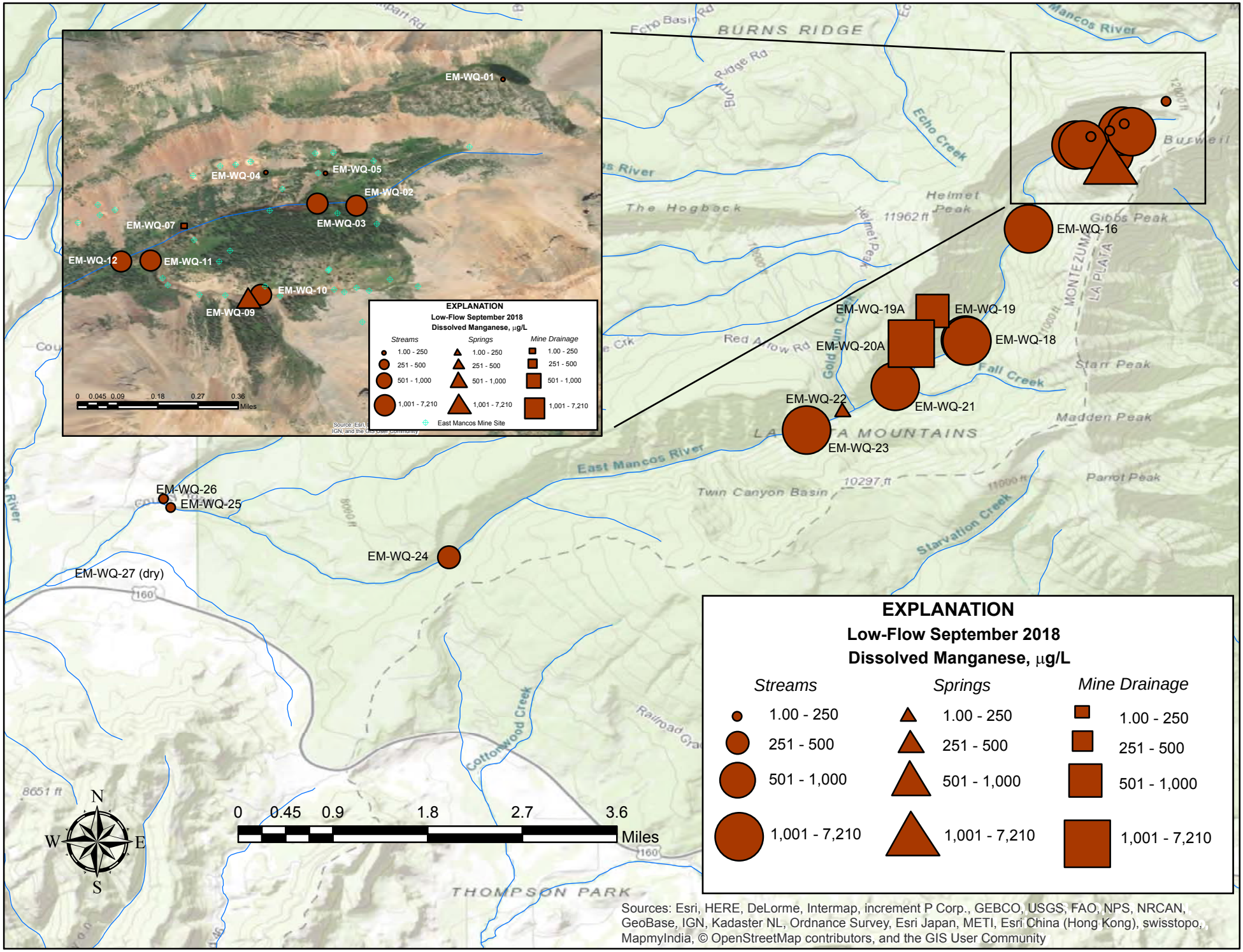

Figure 2-4. Distribution of dissolved manganese concentrations during low flow in water from springs, streams, and mines in the East Mancos Watershed.

Southwest Hydro-Logic, Durango, Colo.

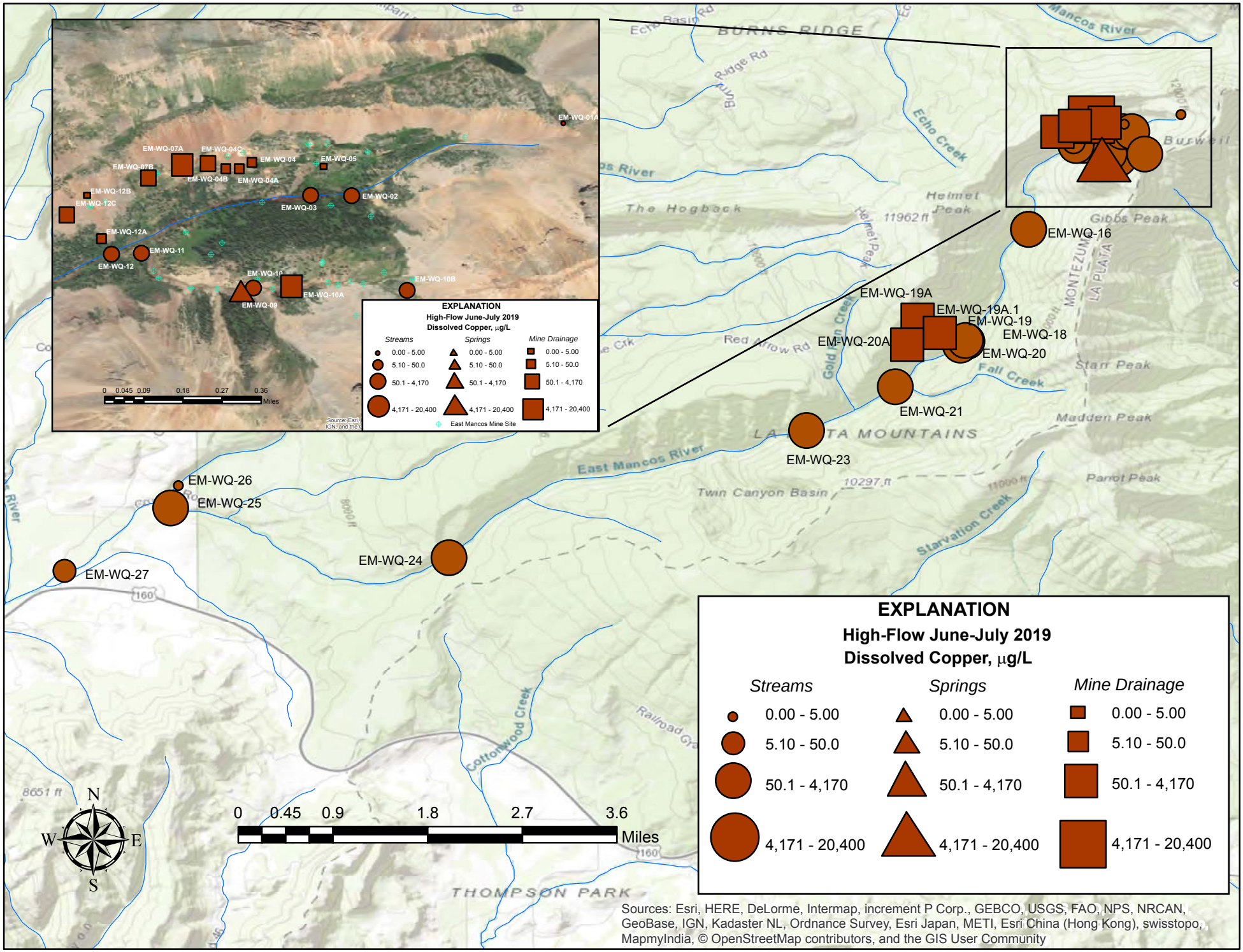

Figure 2-5. Distribution of dissolved copper concentrations during high flow in water from springs, streams, and mines in the East Mancos Watershed.

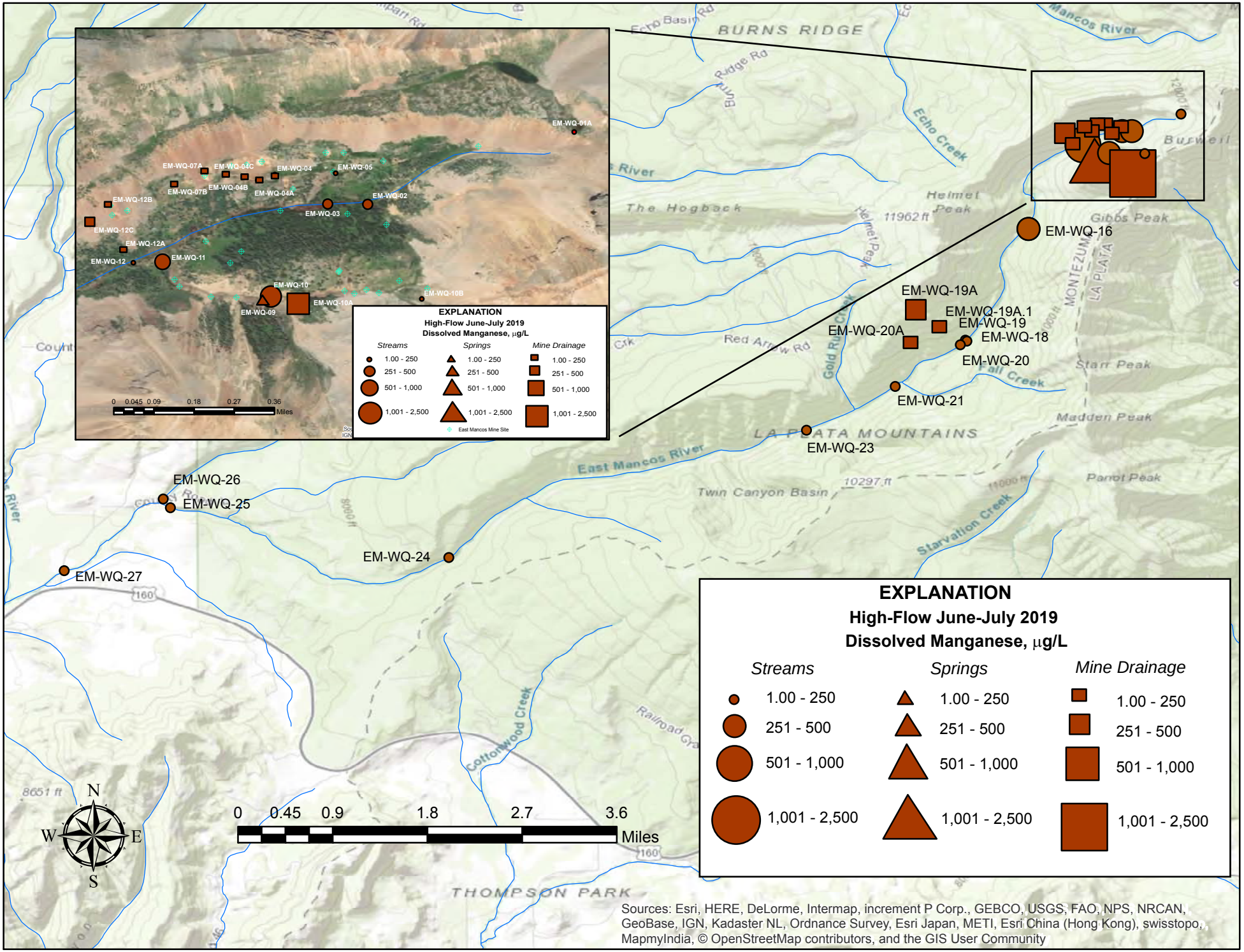

Figure 2-6. Distribution of dissolved manganese concentrations during high flow in water from springs, streams, and mines in the East Mancos Watershed.

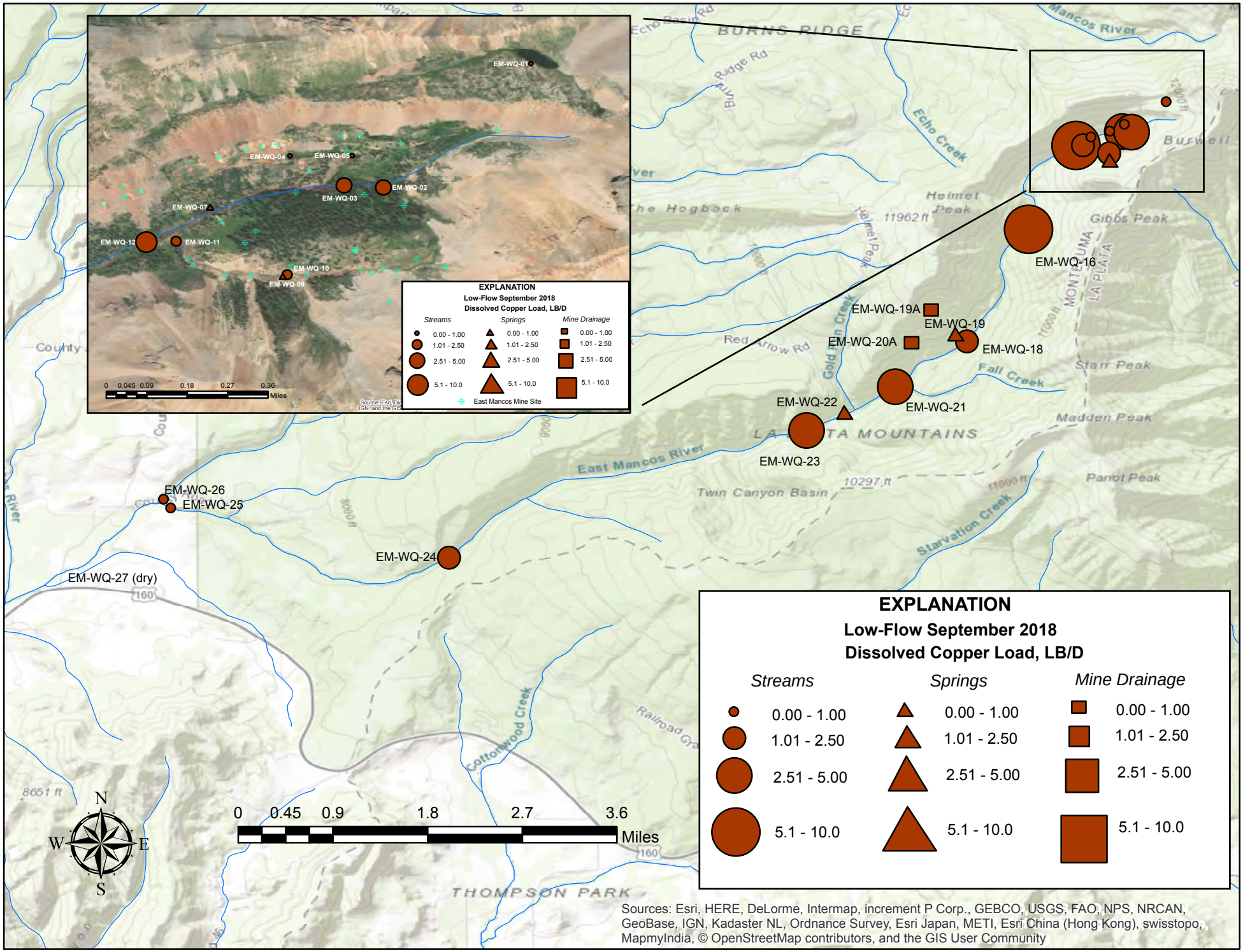

Figure 2-7. Distribution of dissolved copper loads during low flow in water from springs, streams, and mines in the East Mancos Watershed.

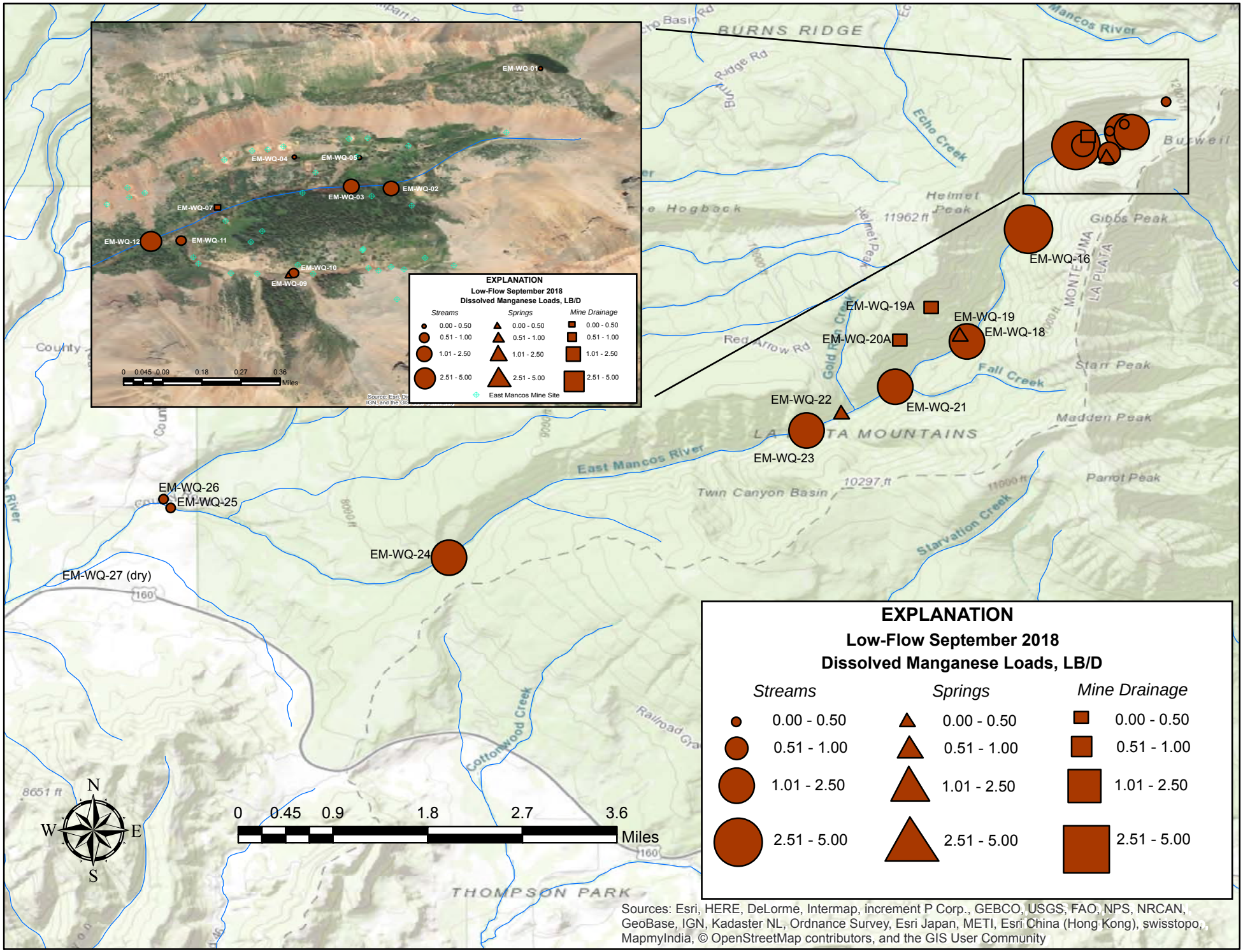

Figure 2-8. Distribution of dissolved manganese loads during low flow in water from springs, streams, and mines in the East Mancos Watershed.

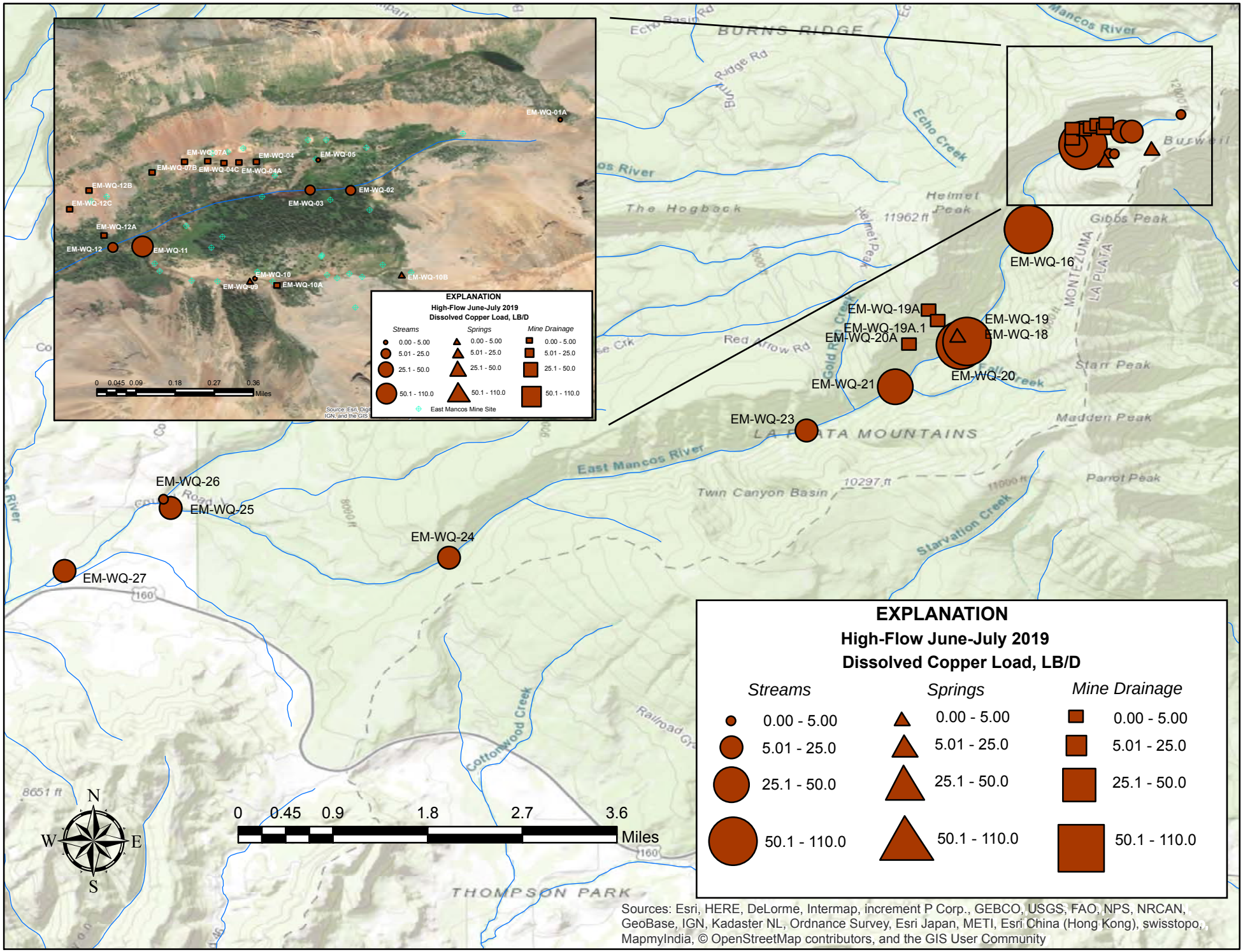

Figure 2-9. Distribution of dissolved copper loads during high flow in water from springs, streams, and mines in the East Mancos Watershed.

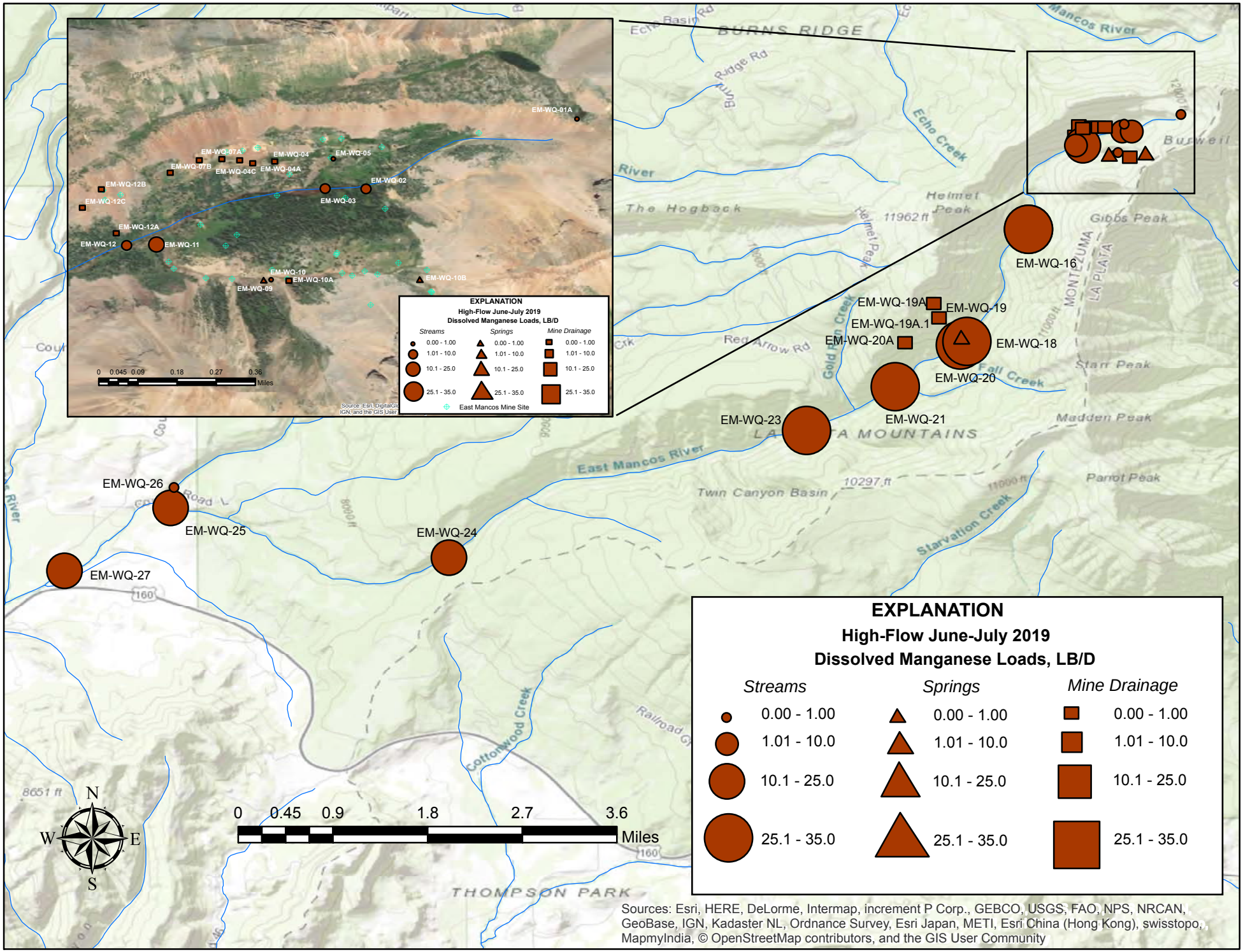

Figure 2-10. Distribution of dissolved manganese loads during high flow in water from springs, streams, and mines in the East Mancos Watershed.

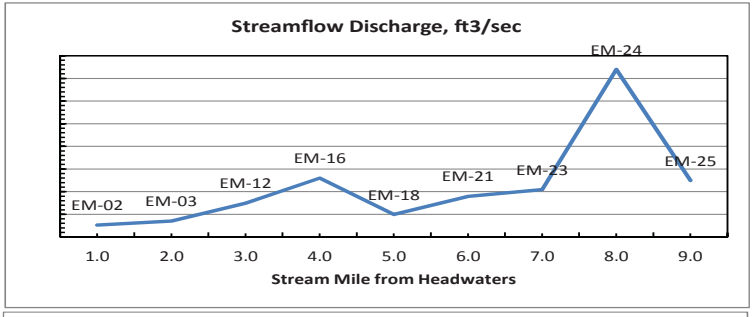

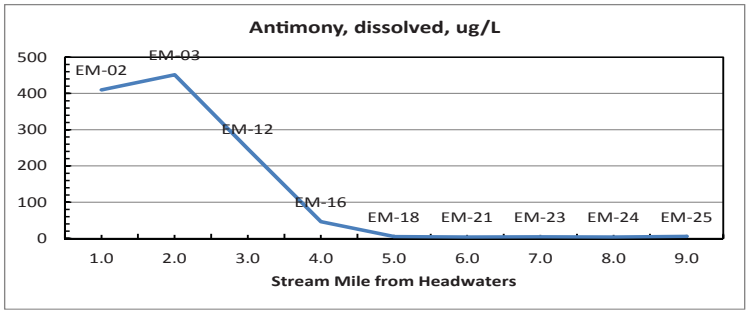

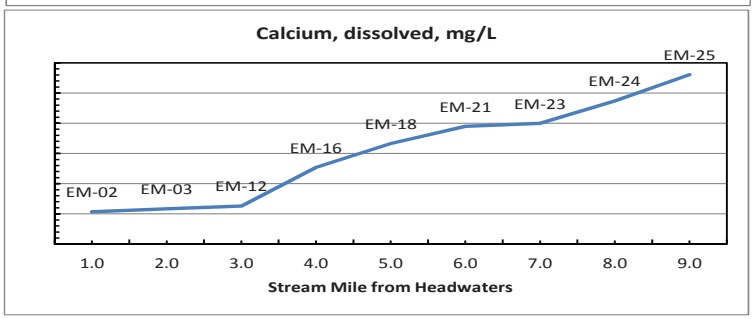

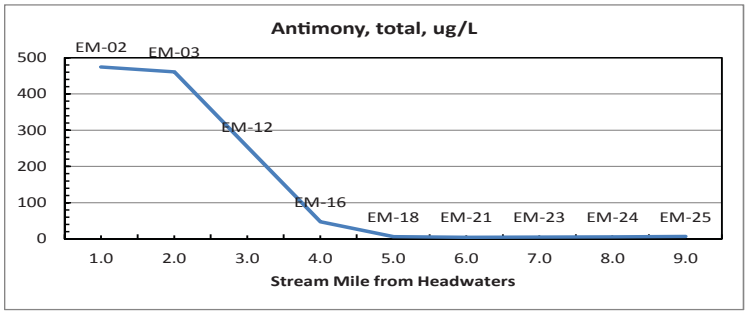

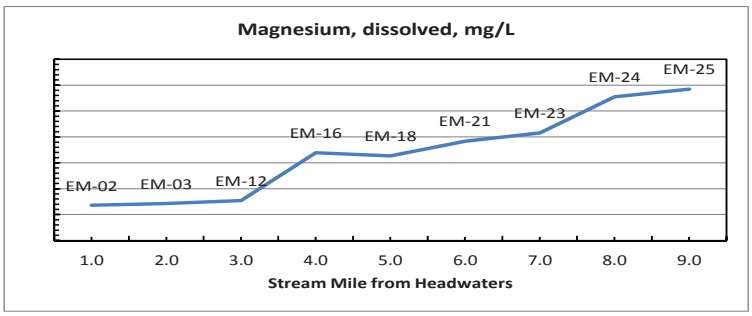

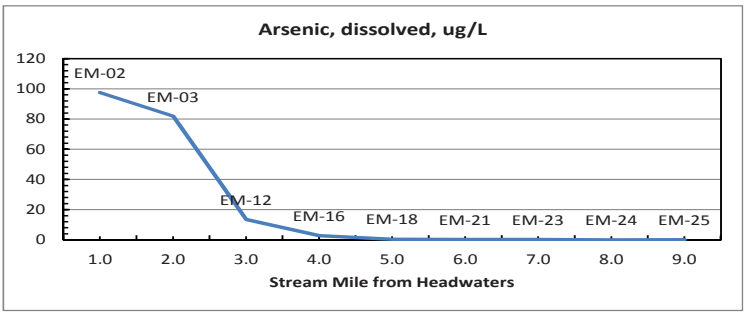

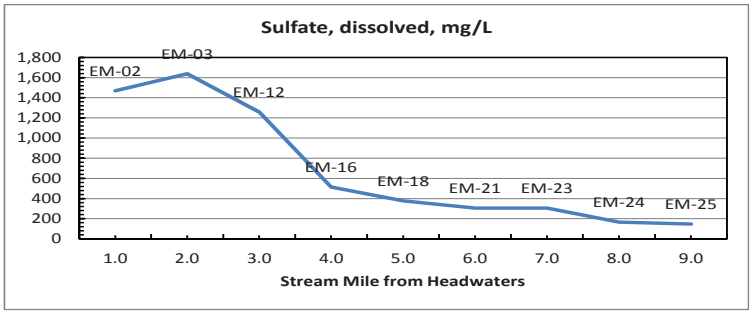

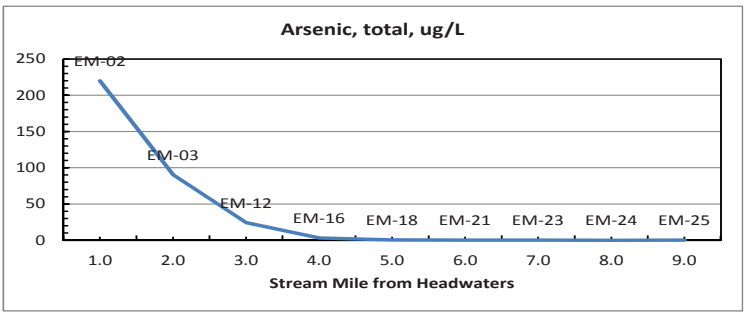

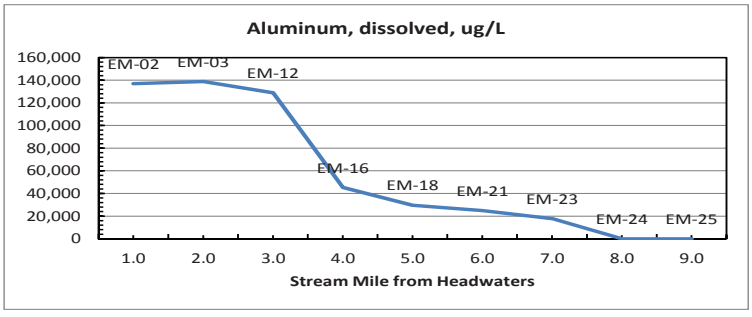

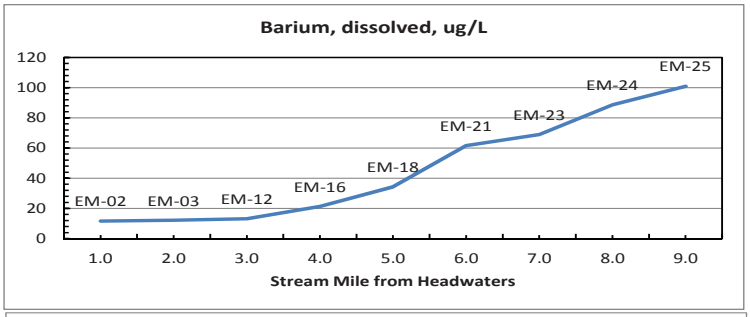

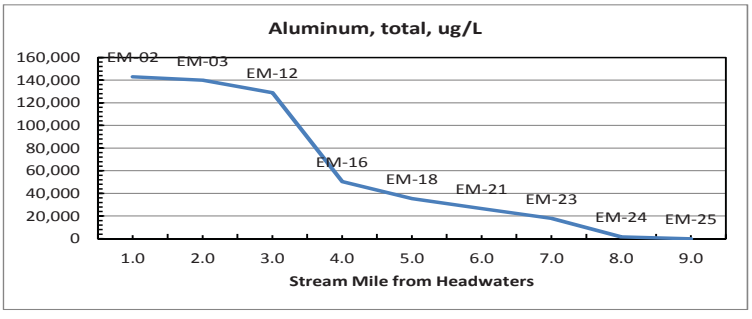

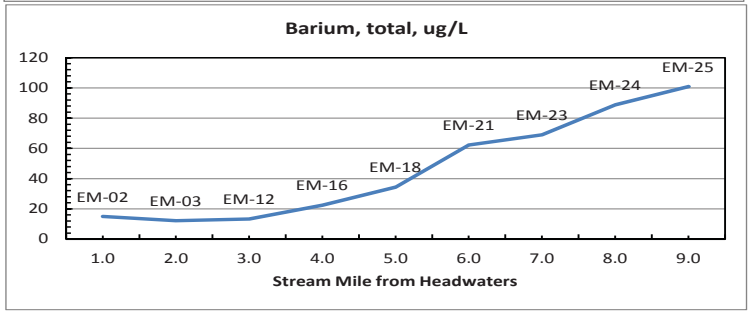

Figure 2-11A. Concentration profiles of dissolved and total metals during low flow in East Mancos River from the headwaters (EM-02) to the mouth (EM-25), September 2018.

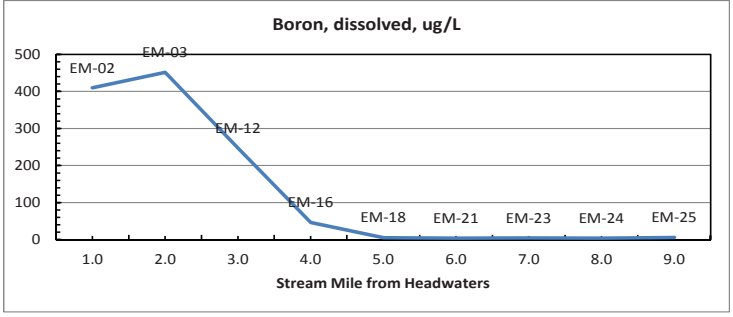

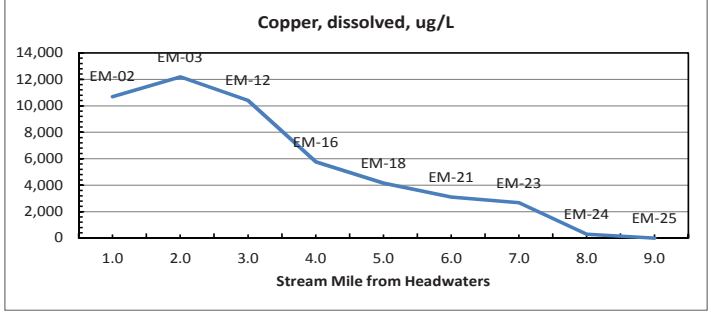

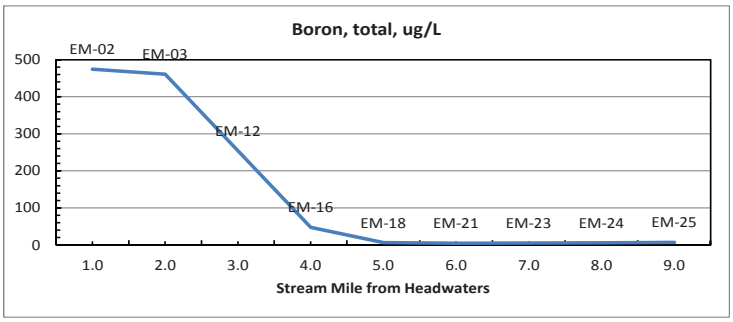

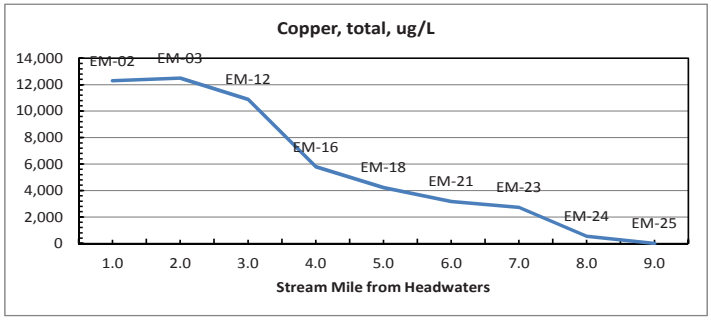

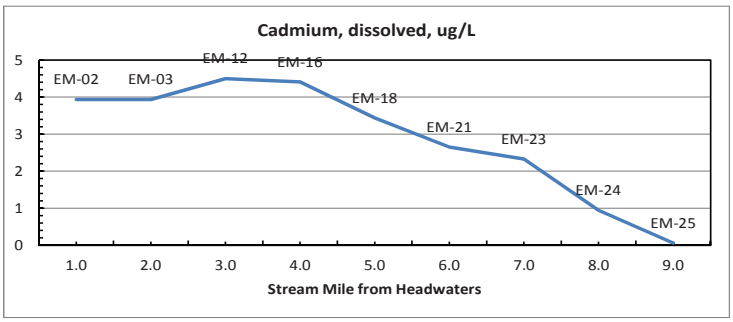

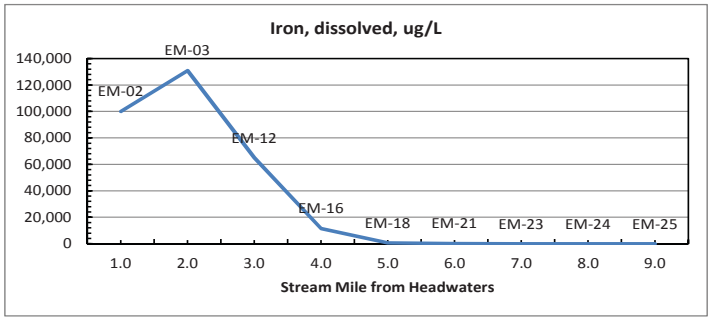

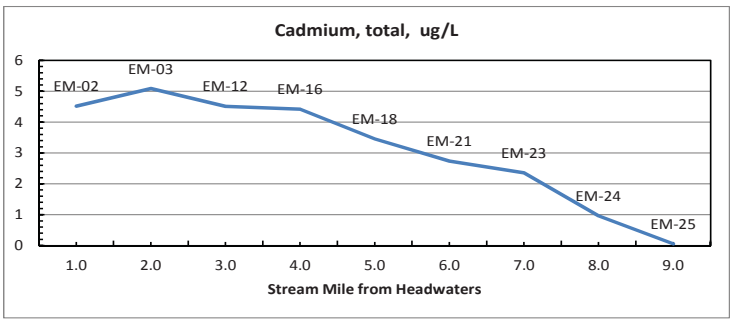

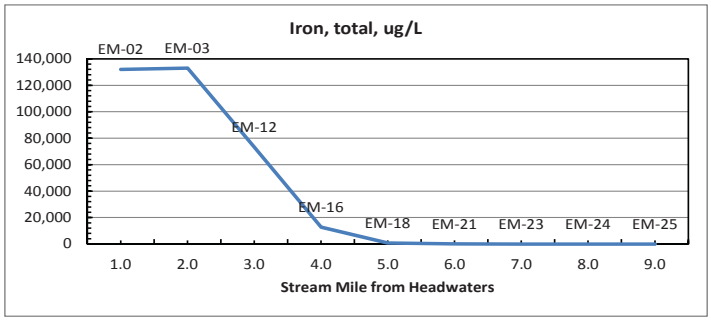

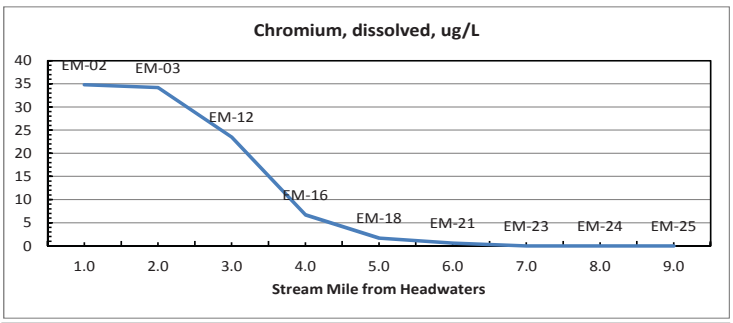

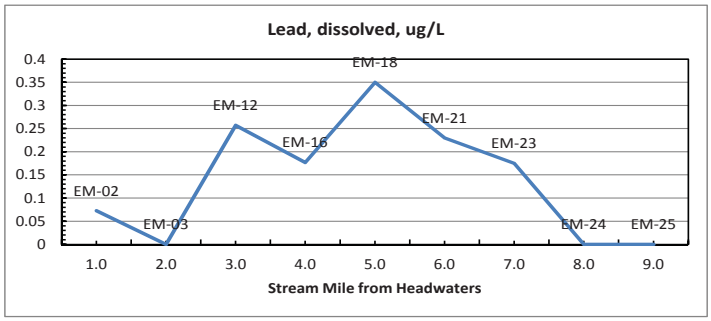

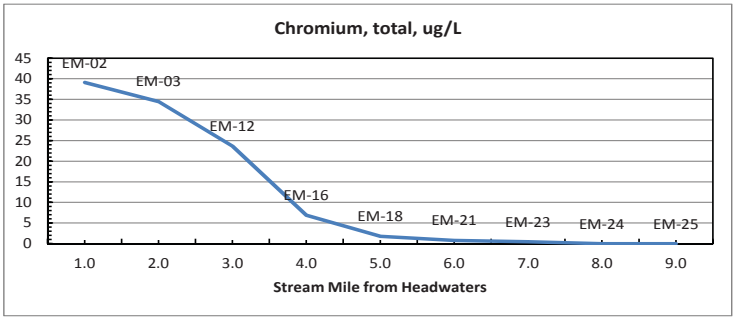

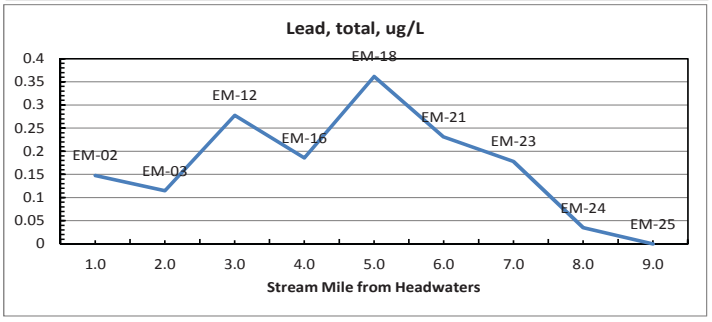

Figure 2-11B. Concentration profiles of dissolved and total metals in East Mancos River from the headwaters (EM-02) to the mouth (EM-25) during low flow, September 2018.

Figure 2-11C. Concentration profiles of dissolved and total metals in East Mancos River from the headwaters (EM-02) to the mouth (EM-25) during low flow, September 2018.

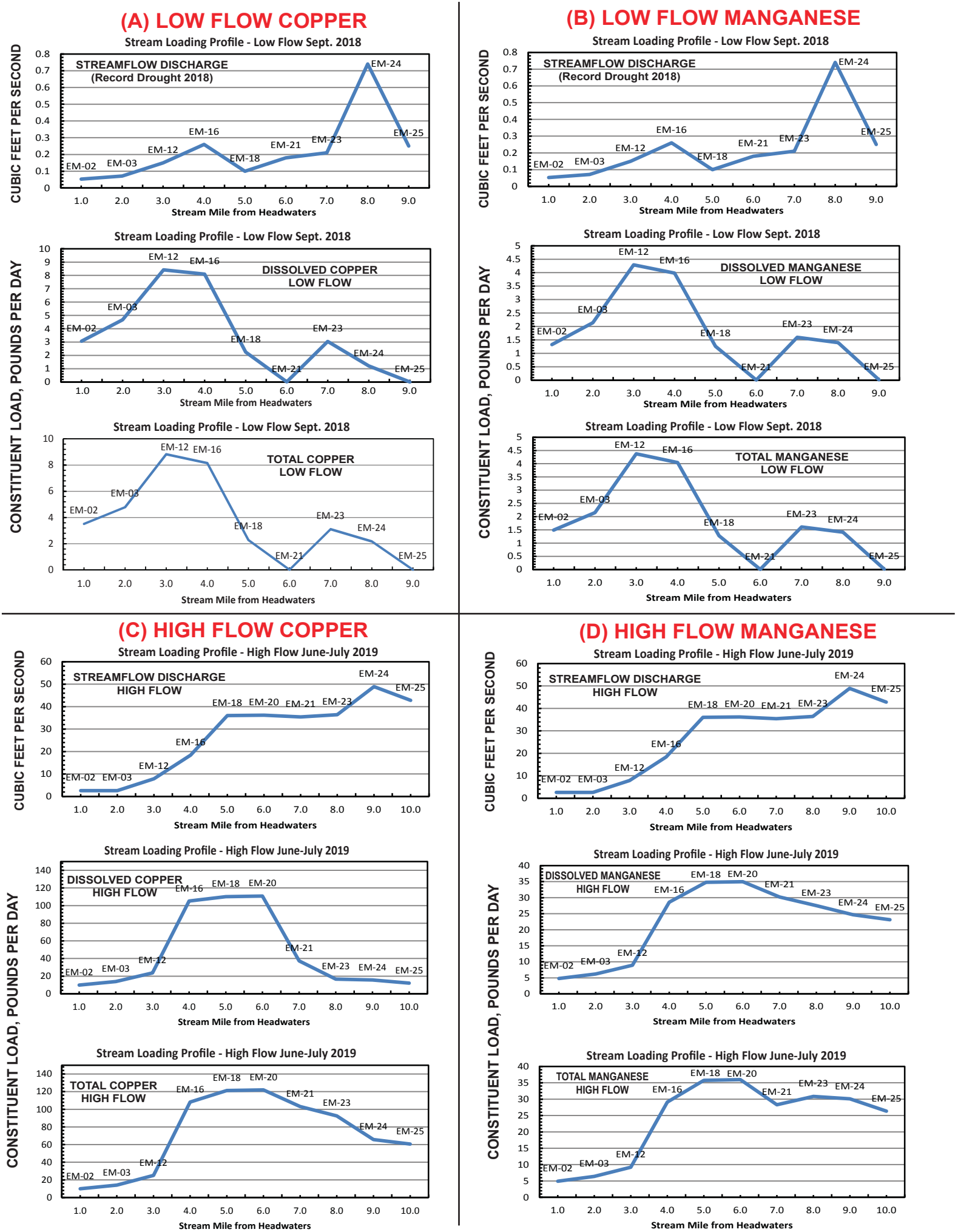

Figure 2-12. Longitudinal stream profiles during low and high flow showing discharge, dissolved and total copper loads, and dissolved and total manganese loads.

(A)

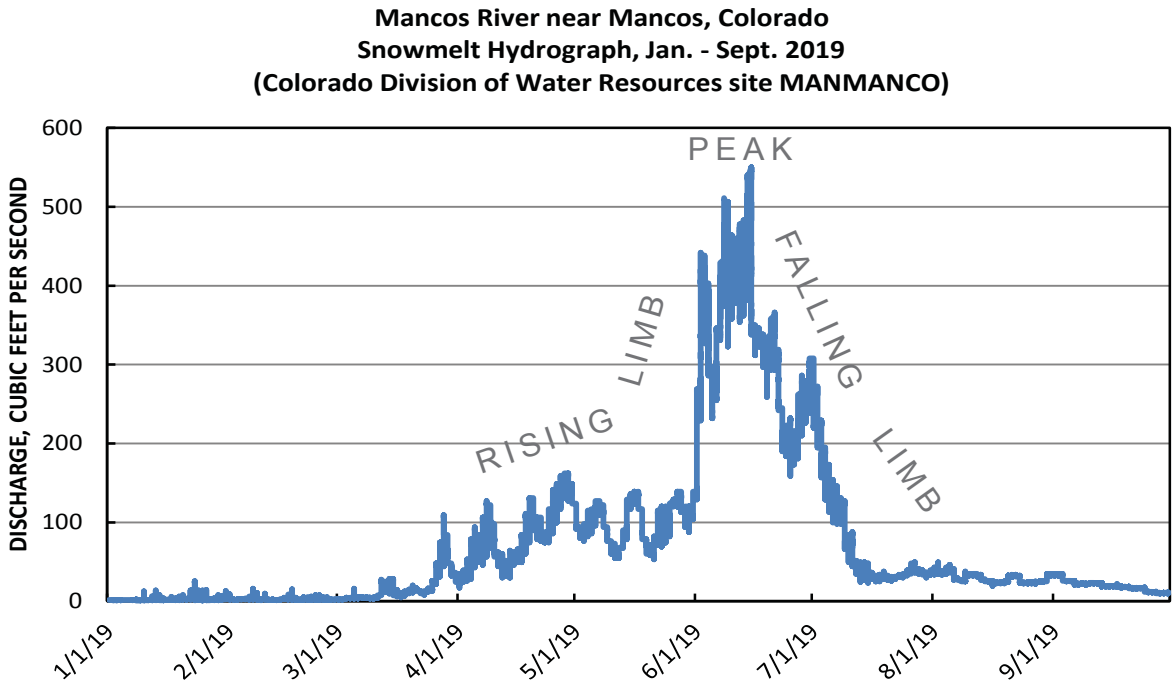

(B)

Date	Time	Streamflow Discharge at EM-WQ-25, ft3/sec	Streamflow Discharge at MANMANCO, ft3/sec
3/20/2019	16:00	5.1	19.4
3/28/2019	16:00	15.9	72.9
4/4/2019	17:45	17.41	72.9
4/9/2019	19:10	30.96	89.9
4/26/2019	18:45	54.98	113
6/12/2019	18:30	156	374
7/3/2019	10:00	42.8	201

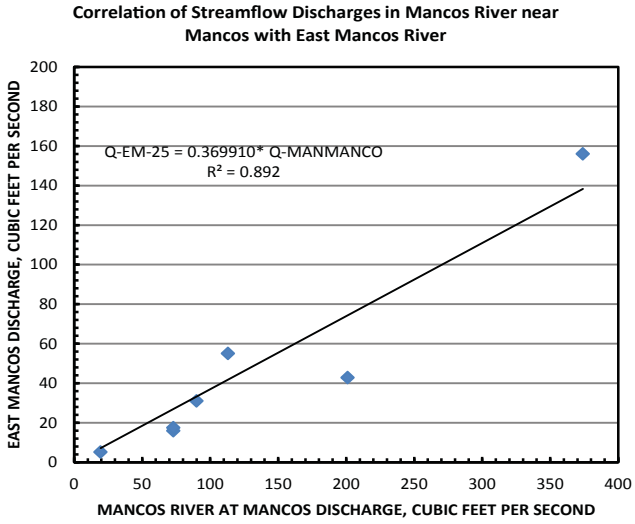

(C)

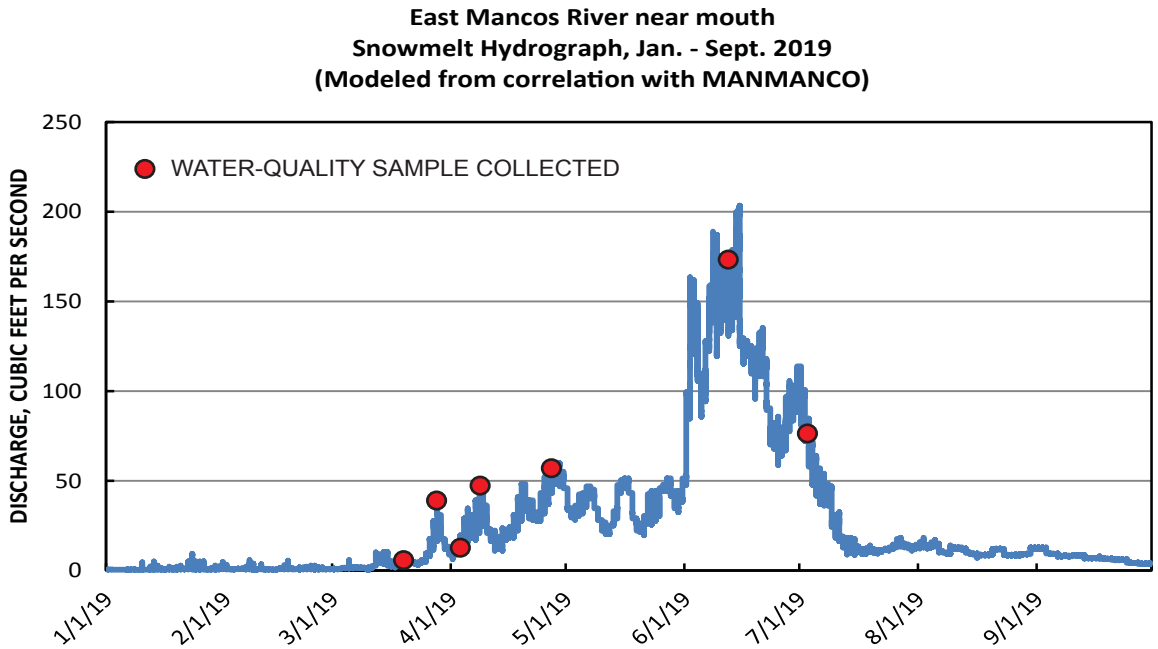

Figure 2-13. (A) Snowmelt runoff hydrograph for the Mancos River near Mancos, Colorado (actual data); (B) Correlation of streamflow discharges in Mancos River with East Mancos River (EM-WQ-25); and (C) modeled snowmelt runoff hydrograph for East Mancos River near mouth.

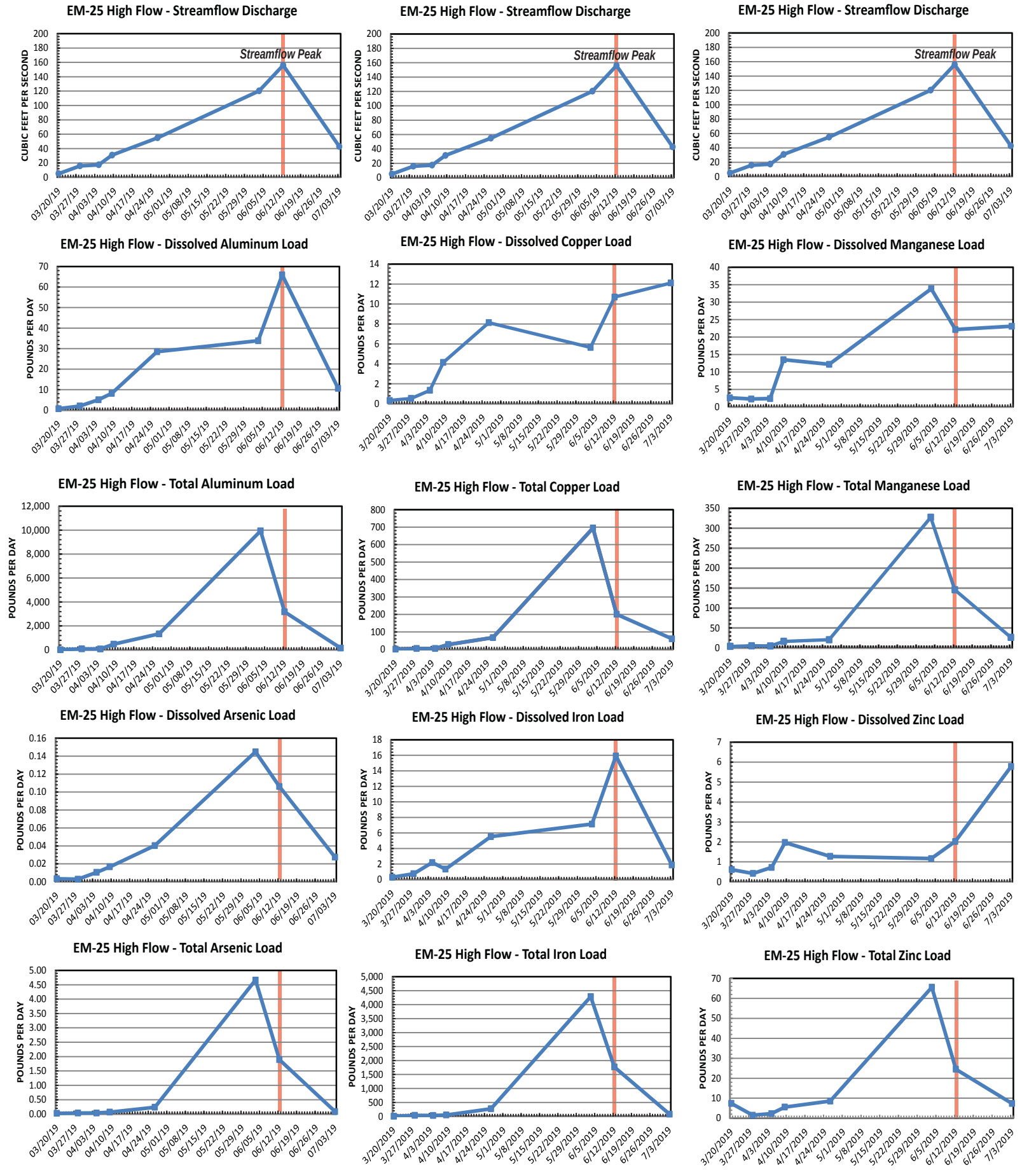

Figure 2-14. Time series of dissolved and total metal loads at site EM-WQ-25 (mouth of watershed) during snowmelt runoff period of March - July 2019. Streamflow peak is indicated by vertical line. Some metals showed a concentration peak before streamflow peak indicating flushing of metal solids accumulated on the streambed during fall and winter low-flow seasons.

10/18/17 -- EM-WQ-03

7/9/19 -- EM-WQ-03

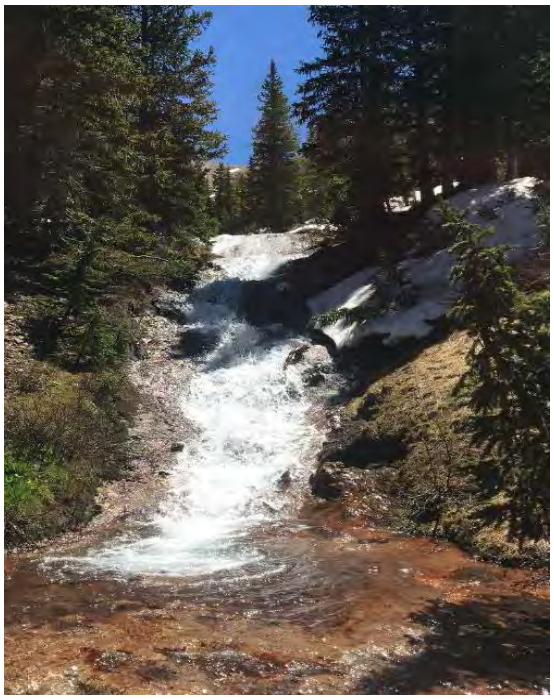

9/14/18 – EM-WQ-12, East Mancos above Burwell Trib

7/10/19 – EMWQ12, East Mancos above Burwell Trib

9/20/18 – EM-WQ-24

6/26/19 – EM-WQ-24

Figure 2-15. Photocomparison of the East Mancos River before snowmelt runoff showing mineral precipitates, and after snowmelt runoff showing that mineral precipitates had been scoured from the streambed. Mineral solids were transported out of the basin, and samples of this runoff was captured at site EM-WQ-25 during March-July 2019 (photos by Scott Roberts).

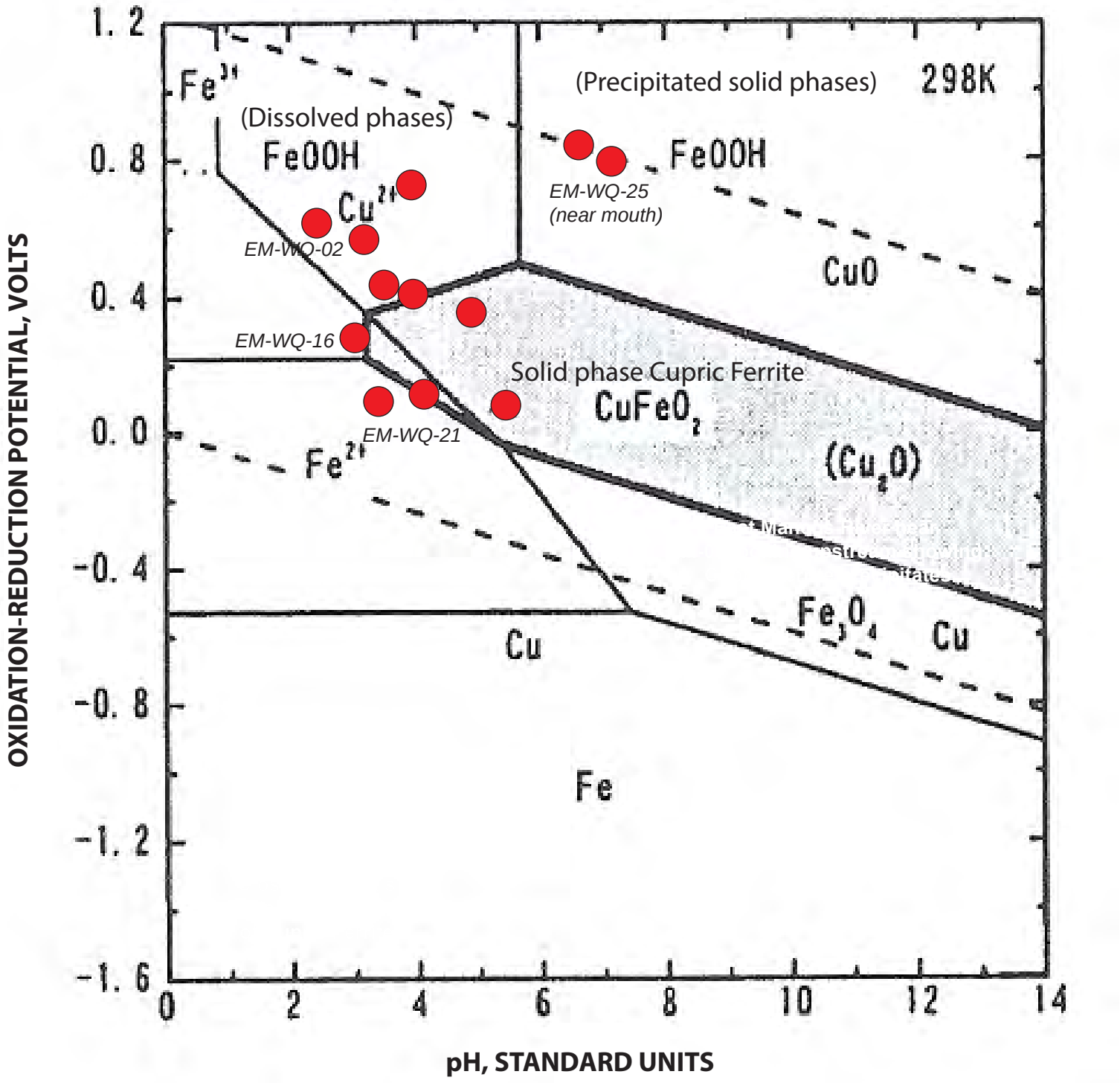

Figure 2-16. Stability field diagram for iron (Fe) and copper (Cu) dissolved and solid phases. Circles indicate data points for water from springs and streams in the East Mancos watershed.

Figure 2-17A. East Mancos River downstream from Rush Basin showing voluminous amounts of copper and and iron mineral precipitates on the streambed during low flow conditions of September 2018.

Figure 2-17B. East Mancos River downstream from Rush Basin showing red- orange, and copper-rust colored mineral precipitates on the streambed.

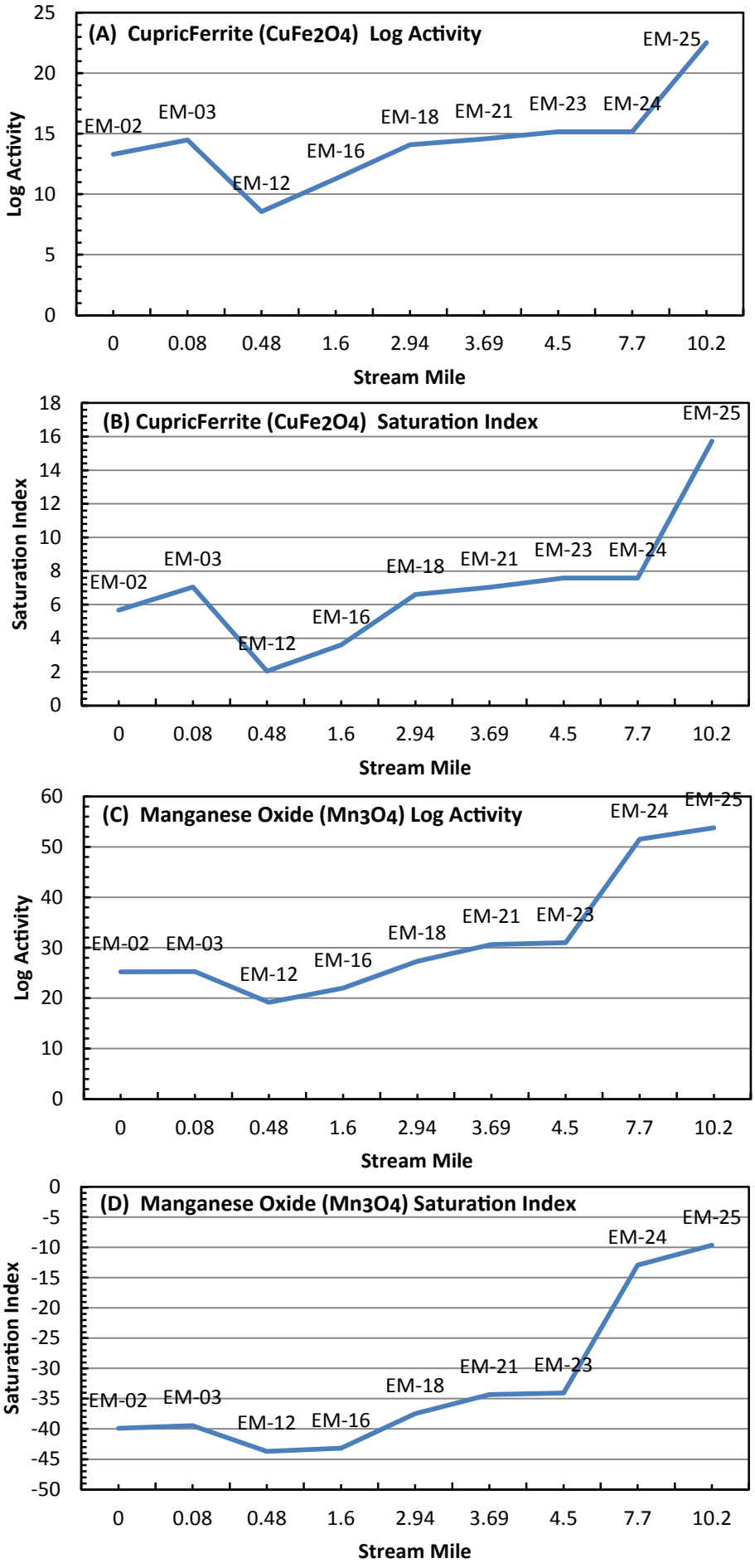

Figure 2-18. Longitudinal stream profile of cupric ferrite and manganese oxide log activity and saturation index, East Mancos River, low-flow samples September 2018.

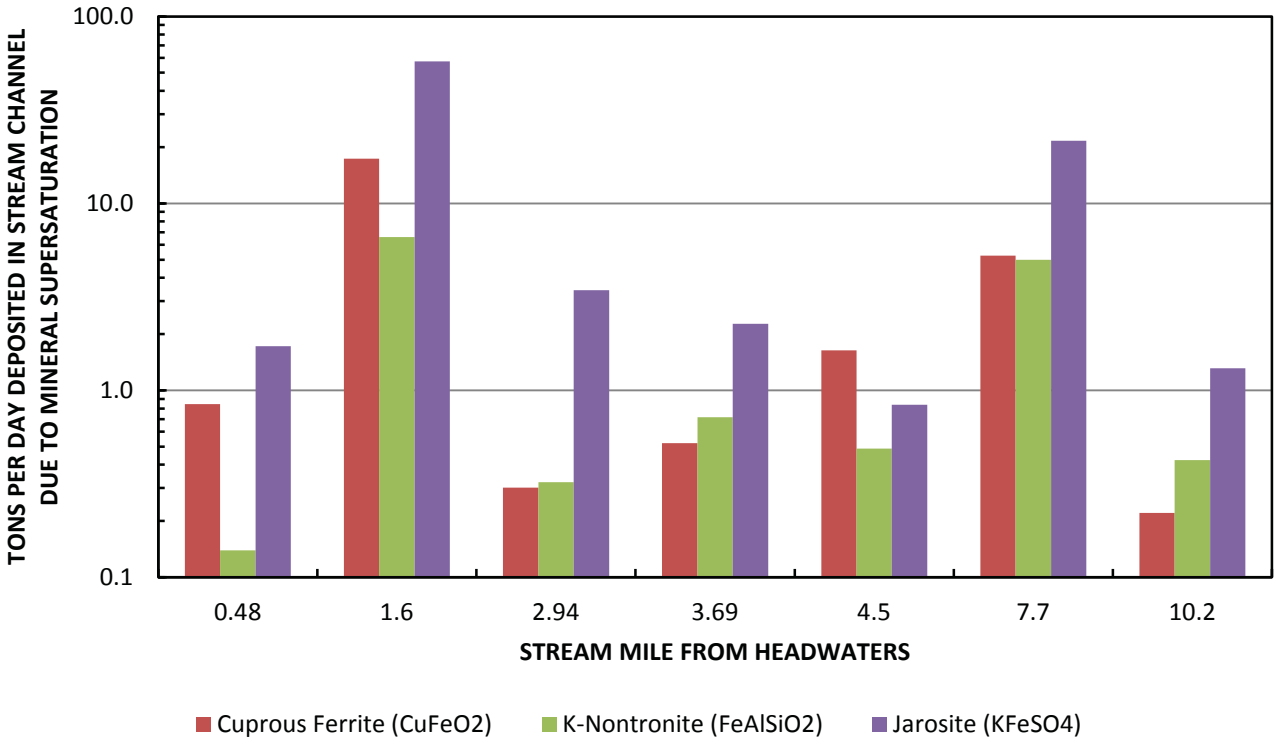

Figure 2-19. Examples of solid phase minerals deposited in the stream channel due to mineral supersaturation (results from geochemical modeling using Sept. 2018 low-flow data).

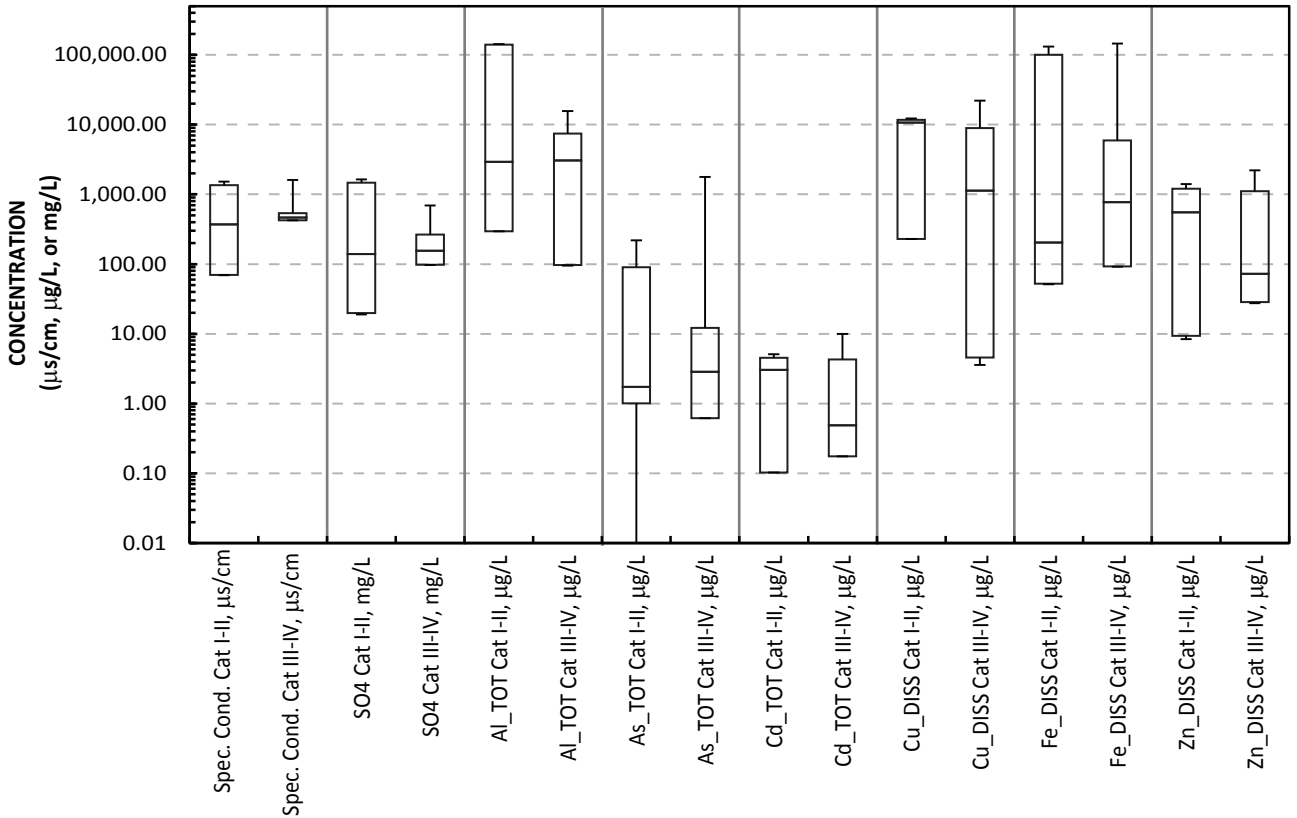

Figure 2-20. Boxplots showing concentration ranges of selected constituents during low flow September 2018.

Table 1-1. Laboratory parameters and detection limits for analysis of water-quality samples

[TR, total recoverable; Diss, dissolved; g/L, micrograms per liter; mg/L, milligrams per liter]

EPA Method	Target Analytes	Instrument	Fraction Evaluated	Units	Laboratory*
200.7	Aluminum	ICP-OES	TR & Diss	µg/L	LDS
	Barium	ICP-OES	TR & Diss	µg/L	LDS
	Beryllium	ICP-OES	TR & Diss	µg/L	LDS
	Boron	ICP-OES	TR & Diss	µg/L	LDS
	Calcium	ICP-OES	Diss	mg/L	LDS
	Iron	ICP-OES	TR & Diss	µg/L	LDS
	Chromium	ICP-OES	TR & Diss	µg/L	LDS
	Copper	ICP-OES	TR & Diss	µg/L	LDS
	Magnesium	ICP-OES	Diss	mg/L	LDS
	Manganese	ICP-OES	TR & Diss	µg/L	LDS
	Potassium	ICP-OES	TR & Diss	mg/L	LDS
	Silica	ICP-OES	Diss	mg/L	GAL
	Strontium	ICP-OES	TR & Diss	µg/L	LDS
	Vanadium	ICP-OES	TR & Diss	µg/L	LDS
2340B	Hardness	Calculated	Diss	mg/L	LDS
200.8	Antimony	ICP-MS	TR & Diss	µg/L	LDS
	Arsenic	ICP-MS	TR & Diss	µg/L	LDS
	Cadmium	ICP-MS	TR & Diss	µg/L	LDS
	Lead	ICP-MS	TR & Diss	µg/L	LDS
	Molybdenum	ICP-MS	TR & Diss	µg/L	LDS
	Nickel	ICP-MS	TR & Diss	µg/L	LDS
	Selenium	ICP-MS	TR & Diss	µg/L	LDS
	Silver	ICP-MS	TR & Diss	µg/L	LDS
	Sodium	ICP-MS	Diss	mg/L	LDS
	Thallium	ICP-MS	TR & Diss	µg/L	LDS
	Uranium	ICP-MS	TR & Diss	µg/L	LDS
	Zinc	ICP-MS	TR & Diss	µg/L	LDS
2320B	Alkalinity	Titration, endpoint	Total	mg/L	LDS,SWHL
245.1	Mercury	Cold Vapor Atomic Absorption	TR	mg/L	LDS
415.3	Carbon, Dissolved Organic	UVA	Diss	mg/L	GAL
300.0	Chloride	Ion chromatography	Diss	mg/L	GAL
	Fluoride		Diss	mg/L	GAL
	Sulfate		Total	mg/L	LDS

* LDS - CDPHE Laboratory Services Division; GAL – Green Analytical Laboratories; SWHL – Southwest Hydro-Logic

Table 1-2. Water-quality field parameters and detection limits

Parameter	Method	Reporting units	Minimum reporting limit	Precision, in RSD
Date, time	--	mm/dd/yyyy, 24 hr	--	--
Stream stage	--	ft	0	±10 percent
Discharge, instantaneous	Flow anemometer (pygmy or AA meter), or flow sensor (Hach 950)	cubic feet per second (ft^3/s)	0.001 ft^3/s	±10 percent
Specific conductance	Field electro-metric meter	microsiemens per centimeter (S/cm)	10 S/cm	±10 percent
pH	Double-junction electrometric probe	Standard Units	1.68	± 0.05 pH units
Water temperature	Digital thermometer	°C	-10 °C	±1 percent
Dissolved oxygen	Field meter, gold cathode probe	milligrams per liter (mg/L)	0 mg/L	±1 percent
Alkalinity, as $CaCO_3$	Incremental breakpoint titration	mg/L as $CaCO_3$	0.5 mg/L as $CaCO_3$	±5 percent
Dissolved copper, cupric	Ion-selective electrode	mg/L	0.010 mg/L	±5 percent
Ferrous iron	1,10 phenanthroline spectrophotometry	mg/L	0.010 mg/L	±0.009 mg/L

Table 1-3. Laboratory parameters and detection limits for analysis of leachate from waste-rock samples

[Diss, dissolved; g/L, micrograms per liter; mg/L, milligrams per liter; MDL, method detection limit; PQL, practical quantitation limit]

EPA Method	Target Analytes	Instrument	Fraction Evaluated	Units	Laboratory*
200.7	Aluminum	ICP-OES	Diss	µg/L	LDS
	Barium	ICP-OES	Diss	µg/L	LDS
	Beryllium	ICP-OES	Diss	µg/L	LDS
	Boron	ICP-OES	Diss	µg/L	LDS
	Calcium	ICP-OES	Diss	mg/L	LDS
	Iron	ICP-OES	Diss	µg/L	LDS
	Chromium	ICP-OES	Diss	µg/L	LDS
	Copper	ICP-OES	Diss	µg/L	LDS
	Magnesium	ICP-OES	Diss	mg/L	LDS
	Manganese	ICP-OES	Diss	µg/L	LDS
	Strontium	ICP-OES	Diss	µg/L	LDS
	Vanadium	ICP-OES	Diss	µg/L	LDS
200.8	Antimony	ICP-MS	Diss	µg/L	LDS
	Arsenic	ICP-MS	Diss	µg/L	LDS
	Cadmium	ICP-MS	Diss	µg/L	LDS
	Lead	ICP-MS	Diss	µg/L	LDS
	Molybdenum	ICP-MS	Diss	µg/L	LDS
	Nickel	ICP-MS	Diss	µg/L	LDS
	Selenium	ICP-MS	Diss	µg/L	LDS
	Silver	ICP-MS	Diss	µg/L	LDS
	Thallium	ICP-MS	Diss	µg/L	LDS
	Uranium	ICP-MS	Diss	µg/L	LDS
	Zinc	ICP-MS	Diss	µg/L	LDS
245.1	Mercury	Cold Vapor AA	Diss	mg/L	LDS

* LDS - CDPHE Laboratory Services Division

Table 2-1. Site Categories for Natural Background Characterization (Mast and others, 2007)

I	No manmade disturbances upgradient or upstream from the water-quality sampling site
II	Some potential manmade disturbances upgradient or upstream from the water-quality sampling site
III	Some manmade disturbances upgradient or upstream from the water-quality sampling site
IV	Definite manmade disturbances upgradient or upstream from the water-quality sampling site
	Information used in assignment of categories
	Number of mines visibly draining w ater upgradient from sampling site
	Number of mines (draining/not draining) upgradient from sampling site
	Number of mine-w aste dumps upgradient from sampling site
	Number of prospects upgradient from sampling site
	Number of shafts upgradient from sampling site
	Inventory of exploration drill holes, abandoned mill sites, buildings and machinery, logging, grazing, roads upgradient from sampling site
	References used for determination of categories:
	• Direct observations
	• Topographic maps
	• Aerial photographs
	• Published mine maps
	• Written documentation
	• Oral communication

Table 2-2. Summary of natural background (Category I-II) and mining-affected (Category III-IV) for selected constituents

Site Category	Specific Conductance us/cm	pH, S.U.	Water temp, oC	Hardness, mg/L as CaCO3	Dissolved Sulfate, mg/L	Dissolved Aluminum, ug/L	Dissolved Cadmium, ug/L	Dissolved Copper, ug/L	Dissolved Iron, ug/L	Dissolved Lead, ug/L	Dissolved Manganese ug/L	Dissolved Nickel, ug/L	Dissolved Thallium, ug/L	Dissolved Zinc, ug/L
MEDIAN VALUES, LOW FLOW SEPTEMBER 2018														
I - II	370.7	4.3	8.1	34.7	139.0	2,910	3.5	10,700	204.0	0.07	1,860	195.0	14.2	551.0
III - IV	465.8	4.6	8.1	158.5	155.0	4,885	0.8	1,131	775.0	0.17	1,255	11.8	51.2	72.5
MEDIAN VALUES, HIGH FLOW JULY 2019														
I - II	81.2	5.2	1.5	7.1	37.6	3,162	0.4	846	49.4	ND	186	15.1	1.3	104.2
III - IV	282.2	3.8	4.0	16.8	44.9	635	0.3	181	953.0	0.33	123	3.9	2.9	30.2

Table 2-3. Locations and descriptions of mine sites where waste-rock samples were tested for leachate potential

Map No.	Site Name	Sample Type*	Latitude, dd	Longitude, dd	Altitude, ft	Leachate pH, S.U.	Specific Conductance, µs/cm	Copper, cupric, µg/L	Acidity, mg/L as $CaCO_3$	Acid neutralizing requirement, kg $CaCO_3$ / 1000 L of wastewater
EM-MS-01	Background 1	B	37.419190	-108.097030	11,731	5.37	41	100	10	0.0
EM-MS-02	Background 2	B	37.421951	-108.094648	11,820	3.98	58	< 1	15	0.1
EM-MS-03	Background 3	B	37.424331	-108.090435	11,796	5.34	14	< 1	< 1.0	< 0.1
EM-MS-04	Doyle 1	WR	37.423943	-108.101241	11,398	3.73	158	346	15	0.1
EM-MS-05	Doyle 10	WR	37.422192	-108.110349	11,520	3.66	142	< 1	< 1.0	< 0.1
EM-MS-06	Doyle 2	WR	37.423666	-108.103326	11,368	2.44	2,680	< 1	1,450	2.4
EM-MS-07	Doyle 3	WR	37.423561	-108.103829	11,372	2.10	5,230	1,032,720	6,080	12.4
EM-MS-08	Doyle 4	WR	37.423517	-108.104322	11,356	4.96	84	< 1	< 1.0	< 0.1
EM-MS-09	Doyle 5	WR	37.423209	-108.105205	11,297	3.72	103	< 1	10	0.01
EM-MS-10	Doyle 6	WR	37.422069	-108.107740	11,298	2.20	3,120	< 1	2,600	3.93
EM-MS-11	Doyle 7	WR	37.422234	-108.108288	11,300	4.86	24	< 1	< 1.0	< 0.1
EM-MS-12	Doyle 8	WR	37.421913	-108.108230	11,217	2.65	1,332	< 1	576	0.95
EM-MS-13	Doyle 8 Repeat	WR	37.421913	-108.108230	11,217	2.68	1,358	< 1	600	1.12
EM-MS-14	Doyle 9	WR	37.421654	-108.108940	11,211	3.06	424	< 1	70	0.1
EM-MS-15	Doyle Mill 2	MT	37.422771	-108.102310	11,262	4.35	48	< 1	< 1.0	< 0.1
EM-MS-16	DRMS-31	WR	37.409119	-108.120677	10,910	4.22	50	< 1	< 1.0	< 0.1
EM-MS-17	Georgia Girl (Lower)	WR	37.417926	-108.113715	10,158	3.92	127	< 1	< 1.0	< 0.1
EM-MS-18	Georgia Girl (Upper)	WR	37.418850	-108.114771	10,590	4.08	62	< 1	10	0.01
EM-MS-19	Gold Dollar Mine	WR	37.393297	-108.131070	10,000	6.81	122	< 1	< 1.0	< 0.1
EM-MS-20	KB-1	WR	37.419583	-108.097917	11,635	4.62	54	< 1	< 1.0	< 0.1
EM-MS-21	KB-2	WR	37.418201	-108.096424	11,880	5.25	15	< 1	< 1.0	< 0.1
EM-MS-22	Kentucky (Lower)	WR	37.393548	-108.139273	9,844	4.91	37	79.5	< 1.0	< 0.1
EM-MS-23	Lady Stafford	WR	37.416417	-108.117614	11,018	4.37	45	< 1	15	0.10
EM-MS-24	Red Arrow Gold Run	WR	37.384347	-108.139552	9,480	5.05	541	< 1	< 1.0	< 0.1
EM-MS-25	Red Arrow Historic Level	WR	37.384310	-108.138644	9,280	6.41	53	< 1	< 1.0	< 0.1
EM-MS-26	Red Arrow River Level	WR	37.383548	-108.138553	9,160	7.03	43	< 1	15	0.02
EM-MS-27	Red Arrow Tailings	MT	37.383884	-108.140843	9,160	4.36	240	798	20	0.13
EM-MS-28	Thunder Mine	WR	37.397058	-108.127764	10,524	2.21	3,410	< 1	880	1.75
EM-MS-29	WR-1	WR	37.418821	-108.097772	11,689	4.06	187	1,965	20	0.13
EM-MS-30	WR-2	WR	37.424164	-108.096233	11,557	4.79	37	< 1	< 1.0	< 0.1
EM-MS-31	WR-3	WR	37.420071	-108.100812	11,513	3.71	128	371	30	0.20
EM-MS-32	WR-4	WR	37.422057	-108.102718	11,222	5.84	22	< 1	10	0.01
EM-MS-33	WR-5	MT	37.421078	-108.105167	11,010	4.20	50	< 1	10	0.01
EM-MS-34	WR-6	WR	37.417434	-108.110734	10,948	2.91	612	< 1	128	0.98
EM-MS-35	WR-7	WR	37.413279	-108.112586	10,498	5.64	14	< 1	< 1.0	< 0.1

*B=background; WR=waste rock; MT=mill tailings

Table 3-1. Mass loading summary for Category III-IV sites compared with mainstem sites during low flow and high flow (waste-rock leachate compared during low flow)

Samples representing	Discharge, ft^3/sec	Field Specific Conduc-tance, µS/cm	Field pH, standard units	Water Temp., °C	Copper, dissolved, LOAD, lb/d	Copper, total, LOAD, lb/d	Iron, dissolved, LOAD, lb/d	Iron, total, LOAD, lb/d	Manganese, dissolved, LOAD, lb/d	Manganese, total, LOAD, lb/d	Zinc, dissolved, LOAD, lb/d	Zinc, total, LOAD, lb/d
LOW FLOW, SEPT 2018												
Mass Loading Sum* for samples from Category III-IV sites (n=5), low flow Sept 2019	0.006	465.8	4.65	8.05	0.21	0.22	2.36	2.43	0.02	0.02	0.02	0.02
Waste rock leachate mass loading* simulating snowmelt and percolation through waste rock piles, sum of 32 mine waste rock sites**	--	124.5	4.21	--	0.29	--	82.50	--	0.68	--	0.17	--
EM-WQ-16, East Mancos River above Silver Falls, 9/21/18	0.26	867	3.10	7.3	8.10	8.15	16.28	18.10	3.99	4.04	0.99	0.99
EM-WQ-21, East Mancos River at river crossing, 9/19/18	0.18	494	4.23	8.5	3.02	3.09	0.14	0.19	1.68	1.70	0.41	0.41
EM-WQ-23, East Mancos River below Red Arrow, 9/19/18	0.21	445	4.31	8.1	3.05	3.11	0.05	0.13	1.60	1.61	0.43	0.44
EM-WQ-24, East Mancos River, downstream reach, 9/20/18	0.74	370	7.07	10.7	1.21	2.18	0.002	0.10	1.40	1.41	0.68	0.70

Samples representing	Discharge, ft^3/sec	Field Specific Conduc-tance, µS/cm	Field pH, standard units	Water Temp., °C	Copper, dissolved, LOAD, lb/d	Copper, total, LOAD, lb/d	Iron, dissolved, LOAD, lb/d	Iron, total, LOAD, lb/d	Manganese, dissolved, LOAD, lb/d	Manganese, total, LOAD, lb/d	Zinc, dissolved, LOAD, lb/d	Zinc, total, LOAD, lb/d
HIGH FLOW, JUNE-JULY 2019												
Mass Loading Sum* for samples from Category III-IV sites (n=13), high flow June-July 2019	0.3	284.9	3.74	4	3.07	3.17	21.54	22.80	0.15	0.15	0.13	0.13
EM-WQ-16, East Mancos River above Silver Falls, 7/8/19	18.39	137.3	4.54	6.9	105.2	108.2	113.2	127.1	28.6	29.1	8.69	8.75
EM-WQ-21, East Mancos River at river crossing, 7/3/19	35.4	110.8	6.31	5.1	37.3	103.2	ND	157.1	30.2	28.3	8.31	9.15
EM-WQ-23, East Mancos River below Red Arrow, 7/3/19	36.4	114	6.56	6.4	16.70	92.54	0.29	123.0	27.5	30.8	6.1	9.2
EM-WQ-24, East Mancos River, downstream reach, 6/26/19	48.9	109.3	6.93	10.1	15.65	65.72	4.778	110.1	24.7	30.1	5.2	7.6

*Median values for specific conductance, pH, and water temperature

**Total analyses were not performed

Figures and Tables for Section 4. WATER-QUALITY STANDARDS AND AQUATIC TOXICITY

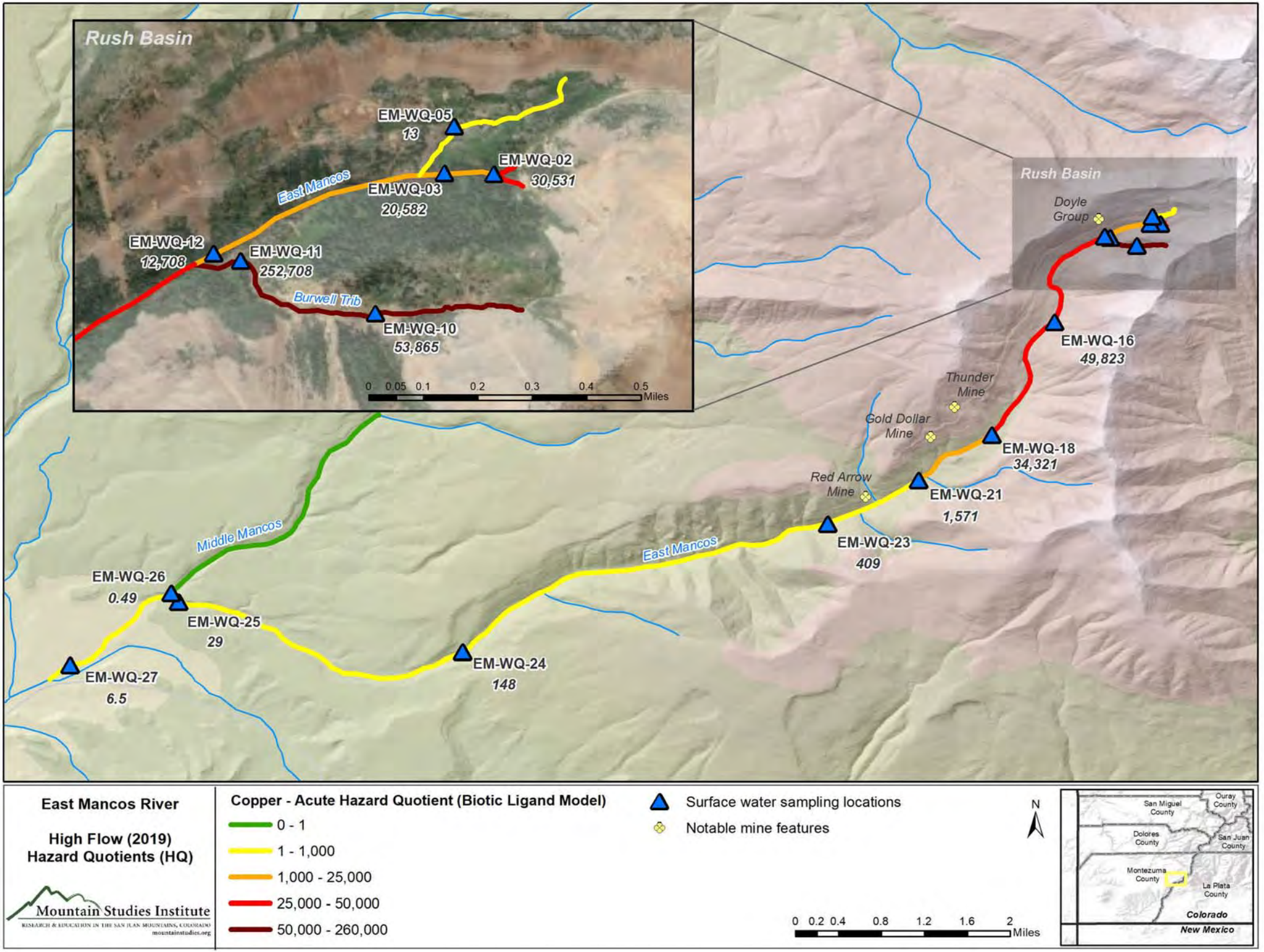

Figure 4-1. Distribution of acute hazard quotient (Biotic Ligand Model) for dissolved copper during high flow in the East Mancos River watershed.

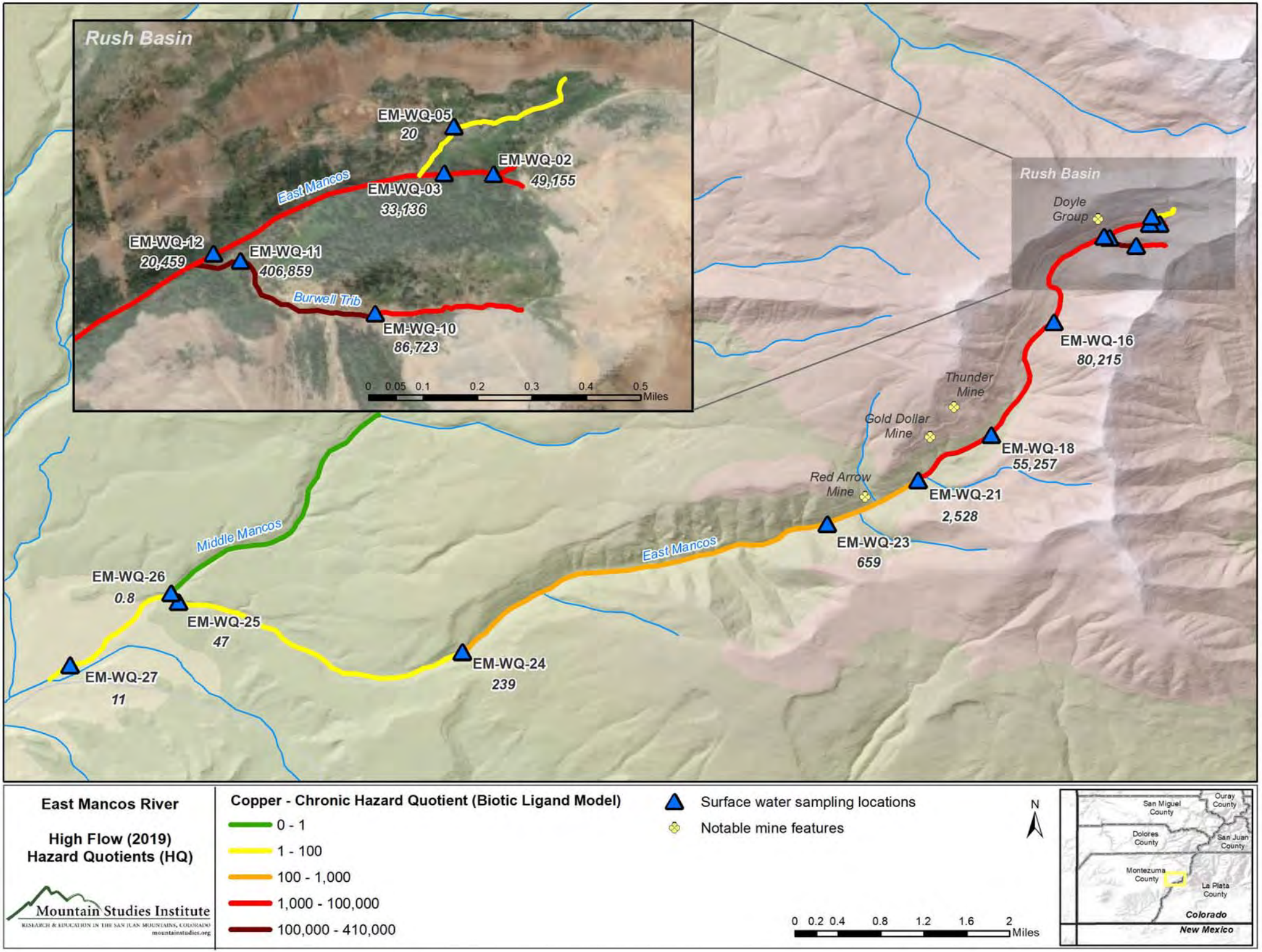

Figure 4-2. Distribution of chronic hazard quotient (Biotic Ligand Model) for dissolved copper during high flow in the East Mancos River watershed.

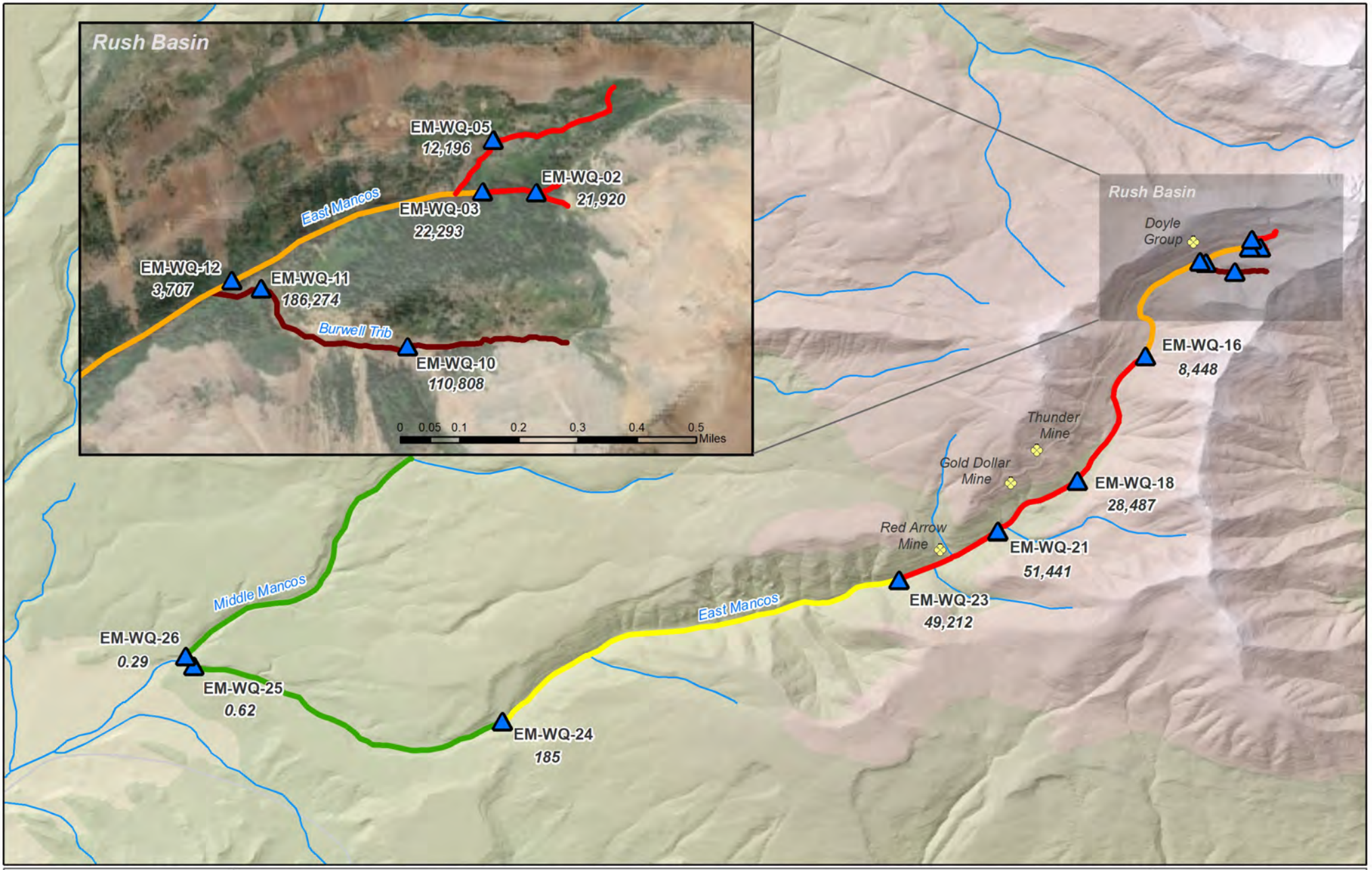

Figure 4-3. Distribution of acute hazard quotient (Biotic Ligand Model) for dissolved copper during low flow in the East Mancos River watershed.

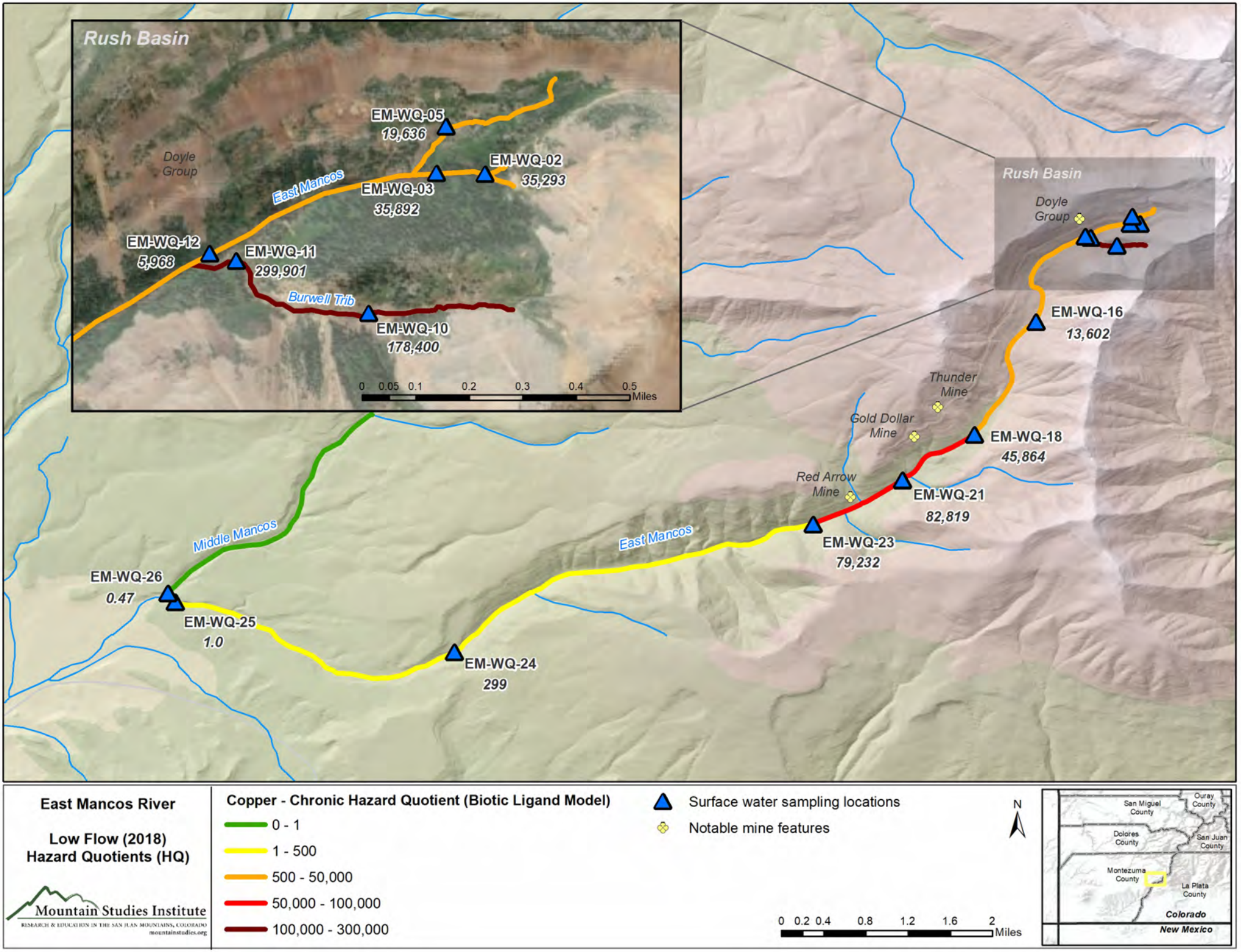

Figure 4-4. Distribution of chronic hazard quotient (Biotic Ligand Model) for dissolved copper during low flow in the East Mancos River watershed.

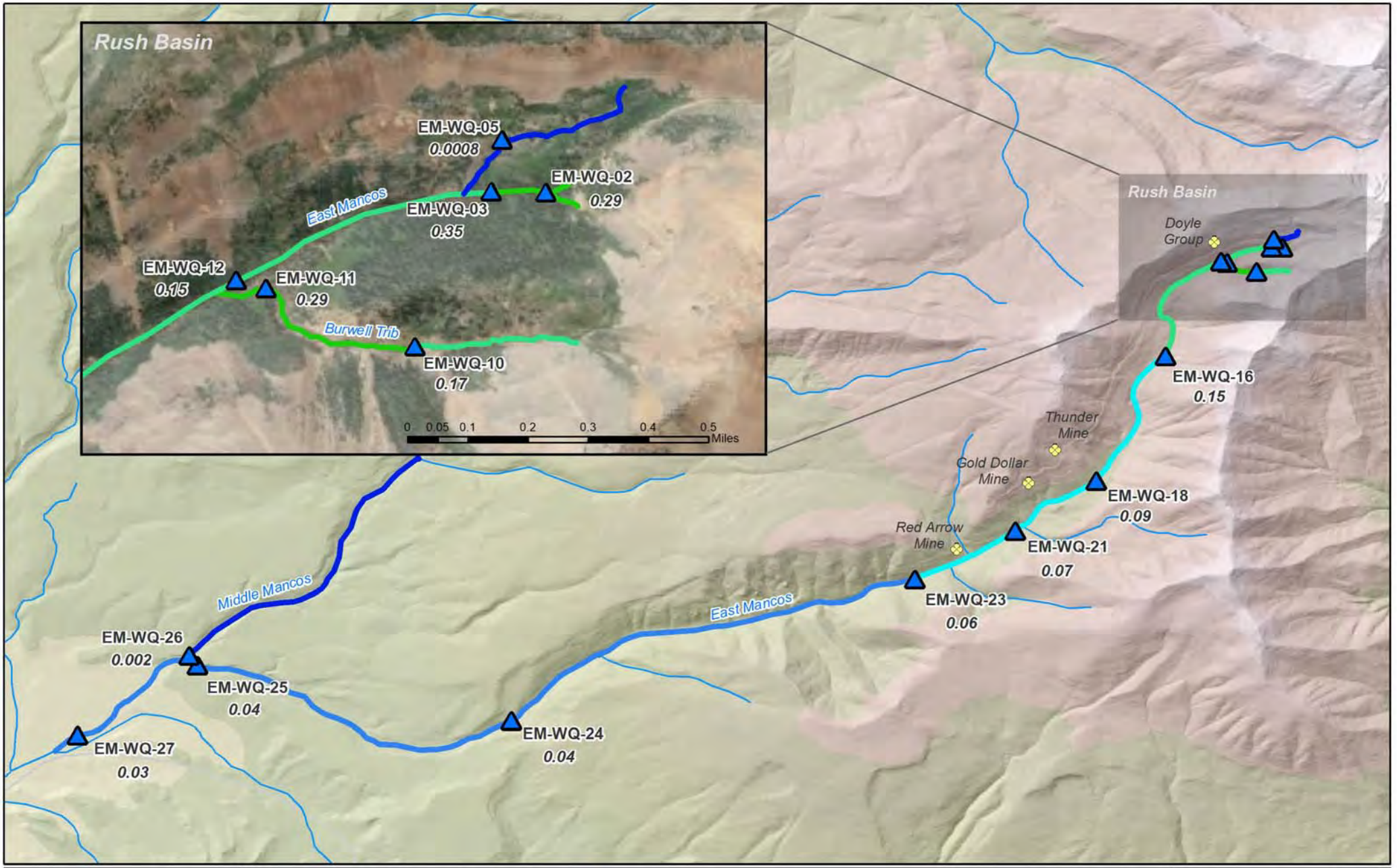

Figure 4-5. Distribution of acute hazard quotient for dissolved manganese during high flow in the East Mancos River watershed.

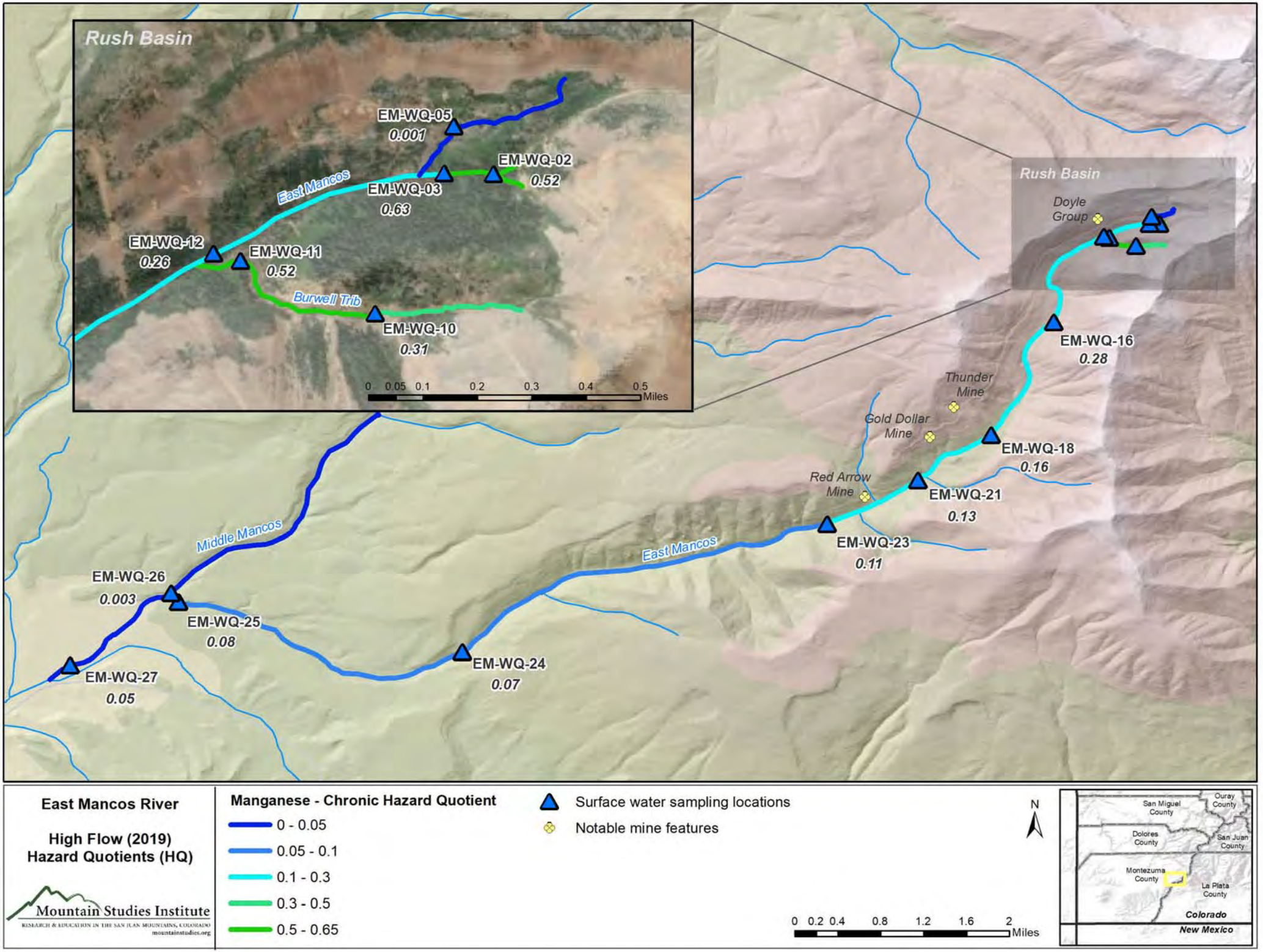

Figure 4-6. Distribution of chronic hazard quotient for dissolved manganese during high flow in the East Mancos River watershed.

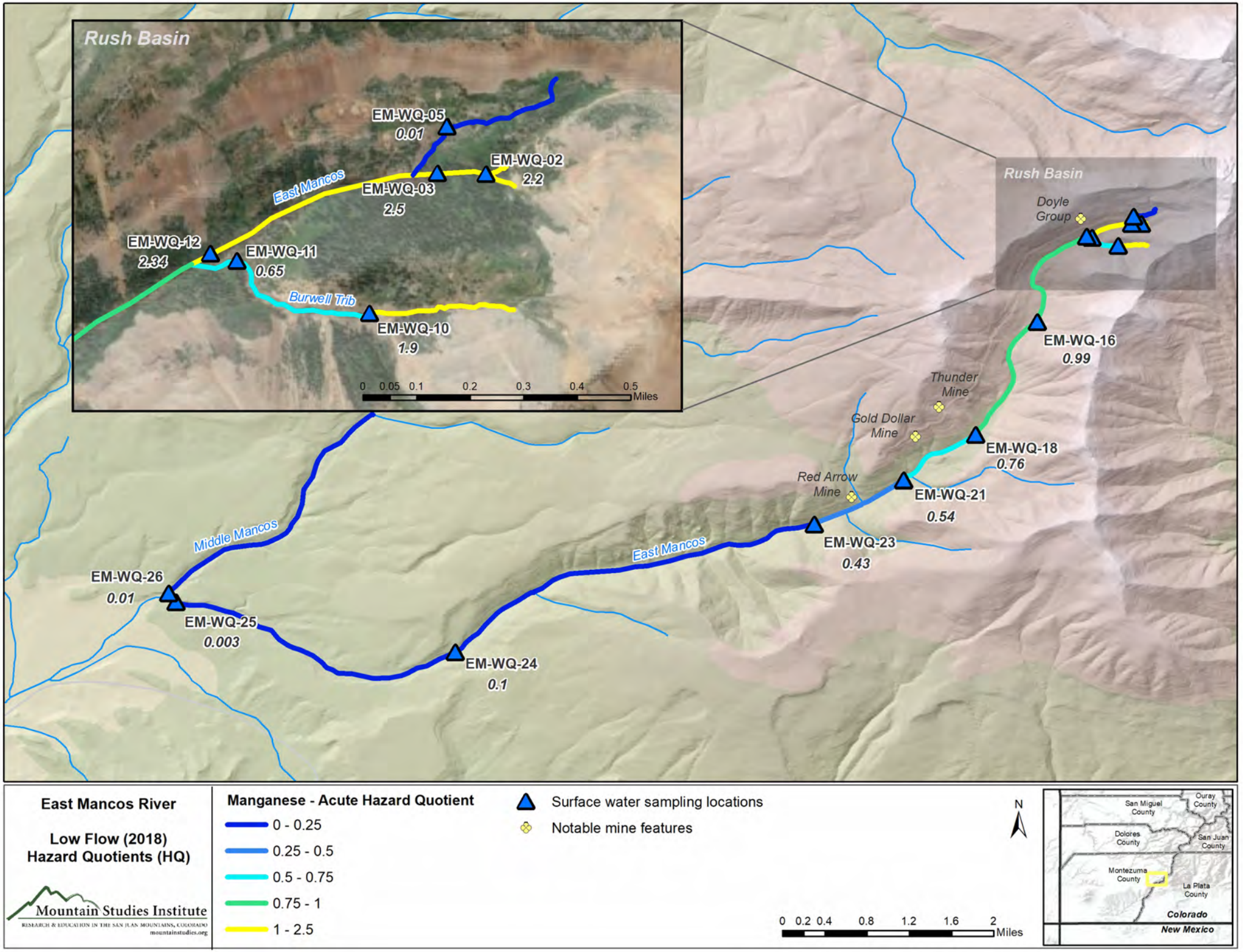

Figure 4-7. Distribution of acute hazard quotient for dissolved manganese during low flow in the East Mancos River watershed.

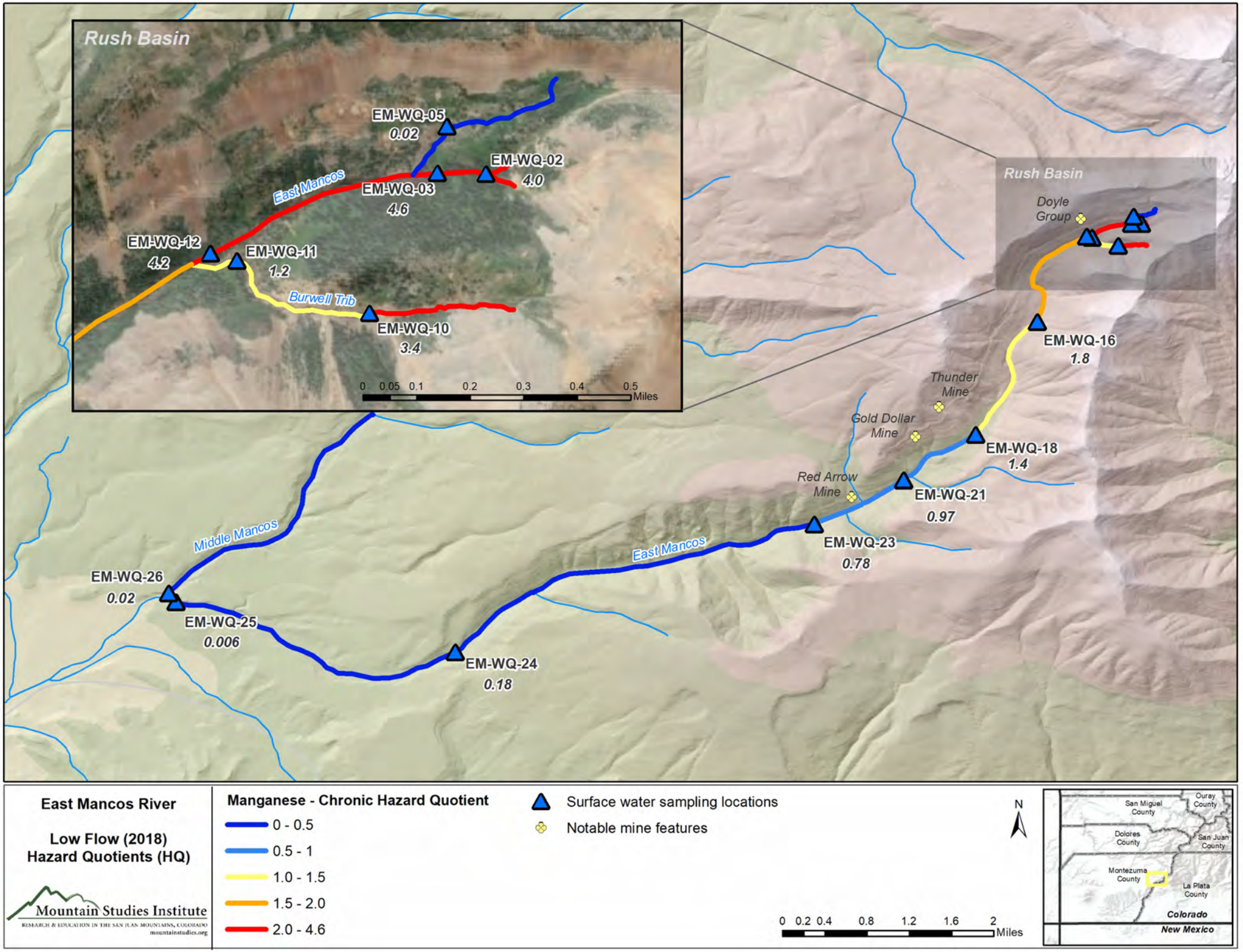

Figure 4-8. Distribution of chronic hazard quotient for dissolved manganese during low flow in the East Mancos River watershed.

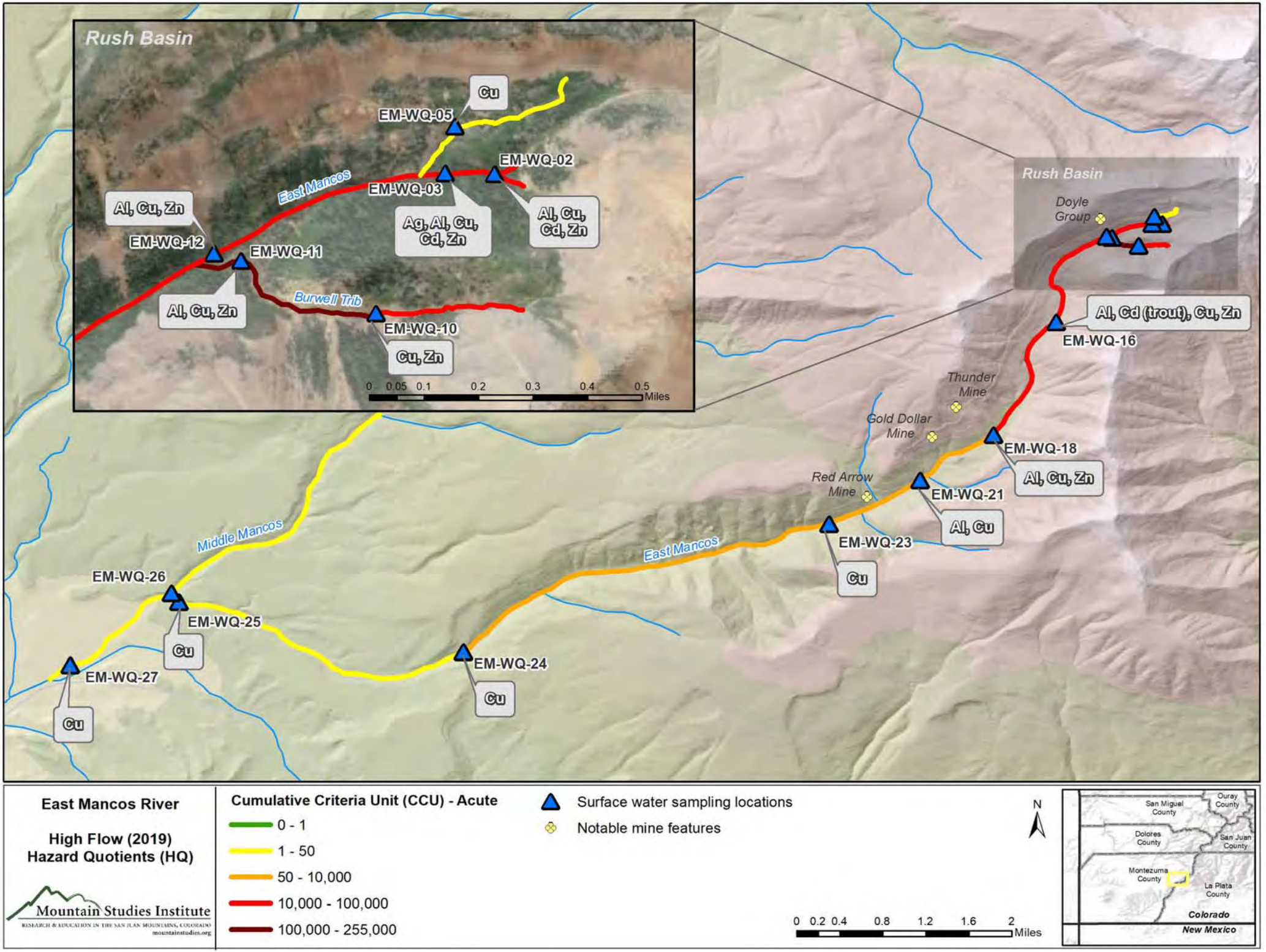

Figure 4-9. Distribution of acute cumulative criteria unit (CCU) during high flow in the East Mancos River watershed.

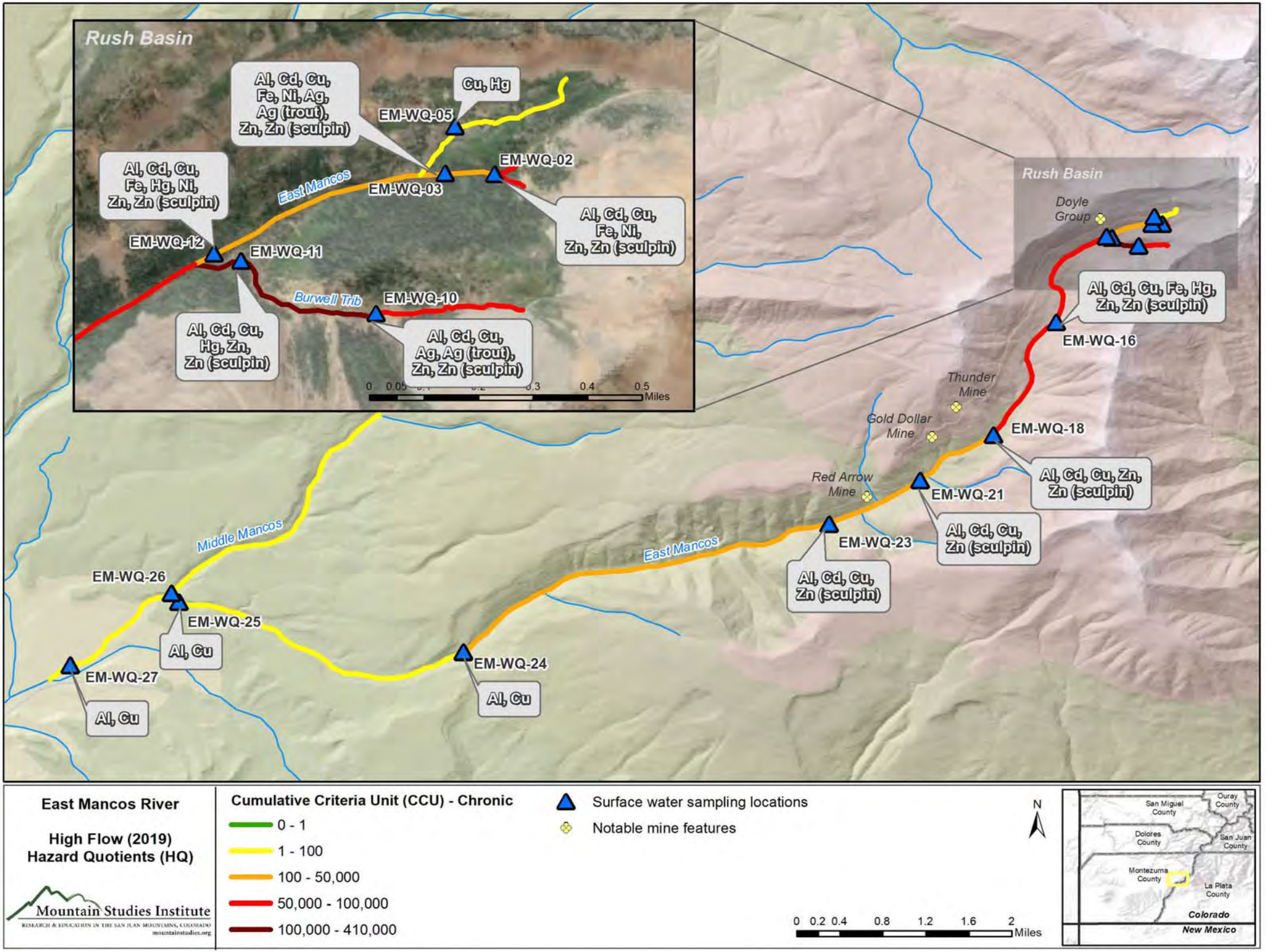

Figure 4-10. Distribution of chronic cumulative criteria unit (CCU) during high flow in the East Mancos River watershed.

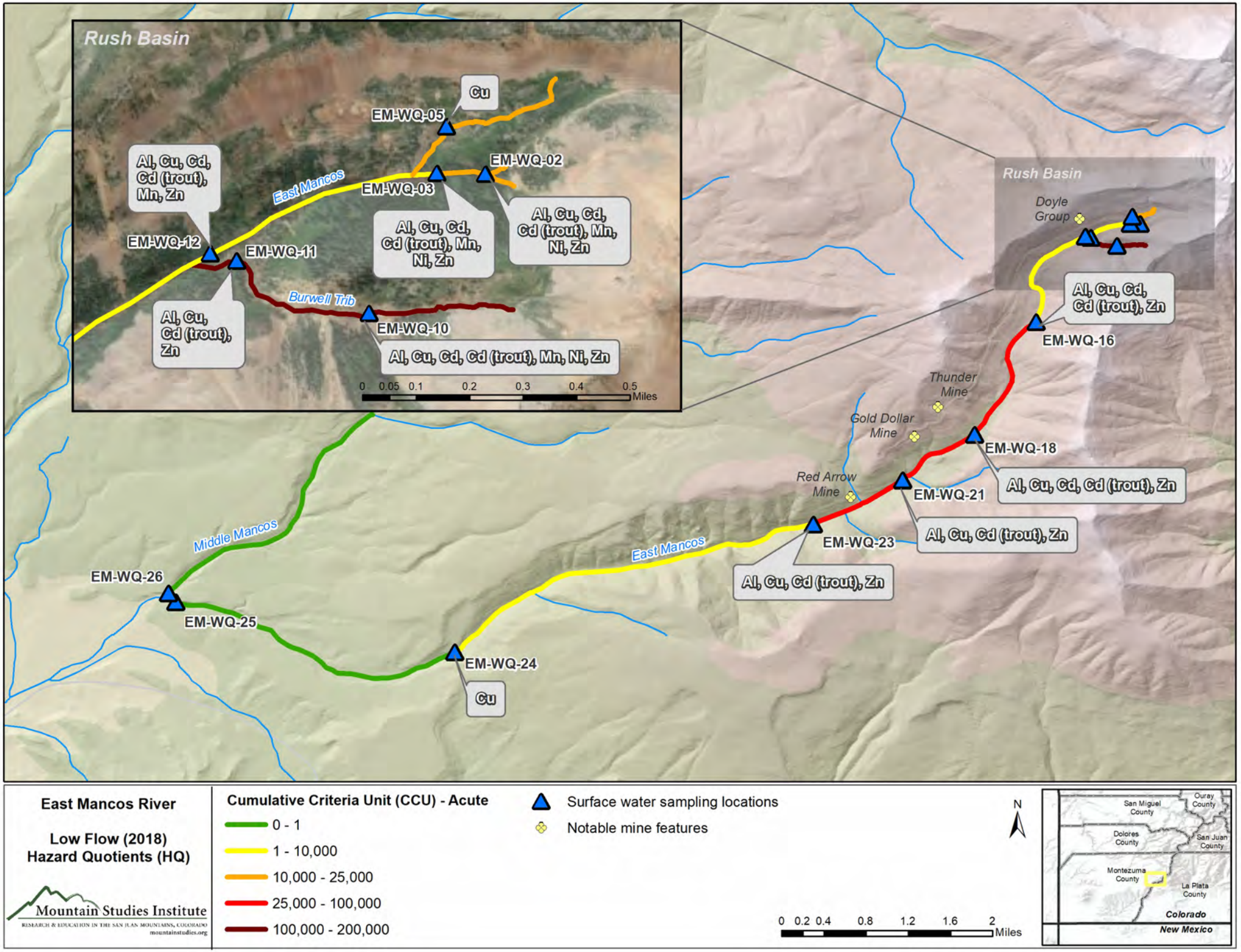

Figure 4-11. Distribution of acute cumulative criteria unit (CCU) during low flow in the East Mancos River watershed.

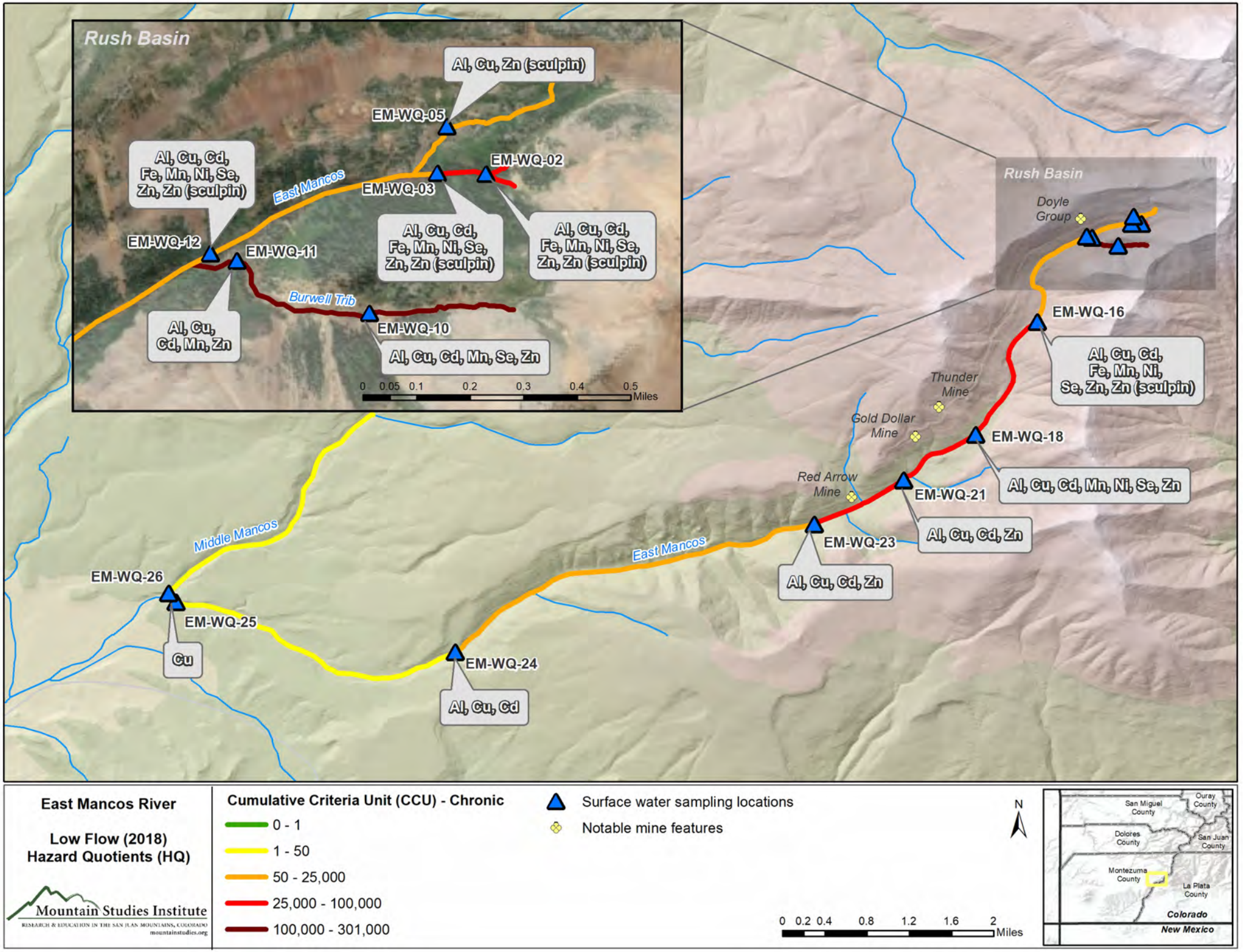

Figure 4-12. Distribution of chronic cumulative criteria unit (CCU) during low flow in the East Mancos River watershed.

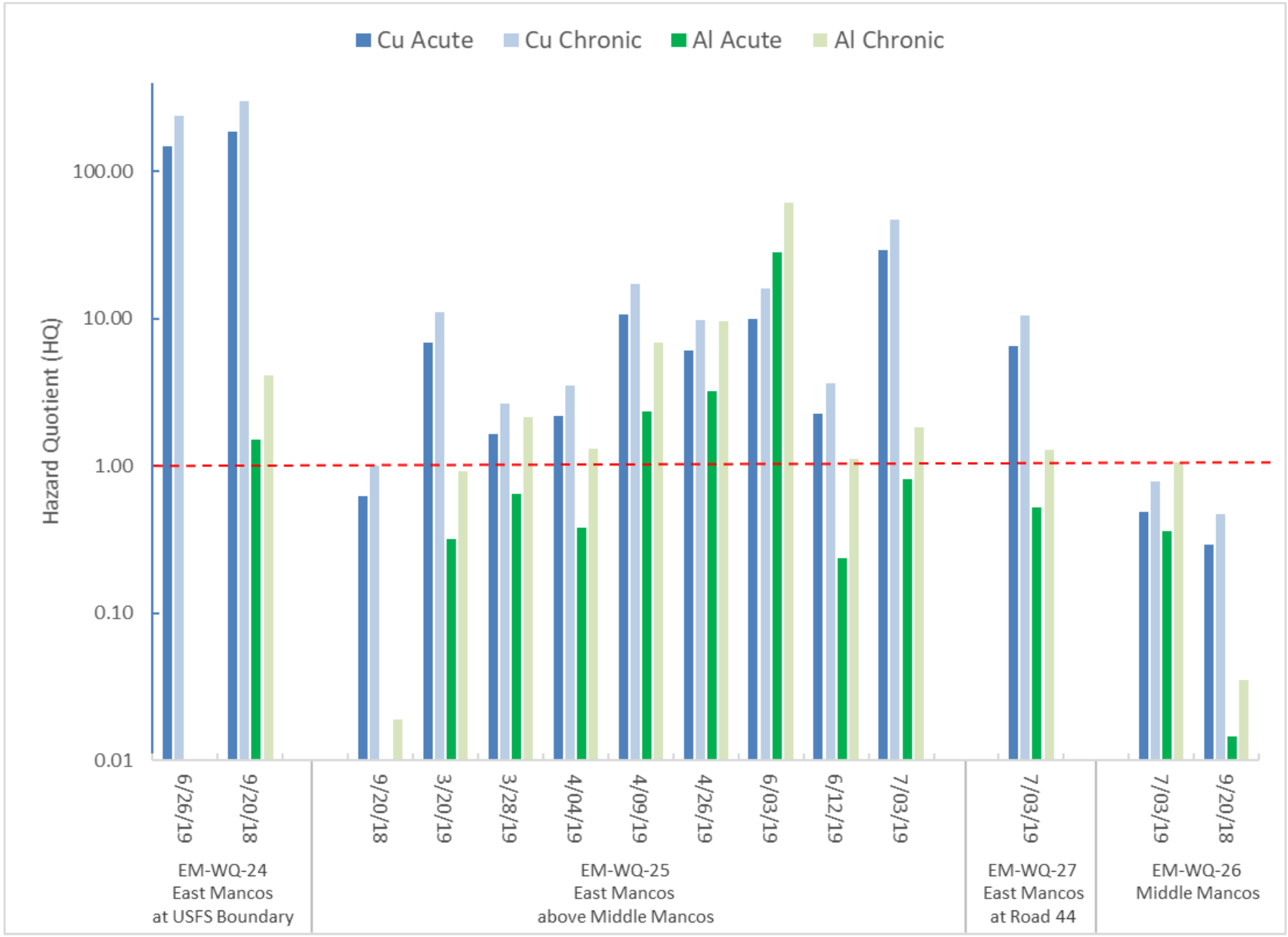

Figure 4-13. Hazard quotients for downstream sites on the East Mancos River watershed.

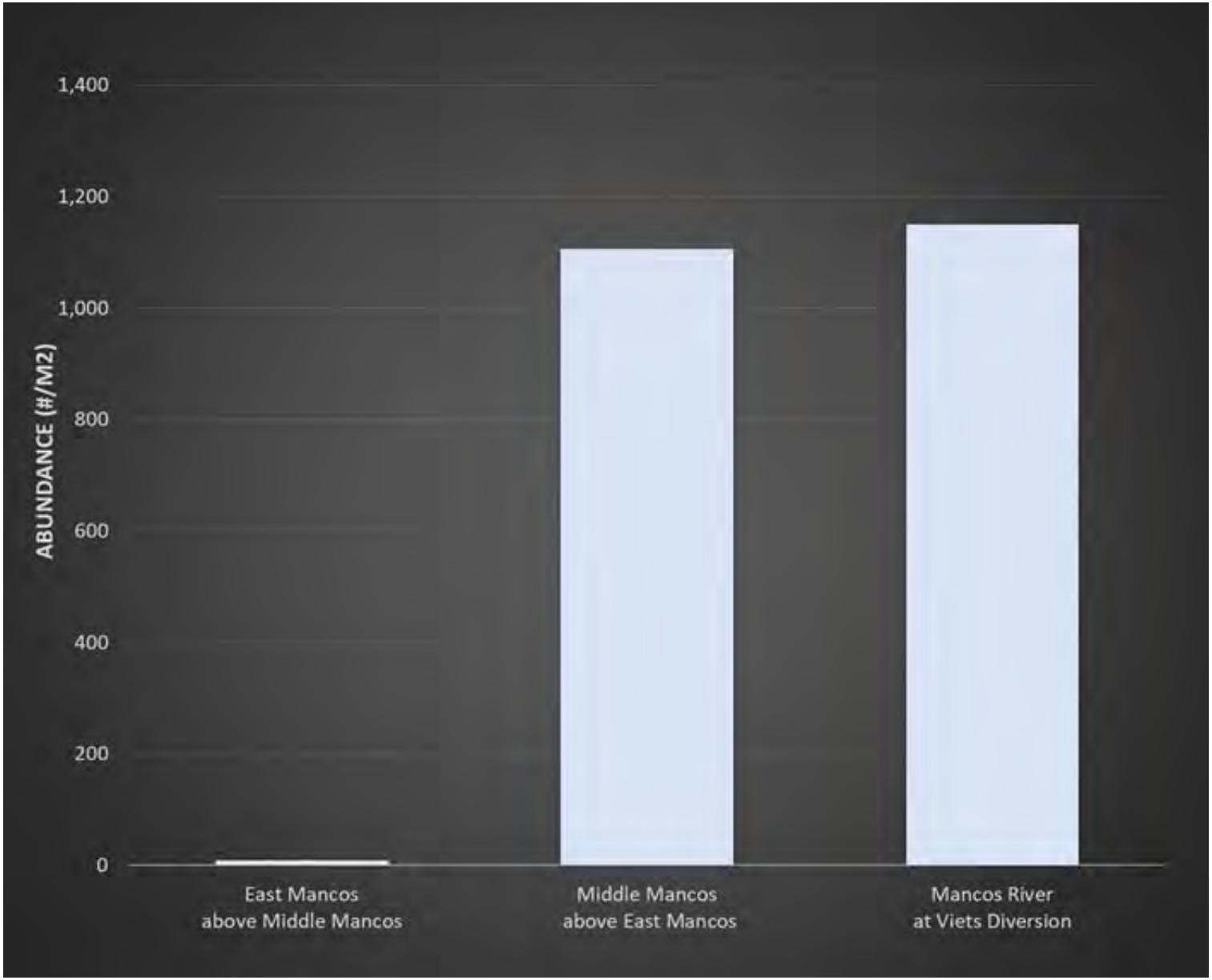

Figure 4-14. Benthic macroinvertebrate abundance in the East Mancos River at mouth (site 25), Middle Mancos River (site 26), and Mancos River at Viets diversion, Sept-Oct 2019.

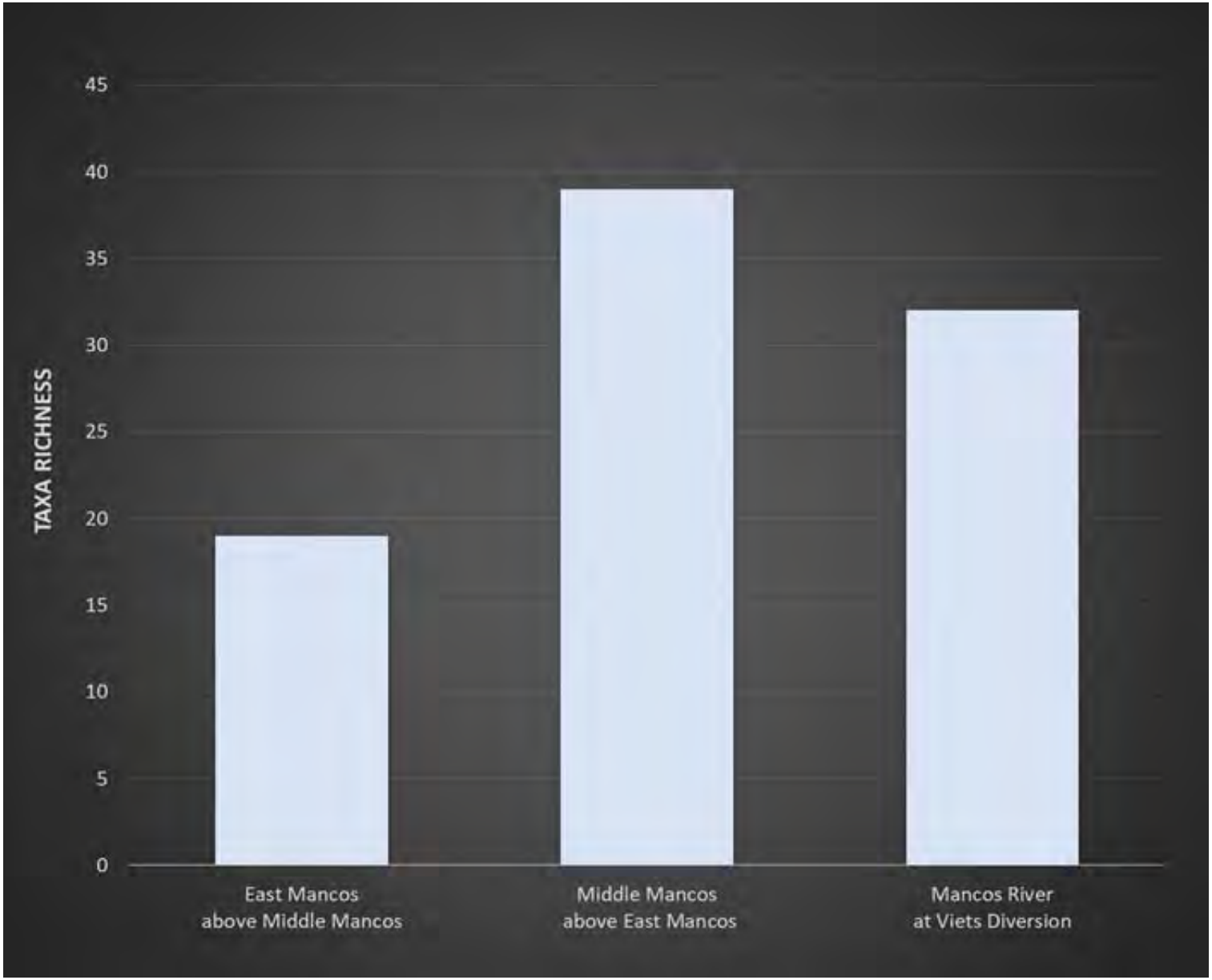

Figure 4-15. Benthic macroinvertebrate taxa richness in the East Mancos River at mouth (site 25), Middle Mancos River (site 26), and Mancos River at Viets diversion, Sept-Oct 2019.

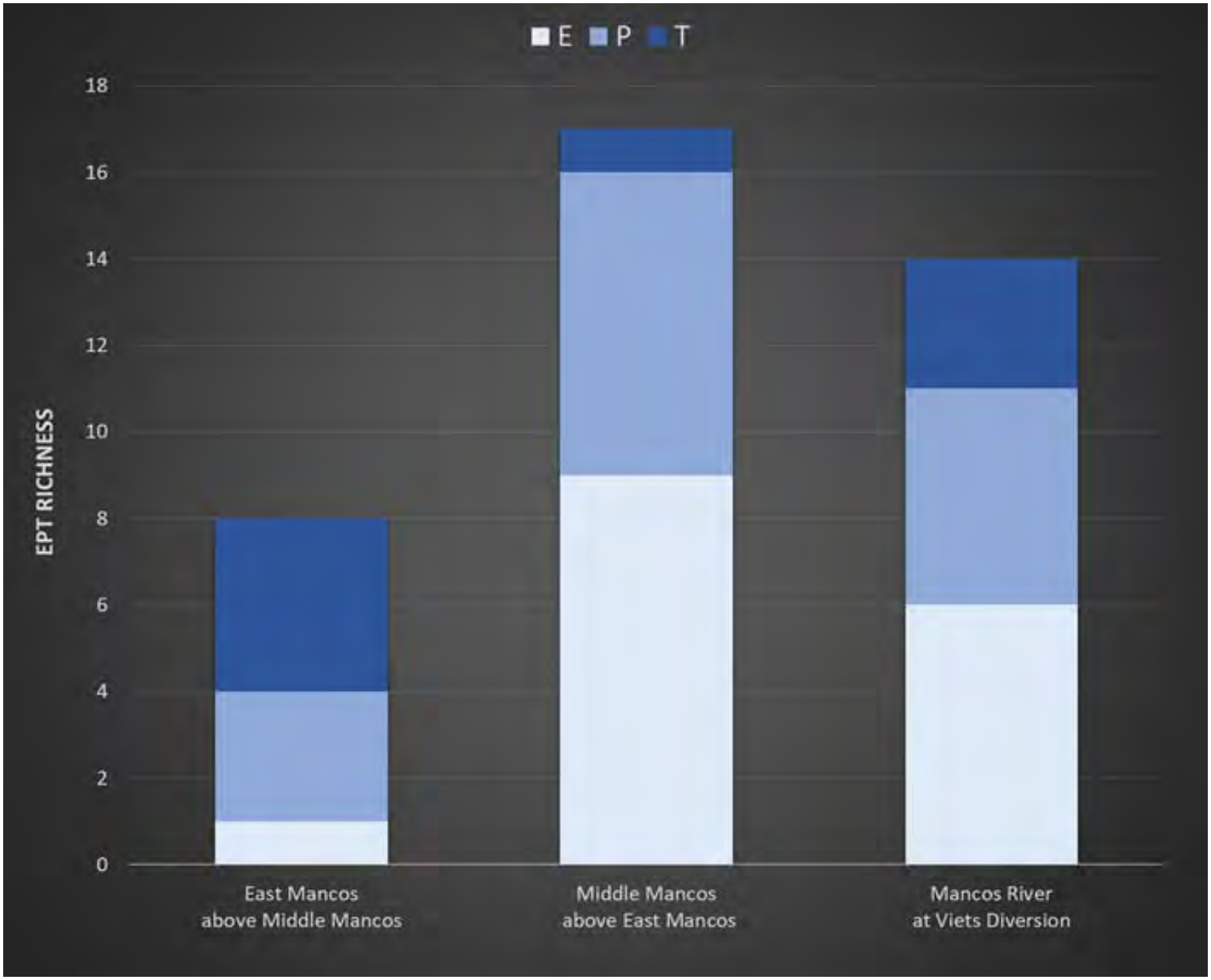

Figure 4-16. Richness of EPT (Ephemeroptera, Plecoptera, and Trichoptera) in the East Mancos River at mouth (site 25), Middle Mancos River (site 26), and Mancos River at Viets diversion, Sept-Oct 2019.

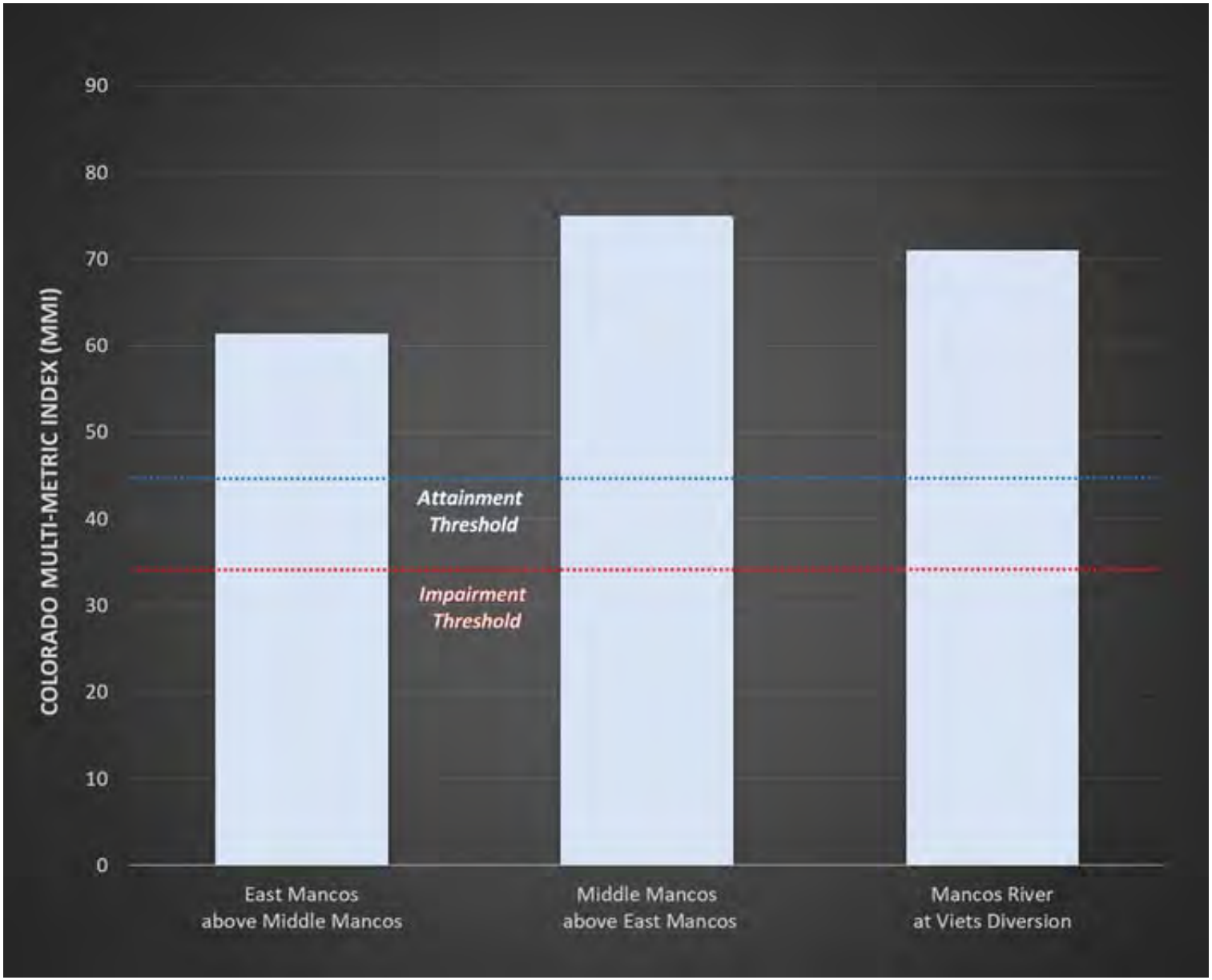

Figure 4-17. Colorado Multi-Metric Index (MMI) in the East Mancos River at mouth (site 25), Middle Mancos River (site 26), and Mancos River at Viets diversion, Sept-Oct 2019.

Table 4-1. Hazard Quotients calculated for water-quality sites in the East Mancos River, 2018-19

Site					Cumulative Criteria Unit*		BLM Copper		EPA Aluminum		CDPHE Aluminum		CDPHE Arsenic		CDPHE Cadmium			CDPHE Copper		CDPHE Iron	CDPHE Lead	
ID	Name	Type	Date	HFLF	Acute	Chronic	Acute	Chronic	Acute	Chronic	Acute	Chronic	Acute	Chronic	Acute	Acute (trout)	Chronic	Acute	Chronic	Chronic	Acute	Chronic
EM-WQ-02	East Mancos above ferricrete	SW	7/9/2019	HF	31,334	50,090	30,531	49,155	n/a	n/a	109	102	0.01	0.03	1.37	2.20	6.42	683	807	6.00	0.02	0.41
EM-WQ-02	East Mancos above ferricrete	SW	9/12/2018	LF	24,291	40,084	21,921	35,293	n/a	n/a	178	1,644	0.29	0.65	3.62	5.82	20.64	2,158	2,952	132	0.004	0.09
EM-WQ-03	East Mancos below ferricrete	SW	7/9/2019	HF	21,549	34,304	20,582	33,136	n/a	n/a	119	137	0.02	0.04	1.53	2.47	7.33	836	1,000	8.79	0.01	0.34
EM-WQ-03	East Mancos below ferricrete	SW	9/12/2018	LF	24,611	40,666	22,293	35,892	n/a	n/a	143	1,609	0.24	0.55	3.18	5.12	18.47	2,142	2,968	133	0.005	0.12
EM-WQ-05	Rush Basin Lake Tributary	SW	7/9/2019	HF	15.30	24.94	12.66	20.38	n/a	n/a	0.13	0.90	0.002	0.004	0.07	0.11	0.35	2.26	2.89	0.02	0.006	0.14
EM-WQ-05	Rush Basin Lake Tributary	SW	9/14/2018	LF	12,280	19,747	12,196	19,636	n/a	n/a	0.84	3.40	0.000	0.001	0.15	0.24	0.79	81.83	106	0.07	0.005	0.12
EM-WQ-10	Burwell Tributary above Porphyry Spring	SW	7/30/2019	HF	54,437	87,520	53,865	86,723	n/a	n/a	0.55	5.99	0.004	0.009	0.43	0.69	2.50	568	785	0.002	0.004	0.09
EM-WQ-10	Burwell Tributary above Porphyry Spring	SW	9/14/2018	LF	111,616	179,881	110,808	178,400	n/a	n/a	1.59	180	0.003	0.008	1.79	2.88	12.68	793	1,273	0.13	0.001	0.03
EM-WQ-11	Burwell Tributary above East Mancos	SW	7/8/2019	HF	253,380	407,812	252,708	406,859	n/a	n/a	1.76	20.23	0.001	0.001	0.88	1.41	5.11	665	922	0.02	0.002	0.05
EM-WQ-12	East Mancos River above Burwell Tributary	SW	7/8/2019	HF	13,060	20,928	12,708	20,459	n/a	n/a	31.37	63.79	0.004	0.008	0.60	0.96	2.99	317	393	3.79	0.008	0.21
EM-WQ-12	East Mancos River above Burwell Tributary	SW	9/14/2018	LF	5,555	9,953	3,707	5,968	n/a	n/a	118	1,483	0.04	0.09	3.40	5.47	19.91	1,699	2,370	73.30	0.01	0.26
EM-WQ-16	East Mancos River above Silver Falls	SW	7/8/2019	HF	50,121	80,640	49,823	80,215	n/a	n/a	5.50	32.76	0.000	0.001	0.73	1.17	4.00	289	384	1.28	0.005	0.12
EM-WQ-16	East Mancos River above Silver Falls	SW	9/21/2018	LF	8,952	14,925	8,449	13,602	n/a	n/a	17.11	580	0.008	0.02	1.77	2.84	11.27	475	706	12.90	0.003	0.08
EM-WQ-18	East Mancos River above Thunder Mine drainage	SW	6/26/2019	HF	34,462	55,459	34,321	55,257	n/a	n/a	1.81	12.87	0.000	0.001	0.47	0.75	2.62	137	184	0.54	0.003	0.08
EM-WQ-18	East Mancos River above Thunder Mine drainage	SW	9/20/2018	LF	28,787	46,716	28,487	45,864	n/a	n/a	9.08	407	0.001	0.003	1.16	1.86	7.55	284	429	0.78	0.005	0.13
EM-WQ-21	East Mancos River above Red Arrow	SW	7/3/2019	HF	1,606	2,591	1,571	2,529	n/a	n/a	1.10	13.22	0.004	0.009	0.26	0.42	1.51	32.78	45.60	0.82	0.002	0.05
EM-WQ-21	East Mancos River above Red Arrow	SW	9/19/2018	LF	51,636	83,419	51,441	82,819	n/a	n/a	5.61	306	0.001	0.002	0.79	1.26	5.22	185	283	0.20	0.003	0.07
EM-WQ-23	East Mancos River below Red Arrow	SW	9/19/2018	LF	49,376	79,689	49,212	79,232	n/a	n/a	3.69	208	0.001	0.002	0.68	1.09	4.51	156	240	0.11	0.002	0.05
EM-WQ-24	East Mancos River at USFS boundary	SW	6/26/2019	HF	158	261	148	239	n/a	n/a	0.58	9.29	0.000	0.001	0.13	0.22	0.80	8.17	11.58	0.42	0.002	0.04
EM-WQ-24	East Mancos River at USFS boundary	SW	9/20/2018	LF	201	325	185	299	1.50	4.13	0.25	1.73	0.000	0.000	0.23	0.36	1.55	14.18	22.21	0.03	0.000	0.005
EM-WQ-25	East Mancos River above Middle Mancos	SW	7/3/2019	HF	37.87	62.99	29.01	46.71	0.82	1.84	0.53	3.68	0.000	0.001	0.14	0.23	0.85	7.61	10.73	0.35	0.002	0.04
EM-WQ-25	East Mancos River above Middle Mancos	SW	9/20/2018	LF	0.92	1.63	0.62	1.00	0.009	0.02	0.002	0.02	0.001	0.002	0.01	0.02	0.09	0.20	0.31	0.02	0.000	0.005
EM-WQ-25	East Mancos River above Middle Mancos	SW	3/20/2019	SR	7.59	16.55	6.88	11.07	0.32	0.92	0.04	4.00	0.000	0.001	0.03	0.04	0.19	0.48	0.77	0.22	0.000	0.009
EM-WQ-25	East Mancos River above Middle Mancos	SW	3/28/2019	SR	3.47	15.97	1.65	2.66	0.65	2.16	0.75	11.17	0.000	0.000	0.03	0.04	0.16	0.92	1.29	0.42	0.002	0.04
EM-WQ-25	East Mancos River above Middle Mancos	SW	4/4/2019	SR	3.15	14.54	2.20	3.54	0.38	1.32	0.14	9.25	0.000	0.001	0.01	0.02	0.10	0.73	1.14	0.34	0.001	0.01
EM-WQ-25	East Mancos River above Middle Mancos	SW	4/9/2019	SR	12.71	52.58	10.62	17.09	2.36	6.90	0.53	32.53	0.000	0.001	0.04	0.07	0.27	1.36	2.10	0.30	0.001	0.01
EM-WQ-25	East Mancos River above Middle Mancos	SW	4/26/2019	SR	10.28	66.40	6.11	9.84	3.21	9.57	1.65	51.72	0.000	0.001	0.03	0.04	0.16	2.39	3.53	0.92	0.001	0.02
EM-WQ-25	East Mancos River above Middle Mancos	SW	6/3/2019	SR	19.12	200	9.90	15.94	28.33	61.20	8.14	176	0.001	0.002	0.02	0.03	0.13	0.98	1.41	6.60	0.001	0.03
EM-WQ-25	East Mancos River above Middle Mancos	SW	6/12/2019	SR	6.74	27.00	2.28	3.66	0.24	1.11	2.63	18.42	0.000	0.001	0.02	0.04	0.14	1.72	2.44	2.10	0.002	0.04
EM-WQ-26	Middle Mancos River above East Mancos River	SW	7/3/2019	HF	1.17	3.68	0.49	0.79	0.36	1.06	0.23	1.59	0.001	0.001	0.01	0.02	0.09	0.39	0.59	0.46	0.001	0.02
EM-WQ-26	Middle Mancos River above East Mancos River	SW	9/20/2018	LF	0.45	1.14	0.29	0.47	0.01	0.04	0.005	0.04	0.002	0.003	0.002	0.003	0.01	0.09	0.15	0.28	0.000	0.005
EM-WQ-27	East Mancos River at Road 44	SW	7/3/2019	HF	10.76	19.60	6.54	10.53	0.52	1.28	0.38	2.68	0.000	0.001	0.05	0.08	0.31	3.59	5.25	0.52	0.001	0.03

*CCU incorporates all metals except BLM Cu, EPA Al, Ag, Hg, and Zn due to differences in the availability of data for each site.

Table 4-1. Hazard Quotients calculated for water-quality sites in the East Mancos River, 2018-19

Site				CDPHE Manganese		CDPHE Mercury	CDPHE Nickel		CDPHE Selenium		CDPHE Silver			CDPHE Thalium	CDPHE Uranium		CDPHE Zinc		
ID	Name	Type	Date	Acute	Chronic	Chronic	Acute	Chronic	Acute	Chronic	Acute	Chronic	Chronic (trout)	Chronic	Acute	Chronic	Acute	Chronic	Chronic (sculpin)
EM-WQ-02	East Mancos above ferricrete	SW	7/9/2019	0.29	0.52	n/a	0.31	2.80	0.06	0.23	n/a	n/a	n/a	0.07	0.04	0.07	6.74	8.90	262
EM-WQ-02	East Mancos above ferricrete	SW	9/12/2018	2.21	3.99	n/a	1.02	9.18	0.66	2.65	n/a	n/a	n/a	0.92	0.12	0.19	19.64	25.93	97.91
EM-WQ-03	East Mancos below ferricrete	SW	7/9/2019	0.35	0.63	n/a	0.36	3.21	0.07	0.27	1.75	11.09	47.28	0.08	0.05	0.08	7.70	10.17	250
EM-WQ-03	East Mancos below ferricrete	SW	9/12/2018	2.53	4.58	n/a	1.00	8.98	0.65	2.61	n/a	n/a	n/a	0.97	0.11	0.17	20.18	26.65	83.97
EM-WQ-05	Rush Basin Lake Tributary	SW	7/9/2019	0.001	0.001	2.70	0.009	0.08	0.008	0.03	n/a	n/a	n/a	0.07	0.000	0.000	0.06	0.07	0.70
EM-WQ-05	Rush Basin Lake Tributary	SW	9/14/2018	0.01	0.02	n/a	0.01	0.09	0.010	0.04	n/a	n/a	n/a	0.07	0.001	0.001	0.27	0.35	2.78
EM-WQ-10	Burwell Tributary above Porphyry Spring	SW	7/30/2019	0.17	0.31	n/a	0.03	0.25	0.07	0.26	0.63	4.02	17.14	0.67	0.000	0.000	1.69	2.23	7.27
EM-WQ-10	Burwell Tributary above Porphyry Spring	SW	9/14/2018	1.87	3.38	n/a	0.04	0.39	0.54	2.16	0.01	0.07	0.30	0.07	0.001	0.001	6.83	9.01	n/a
EM-WQ-11	Burwell Tributary above East Mancos	SW	7/8/2019	0.29	0.52	2.70	0.03	0.25	0.07	0.28	n/a	n/a	n/a	0.07	0.001	0.001	3.13	4.13	12.82
EM-WQ-12	East Mancos River above Burwell Tributary	SW	7/8/2019	0.14	0.26	3.00	0.12	1.07	0.03	0.14	n/a	n/a	n/a	0.07	0.02	0.02	2.63	3.47	51.07
EM-WQ-12	East Mancos River above Burwell Tributary	SW	9/14/2018	2.34	4.24	n/a	0.88	7.91	0.67	2.67	n/a	n/a	n/a	0.83	0.09	0.14	17.89	23.62	67.74
EM-WQ-16	East Mancos River above Silver Falls	SW	7/8/2019	0.15	0.28	4.30	0.05	0.43	0.03	0.11	n/a	n/a	n/a	0.07	0.003	0.005	1.92	2.53	14.16
EM-WQ-16	East Mancos River above Silver Falls	SW	9/21/2018	0.99	1.78	n/a	0.19	1.72	0.32	1.29	0.02	0.15	0.66	0.25	0.02	0.02	4.85	6.40	7.50
EM-WQ-18	East Mancos River above Thunder Mine drainage	SW	6/26/2019	0.09	0.16	n/a	0.02	0.21	0.01	0.06	n/a	n/a	n/a	0.07	0.001	0.001	1.11	1.47	7.02
EM-WQ-18	East Mancos River above Thunder Mine drainage	SW	9/20/2018	0.76	1.37	n/a	0.13	1.13	0.25	1.00	n/a	n/a	n/a	0.19	0.008	0.01	3.18	4.19	n/a
EM-WQ-21	East Mancos River above Red Arrow	SW	7/3/2019	0.07	0.13	n/a	0.01	0.12	0.008	0.03	n/a	n/a	n/a	0.07	0.000	0.000	0.60	0.79	2.35
EM-WQ-21	East Mancos River above Red Arrow	SW	9/19/2018	0.54	0.97	n/a	0.08	0.74	0.20	0.82	n/a	n/a	n/a	0.14	0.006	0.009	2.13	2.82	n/a
EM-WQ-23	East Mancos River below Red Arrow	SW	9/19/2018	0.43	0.78	n/a	0.07	0.62	0.16	0.64	n/a	n/a	n/a	0.12	0.004	0.007	1.85	2.44	n/a
EM-WQ-24	East Mancos River at USFS boundary	SW	6/26/2019	0.04	0.07	n/a	0.006	0.05	0.008	0.03	n/a	n/a	n/a	0.07	0.000	0.000	0.22	0.29	0.67
EM-WQ-24	East Mancos River at USFS boundary	SW	9/20/2018	0.10	0.18	n/a	0.02	0.18	0.03	0.10	n/a	n/a	n/a	0.07	0.000	0.000	0.68	0.89	n/a
EM-WQ-25	East Mancos River above Middle Mancos	SW	7/3/2019	0.04	0.08	n/a	0.007	0.06	0.008	0.03	n/a	n/a	n/a	0.07	0.000	0.000	0.30	0.39	0.97
EM-WQ-25	East Mancos River above Middle Mancos	SW	9/20/2018	0.003	0.006	n/a	0.002	0.01	0.009	0.04	n/a	n/a	n/a	0.07	0.000	0.000	0.04	0.06	n/a
EM-WQ-25	East Mancos River above Middle Mancos	SW	3/20/2019	0.03	0.05	n/a	0.003	0.03	0.01	0.05	n/a	n/a	n/a	0.07	0.000	0.000	0.08	0.10	n/a
EM-WQ-25	East Mancos River above Middle Mancos	SW	3/28/2019	0.01	0.02	n/a	0.004	0.03	0.008	0.03	n/a	n/a	n/a	0.07	0.000	0.000	0.06	0.08	0.19
EM-WQ-25	East Mancos River above Middle Mancos	SW	4/4/2019	0.008	0.01	n/a	0.001	0.01	0.008	0.03	n/a	n/a	n/a	0.07	0.000	0.000	0.03	0.04	n/a
EM-WQ-25	East Mancos River above Middle Mancos	SW	4/9/2019	0.02	0.04	n/a	0.006	0.05	0.008	0.03	n/a	n/a	n/a	0.07	0.000	0.000	0.06	0.07	n/a
EM-WQ-25	East Mancos River above Middle Mancos	SW	4/26/2019	0.01	0.03	n/a	0.004	0.03	0.008	0.03	n/a	n/a	n/a	0.07	0.000	0.000	0.03	0.04	0.05
EM-WQ-25	East Mancos River above Middle Mancos	SW	6/3/2019	0.02	0.04	n/a	0.003	0.03	0.008	0.03	0.03	0.21	0.90	0.07	0.000	0.000	0.02	0.02	0.04
EM-WQ-25	East Mancos River above Middle Mancos	SW	6/12/2019	0.01	0.02	n/a	0.003	0.03	0.01	0.04	n/a	n/a	n/a	0.07	0.000	0.000	0.03	0.04	0.08
EM-WQ-26	Middle Mancos River above East Mancos River	SW	7/3/2019	0.002	0.003	n/a	0.002	0.02	0.01	0.05	n/a	n/a	n/a	0.07	0.000	0.000	0.01	0.01	n/a
EM-WQ-26	Middle Mancos River above East Mancos River	SW	9/20/2018	0.01	0.02	n/a	0.002	0.01	0.009	0.04	n/a	n/a	n/a	0.07	0.000	0.000	0.03	0.04	n/a
EM-WQ-27	East Mancos River at Road 44	SW	7/3/2019	0.03	0.05	n/a	0.003	0.02	0.01	0.04	n/a	n/a	n/a	0.07	0.000	0.000	0.08	0.11	0.16